Medical Imaging
(The Whole Course in Two Lectures)

On the website you will find papers connected to this Material. Please choose one, and do the following:

(1) Read it and understand it
(2) Write a report on the work (10 pages)
(3) Implement the algorithm on computer
(4) Give me the code and some test images
(5) This is your final project
(6) Contact info: allen.tannenbaum@stonybrook.edu

Outline of Course

- Medical Imaging Devices: (Notes provided online)
- Enhancement
- Segmentation
- Registration
- Visualization

Medical Applications: IGT and IGS

- Biomedical Engineering principles to develop general-purpose software methods that can be integrated into complete therapy delivery systems.
- Four main components of image-guided therapy (IGT): localization, targeting, monitoring and control.
- Develop robust algorithms for:
  - Segmentation - automated methods that create patient-specific models of relevant anatomy from multi-modal data.
  - Registration – automated methods that align multiple data sets with each other and with the patient.

Segmentation

- Conformal curvature flow (CCF) methods find 3-D objects in 3-D space, avoiding distortion from 2-D mapping.

- In CCF methods, a curve or bubble is drawn by the user. This curve moves according to a differential equation, and can wrap around objects:

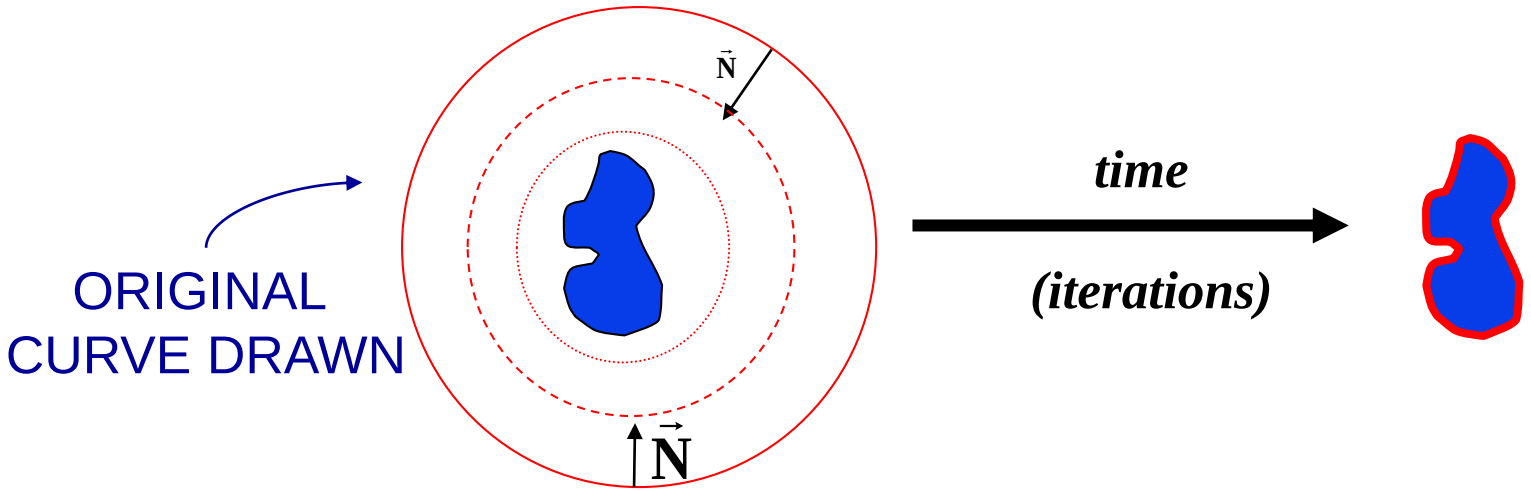

- Curve or surface movement is based on 2-D or 3-D data using the differential equation:

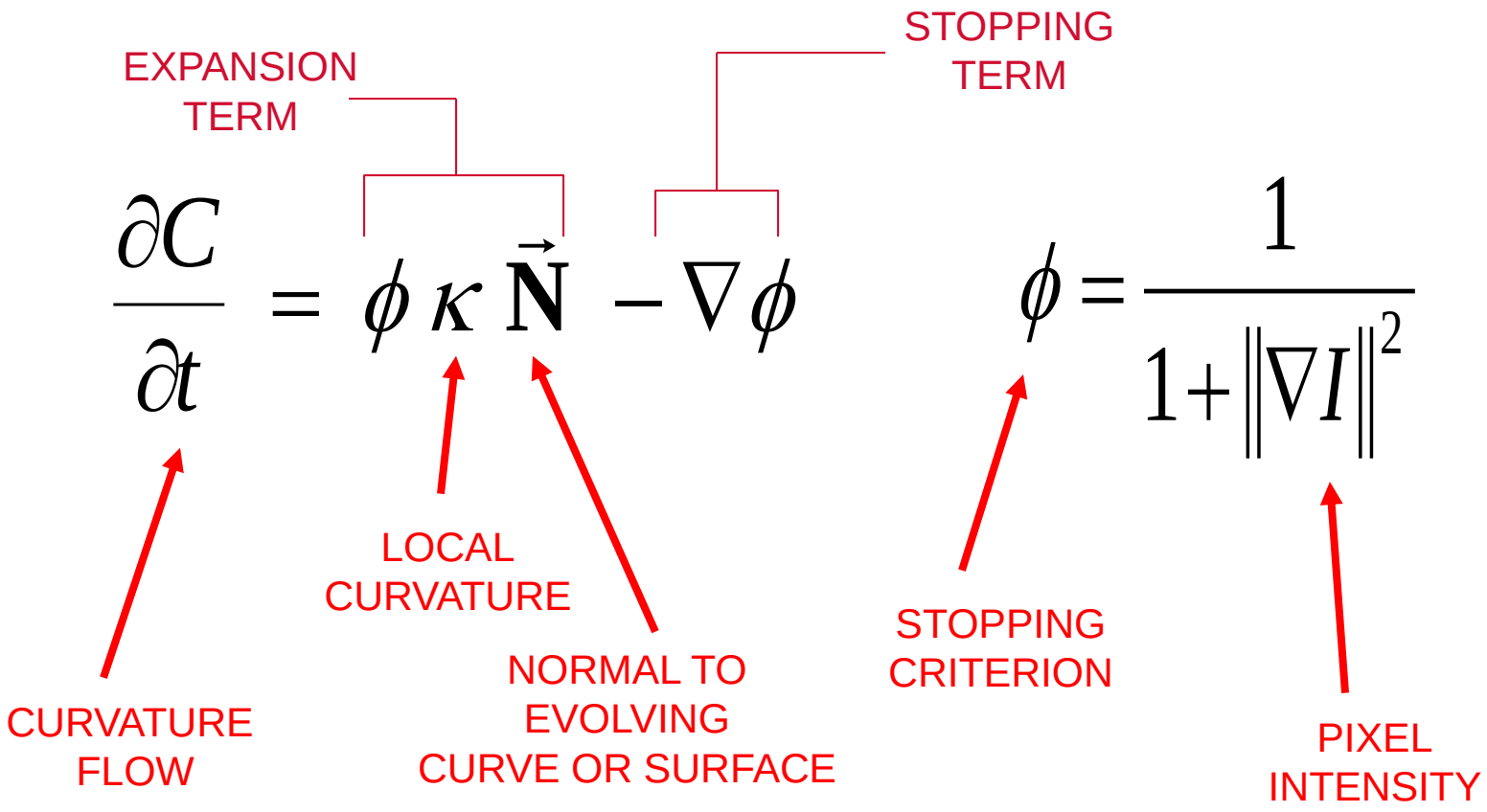

Active Contours-Geometric Heat Equation

The following equation gives the gradient direction in which the length of a closed, embedded plane curve is shrinking as fast as possible using only local information:

$$\frac{\partial C}{\partial t} = \kappa \vec{N}$$

The next equation gives the gradient direction in which the area of a closed, compact embedded surface is shrinking as fast as possible using only local information:

$$\frac{\partial S}{\partial t} = H \vec{N}$$

Conformal Metrics

We now use conformal metrics to modify the geometric heat equation in order to derive our geometric snakes models.

Curves:

$$ds \longrightarrow \phi ds$$

$$\frac{\partial C}{\partial t} = (\phi\kappa - \nabla\phi \cdot \vec{N})\vec{N}$$

Surfaces:

$$dA \longrightarrow \phi dA$$

$$\frac{\partial S}{\partial t} = (\phi H - \nabla\phi \cdot \vec{N})\vec{N}$$

Gradient Flows

The two flows were derived using the calculus of variations. For the curve case, the variational problem was to determine the direction in which the arc-length functional with respect to the conformal Euclidean metric is decreasing as fast as possible. We outine the steps now. Set

$$L_\phi(t) := \int_0^1 ||\frac{\partial C}{\partial p}||\phi dp$$

and

$$U := (\phi\kappa - \nabla\phi \cdot \vec{N})\vec{N}$$

One can compute that the first variation of this weighted arc-length functional is:

$$L'_\phi(t) = -\int_0^{L_\phi(t)} \langle \frac{\partial C}{\partial t}, U \rangle$$

This gives the flow for curves written down above.

Level Sets

If the initial curve is defined implicitly as a function

$$\psi(x, y) = 0$$

then the same evolution will be achieved by the following level set version of the active contour evolution equation:

$$\Psi_t = \phi ||U|| \ \text{div} \ (\frac{U}{||U||}) + \nabla\phi \cdot U,$$

where

$$\boldsymbol{U} := \nabla\boldsymbol{\Psi}.$$

Level sets allow automatic changes in topology.

Medical Applications of Active Contours

- Active contours can find interesting anatomical structures.
- Used in neurosciences for brain segmentation.
- Can also be used to determine pathologies.

Active Contours Find Cortical Surface

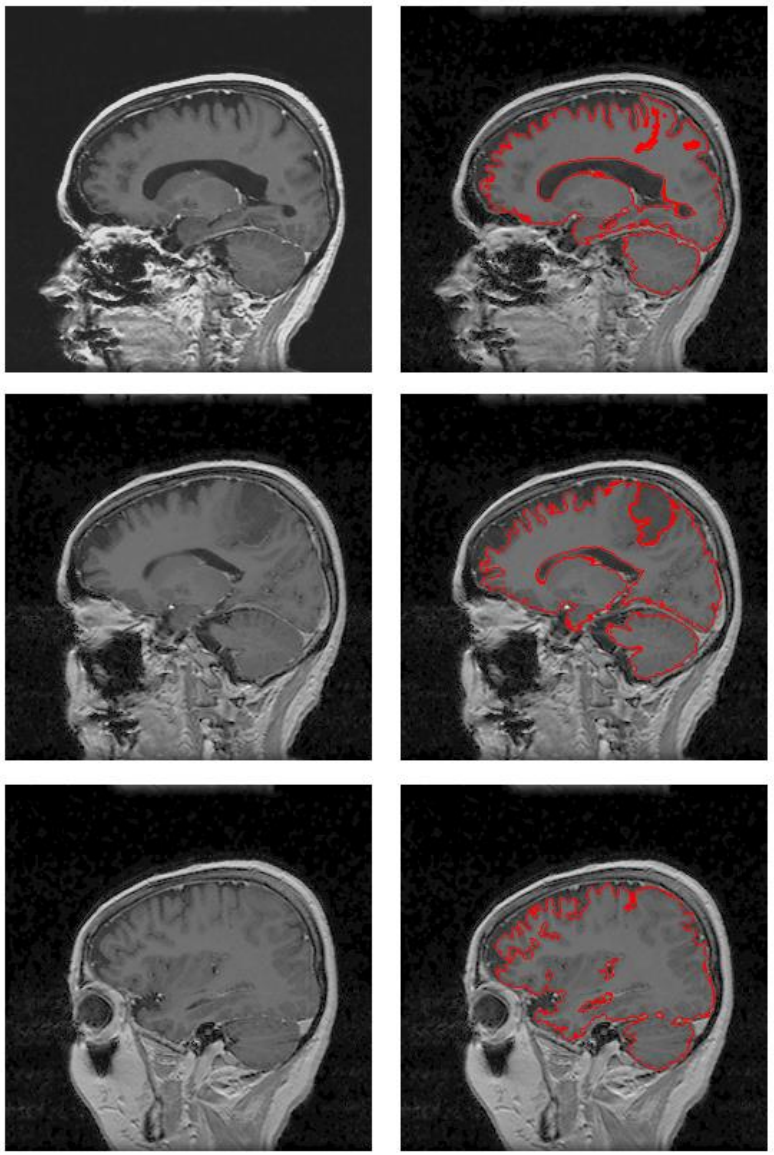

Blood Vessels in the Brain

Segmentation was performed
using codimension 2 active contours.

Knowledge-Based Segmentation

- Combination of Statistical and Partial Differential Equation Methods
- Bayesian Approach to Segmentation + Curvature Driven Flows
- Methodology Used in Conjunction with Geometric Active Contours

Anisotropic Diffusion

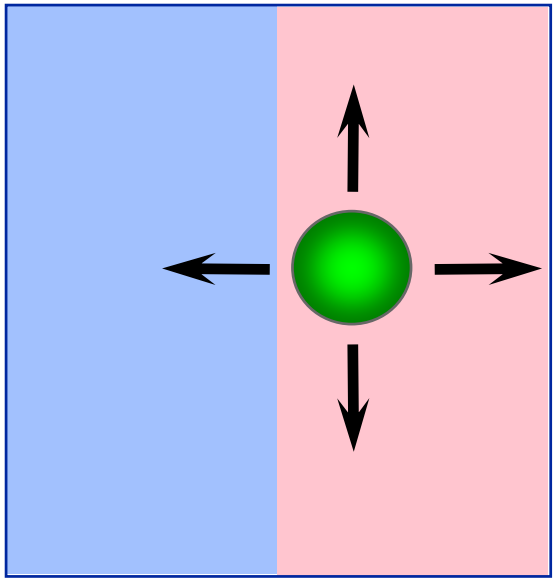

Isotropic smoothing

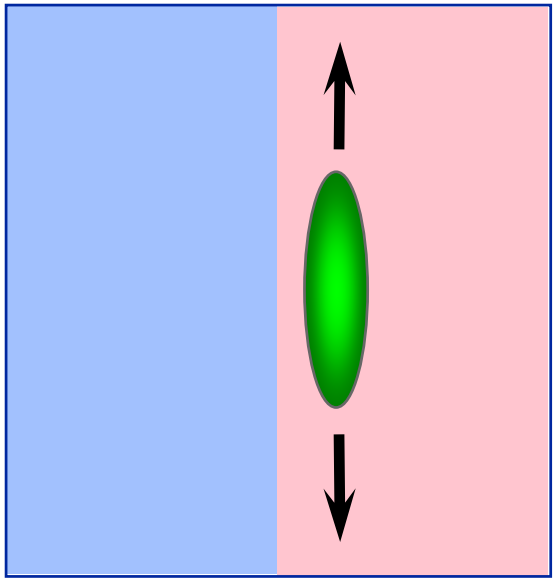

Anisotropic smoothing

The main problem

- Anisotropic diffusion is "blind" to information about types of objects in the scene

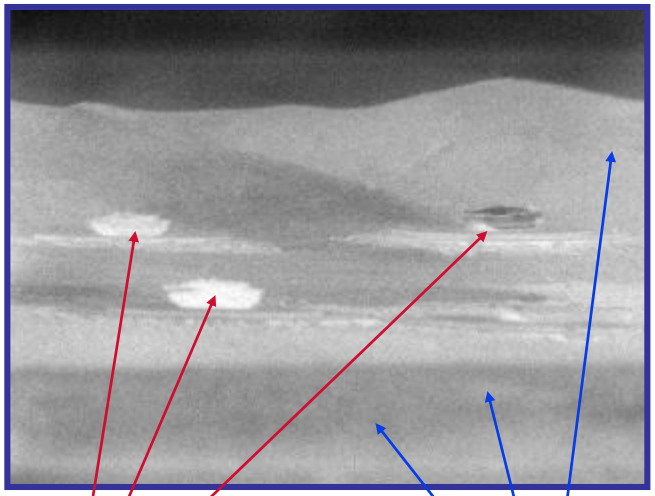

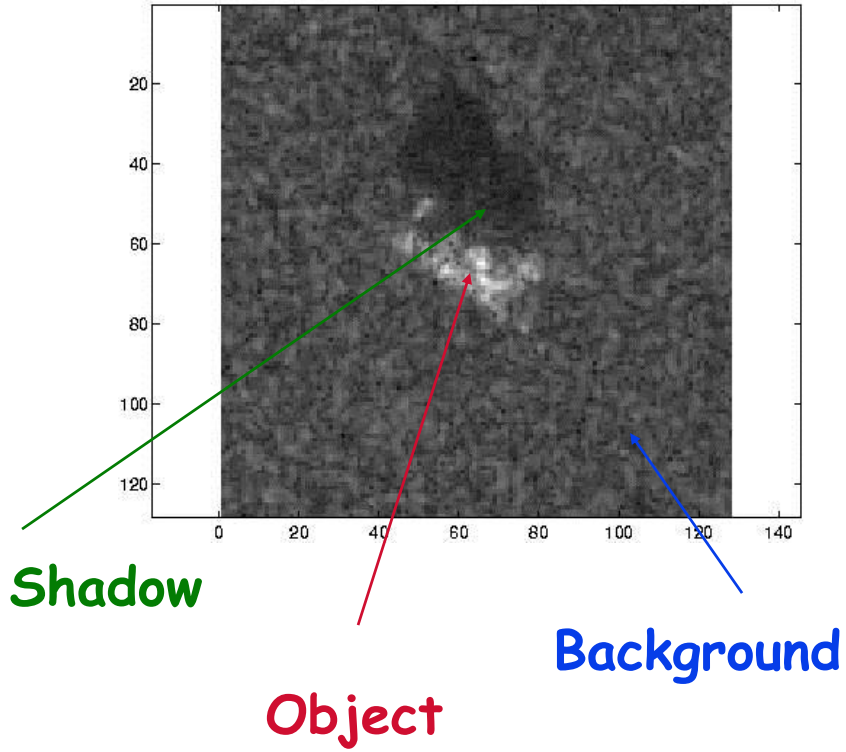

ONLY "TWO CLASSES"

ONLY "THREE CLASSES"

Approach

- Introduce prior information about classes in the image
- Work also with non-additive noise
- Add learning capabilities

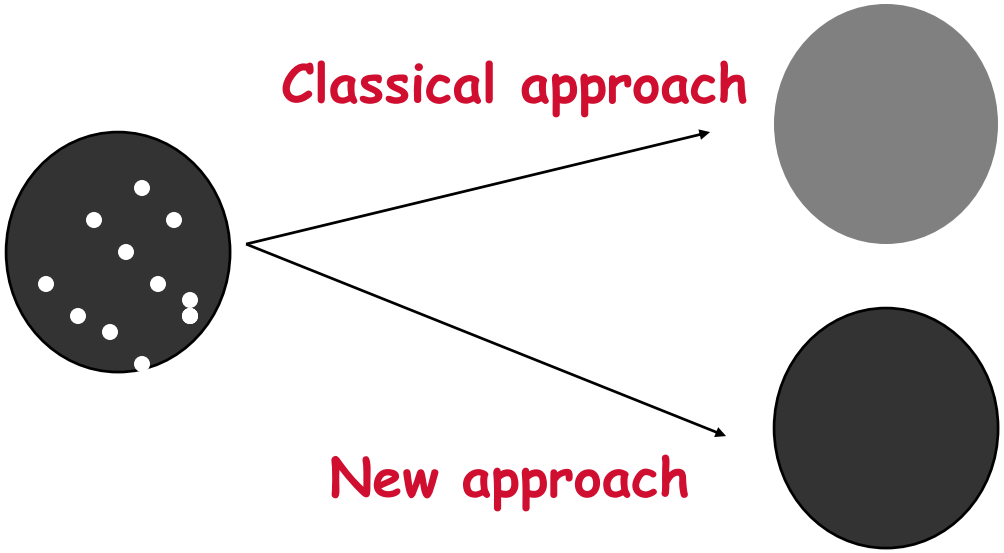

Anisotropic Smoothing of Posterior Probabilities

Posterior Probabilities for each class

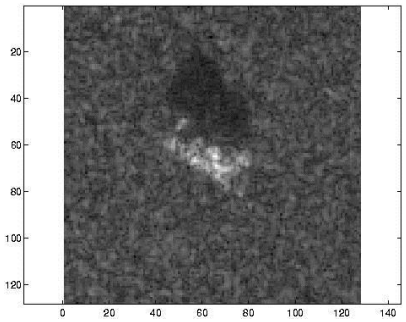

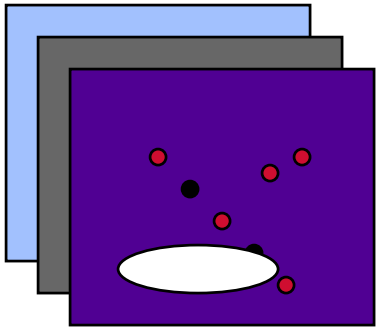

MAP Estimation

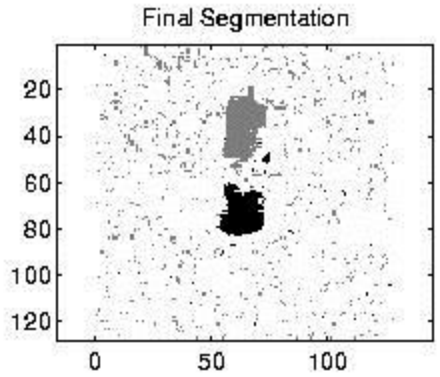

Intensity Image of SAR data

Anisotropic Smoothing

Anisotropically Smoothed **Posterior Probabilities for each class**

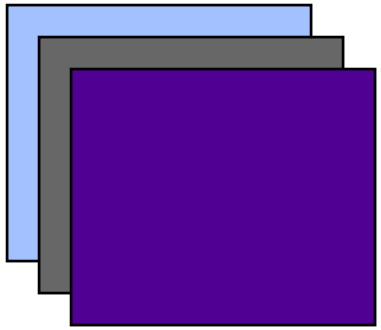

MAP Estimation

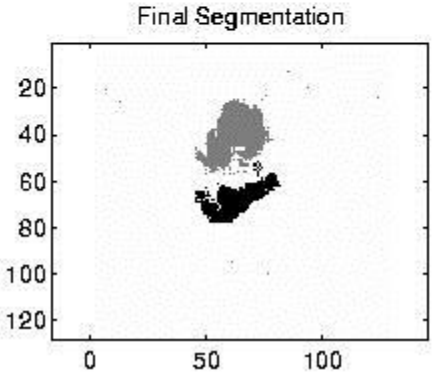

MAP Estimation

- Classes C
- Prior (given) probability: Pr (class=C)
- Posterior probability: Pr(class=C | data)
- *MAP*: Choose class C that maximizes posterior:

$$C^* = \arg\max_C \Pr(\text{class}=C \mid \text{data})$$

- *Bayes' Rule*:

$$\Pr(\text{class}=C \mid \text{data}) = \frac{\Pr(\text{data} \mid \text{class}=C).\Pr(\text{class}=C)}{\Pr(\text{data})}$$

Pr(class=C | data) = Likelihood . Prior Information

Differences with Anisotropic Smoothing of Raw Data

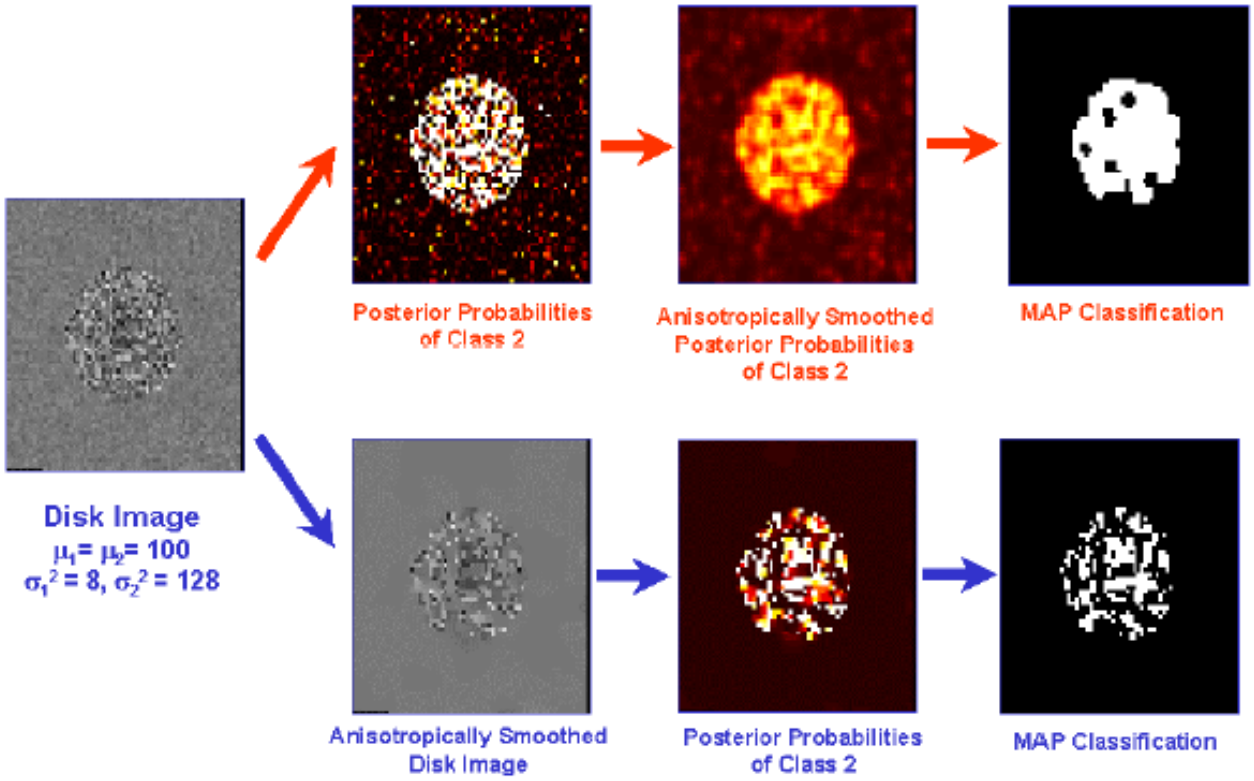

Figure : Toy example of the posterior diffusion algorithm. Two classes of the same average and different standard deviation are present in the image. The first row show the result of our algorithm (posterior, diffusion, MAP), while the second row shows the result of classical techniques (diffusion, posterior, MAP).

Gray-White-Black MR Segmentation-I

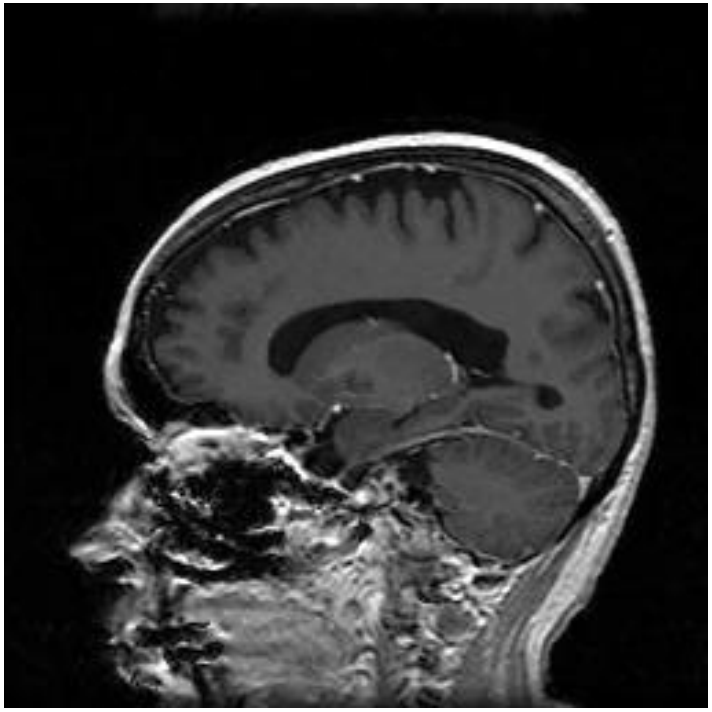

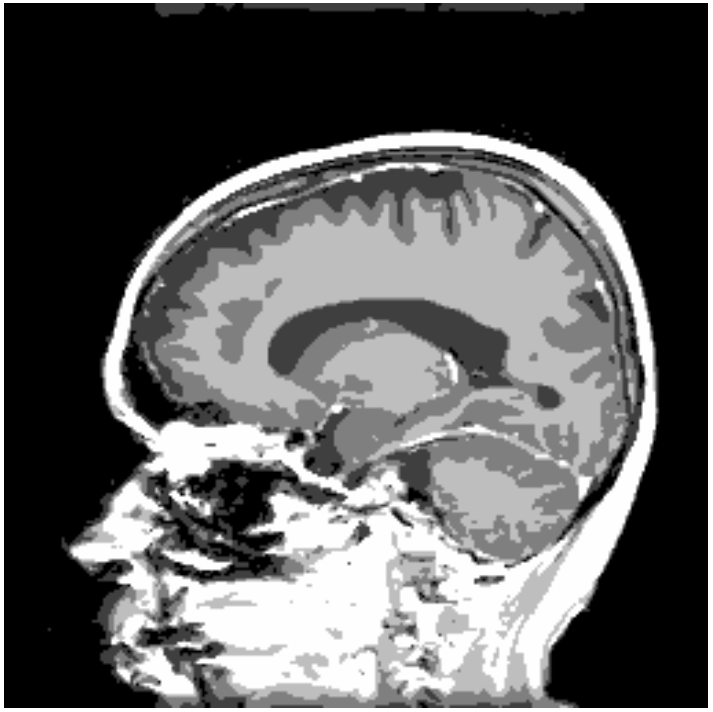

Gray-White-Black MR Segmentation-II

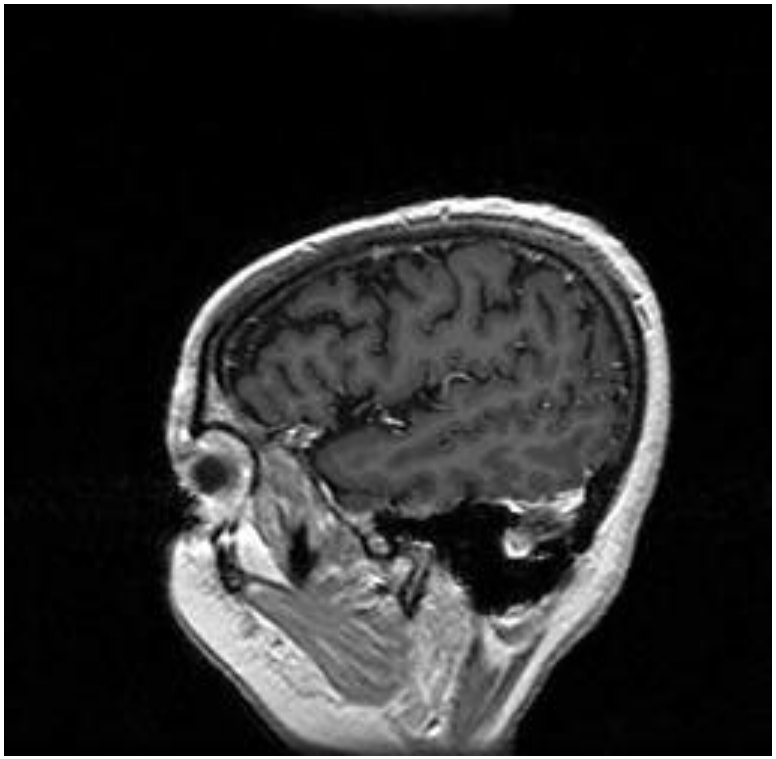

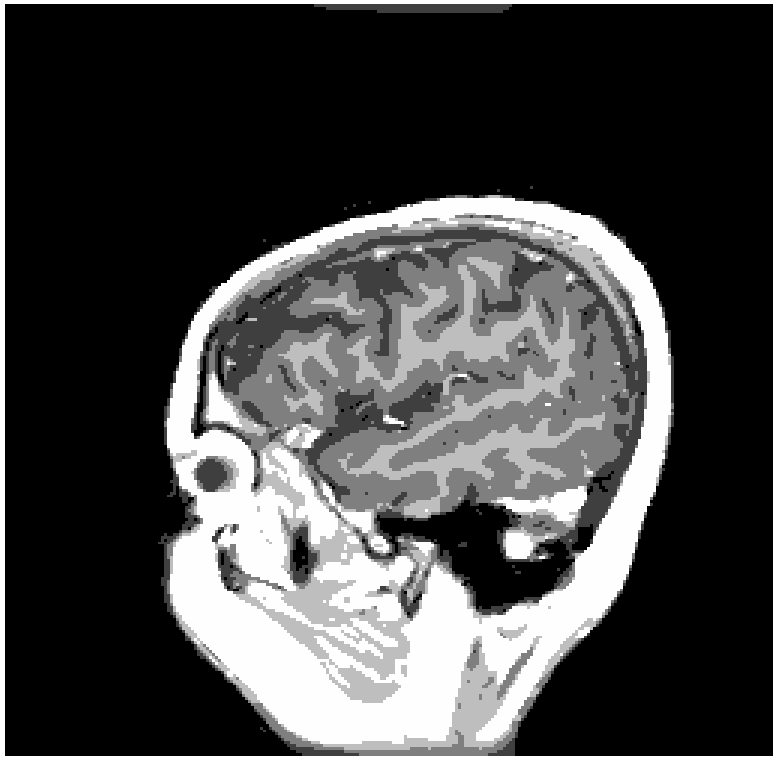

MRF's and Smoothing Posteriors

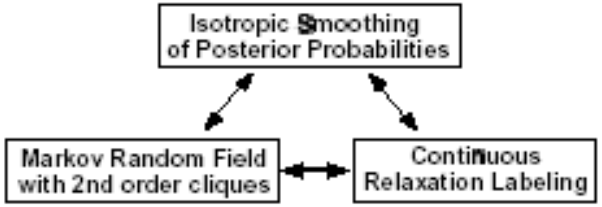

Figure : Equivalence between isotropic smoothing of posterior probabilities, Markov random fields with 2nd order cliques, and continuous relaxation labeling.

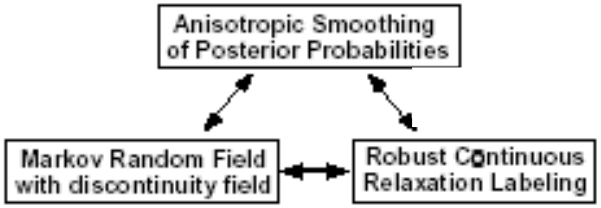

Figure : Equivalence between anisotropic smoothing of posterior probabilities, Markov random fields with discontinuity fields, and robust continuous relaxation labeling.

Maximizing Posterior = Minimizing Energy

MAP Estimation and MRF's in General

We consider degradation model of the form

$$u_o = u + n$$

where *u* is the original image and *n* iid noise process.

MAP estimator is given by :

$$\hat{u} = \arg\max_u \{\log p(u_o|u) + \log p(u)\}$$

μ

MRF is given by Gibbs distribution:

$$p(u) = 1/Z \exp\{\frac{-F(u)}{\lambda}\}$$

Under our assumptions

$$p(u_o|u) = K \exp\{-\frac{|u_o - u|^2}{2\sigma^2}\}$$

and so

$$\hat{u} = \arg\min_u \{F(u) + \lambda/2|u - u_0|^2\}$$

Markov Random Field Theory-I

Spatial properties can be modelled through different aspects, among which, the *contextual constraint* is a general and powerful one. Markov random field (MRF) theory provides a convenient and consistent way to model context-dependent entities such as image pixels and correlated features. This is achieved by characterizing mutual influences among such entities using conditional MRF distributions. In an MRF, the sites in S are related to one another via a *neighborhood system*, which is defined as

$$\mathcal{N} = \{\mathcal{N}_i, i \in S\}$$

where $\mathcal{N}_i$ is the set of sites neighboring i, $i \notin \mathcal{N}_i$ and $i \in \mathcal{N}_j \iff j \in \mathcal{N}_i$. A random field $\boldsymbol{X}$ said to be an MRF on S with respect to a neighborhood system $\mathcal{N}$ if and only if

$$P(\mathbf{x}) > 0, \forall \mathbf{x} \in \mathcal{X}$$

$$P(x_i | x_{S-\{i\}}) = P(x_i | x_{\mathcal{N}_i})$$

Note, the neighborhood system can be multi-dimensional.

Markov Random Field Theory-II

According to the Hammersley-Clifford theorem, an MRF can equivalently be characterized by a Gibbs distribution. Thus,

$$P(x) = Z^{-1} \exp(-U(x))$$

where

$$Z = \sum_{x \in \mathcal{X}} \exp(-U(x))$$

is a normalizing constant called the *partition function*, and $U(x)$ is an *energy function* of the form

$$U(x) = \sum_{c \in \mathcal{C}} V_c(x),$$

which is a sum of *clique potentials* $V_c(x)$ over all possible cliques $\mathcal{C}$. A *clique* c is defined as a subset of sites in $\mathcal{S}$ in which every pair of distinct sites are neighbors, except for single-site cliques. The value of $V_c(x)$ depends on the local configuration on clique c.

Specialization to Images

We specialize our notation to MRF's defined on image grids. Let $\mathcal{S} = \{1, \ldots, n\}$ be a set of sites where each $s \in \mathcal{S}$ corresponds to a single pixel in the image. For simplicity, we assume that each site can take on labels from a common set $\mathcal{L} = \{1, \ldots, k\}$. Adjacency relationships between sites are encoded by $\mathcal{N} = \{\mathcal{N}_i | i \in \mathcal{S}\}$ where $\mathcal{N}_i$ is the set of sites neighboring site i. Cliques are then defined as subsets of sites so that any pair of sites in a clique are neighbors. In this paper, we will only consider 4-neighbor adjacency for images (and 8-neighbor adjacency for volumes) and cliques of sizes no greater than two. By considering each site as a discrete random variable f_i with a probability mass function over $\mathcal{L}$, a discrete MRF $\mathbf{f}$ can be defined over the sites with a Gibbs probability distribution.

If data $d_i \in \mathbf{d}$ is observed at each site i, and is dependent only on its label f_i, then the posterior probability is itself a Gibbs distribution and by the Hammersley-Clifford theorem, also a MRF, albeit a different one [6]: $P(\mathbf{f}|\mathbf{d}) = Z^{-1} \times \exp\{-E(\mathbf{f}|\mathbf{d})\}$ where

$$E(\mathbf{f}|\mathbf{d}) = \sum_{i \in \mathcal{C}_1} V_1(f_i|d_i) + \sum_{(i,j) \in \mathcal{C}_2} V_2(f_i, f_j) \tag{5}$$

where $V_1(f_i|d_i)$ is a combination of the single site clique potential and the independent likelihood and $V_2(f_i, f_j)$ is the pairwise-site clique potential. The notation (i, j) refers to a pair of sites; thus, the sum is actually a double sum. Maximizing the posterior probability $P(\mathbf{f}|\mathbf{d})$ is equivalent to minimizing the energy $E(\mathbf{f}|\mathbf{d})$.

Continuous Relaxation Labelling

Continuous Relaxation Labeling. The continuous relaxation labeling approach to solving this problem was introduced by Li *et. al.* [11]. In CRL, the class (label) of each site i is represented by a vector $p_i = [p_i(f_i)|f_i \in \mathcal{L}]$ subject to the constraints: (1) $p_i(f_i) \geq 0$ for all $f_i \in \mathcal{L}$, and (2) $\sum_{f_i \in \mathcal{L}} p_i(f_i) = 1$. Within this framework, the energy $E(\mathbf{f}|\mathbf{d})$ to be minimized is rewritten as

$$E(\mathbf{p}|\mathbf{d}) = \sum_{i \in \mathcal{C}_1} \sum_{f_i \in \mathcal{L}} V_1(f_i|d_i) p_i(f_i) + \sum_{(i,j) \in \mathcal{C}_2} \sum_{(f_i, f_j) \in \mathcal{L}^2} V_2(f_i, f_j) p_i(f_i) p_j(f_j). \tag{7}$$

Note that when $p_i(f_i)$ is restricted to $\{0, 1\}$, $E(\mathbf{p}|\mathbf{d})$ reverts to its original counterpart $E(\mathbf{f}|\mathbf{d})$. Hence, CRL embeds the actual combinatorial problem into a larger, continuous, constrained minimization problem.

The constrained minimization problem is typically solved by iterating two steps: (1) gradient computation, and (2) normalization and update. The first step decides the direction that decreases the objective function while the second updates the current estimate while ensuring compliance with the constraints. A review of the normalization techniques that have been proposed are summarized in [11]. Ignoring the need for normalization, continuous relaxation labeling is similar to traditional gradient descent: $p_i^{t+1}(f_i) \leftarrow p_i^t(f_i) - \frac{\partial E(\mathbf{p}|\mathbf{d})}{\partial p_i^t(f_i)}$ where

$$\frac{\partial E(\mathbf{p}|\mathbf{d})}{\partial p_i^t(f_i)} \doteq V_1(f_i|d_i) + 2 \sum_{j:(i,j) \in \mathcal{C}_2} \sum_{f_j \in \mathcal{L}} V_2(f_i, f_j) p_j^t(f_j). \tag{8}$$

Isotropic Smoothing

Isotropic Smoothing. A convenient way of visualizing the above operation is as isotropic smoothing. Since the sites represent pixels in an image, for each class

f_i, $p_i(f_i)$ can be represented by an image (of posterior probabilities) such that k classes imply k such image planes. Together, these k planes form a volume of posterior probabilities. Each step of Eqn. 8 then essentially replaces the current estimate $p_i^t(f_i)$ with a weighted average of the neighboring assignment probabilities $p_j^t(f_j)$. In other words, the volume of posterior probabilities is linearly *filtered*. If the potential functions $V_2(f_i, f_j)$ favor similar labels, then the weighted average is essentially low-pass among sites with common labels and hi-pass among sites with differing labels.

MRF: Non-Interacting Discontinuity Fields

We extend the original MRF problem to include a non-interacting, analog discontinuity field on a displaced lattice. Thus, the new energy to be minimized is:

$$E(\mathbf{f},\mathbf{l}) = \sum_{(i,j)\in\mathcal{C}_2} \left[\frac{1}{2\sigma^2} V_2(f_i,f_j)\cdot l_{i,j} + (l_{i,j} - 1 - \log l_{i,j})\right] \tag{9}$$

where $V_1(f_i)$ has been dropped for simplicity since the discontinuity field does not interact with it. The individual sites in the discontinuity field $\mathbf{l}$ are denoted by $l_{i,j}$ which represent either the horizontal or vertical separation between sites i and j in $\mathcal{S}$. When $l_{i,j}$ is small, indicating the presence of a discontinuity, the effect of the potential $V_2(f_i,f_j)$ is suspended; meanwhile, the energy is penalized by the second term in Eqn. 9. There are a variety of penalty functions that could be derived from the robust estimation framework (see [3]). The penalty function in Eqn. 9 was derived from the Lorentzian robust estimator.

The minimization of $E(\mathbf{f},\mathbf{l})$ is now over both $\mathbf{f}$ and $\mathbf{l}$. Since the discontinuity field is non-interacting, $\mathbf{l}$ can be minimized analytically by computing the partial derivatives of $E(\mathbf{f},\mathbf{l})$ with respect to $l_{i,j}$ and setting that to zero. Doing so and inserting the result back into $E(\mathbf{f},\mathbf{l})$ gives us

$$E(\mathbf{f}) = \sum_{(i,j)\in\mathcal{C}_2} \log\left[1 + \frac{1}{2\sigma^2} V_2(f_i,f_j)\right]. \tag{10}$$

Rewriting this equation in a form suitable for CRL, we get

$$E(\mathbf{p}) = \sum_{(i,j)\in\mathcal{C}_2} \log\left[1 + \frac{1}{2\sigma^2} \sum_{(f_i,f_j)\in\mathcal{L}^2} V_2(f_i,f_j) p_i(f_i) p_j(f_j)\right]. \tag{11}$$

Note that when $p_i(f_i)$ is restricted to $\{0,1\}$, Eqn. 6 reduces to Eqn. 5.

Anisotropic Smoothing

Anisotropic Smoothing. To compute the update equation for CRL, we take the derivative of $E(\mathbf{p})$ with respect to $p_i(f_i)$:

$$\frac{\partial E(\mathbf{p})}{\partial p_i(f_i)} \doteq \sum_{j:(i,j)\in\mathcal{C}_2} w_{i,j} \left[\sum_{f_j\in\mathcal{L}} V_2(f_i, f_j) p_j(f_j) \right] \tag{12}$$

where

$$w_{i,j} = 2\sigma^2 / \left[2\sigma^2 + \sum_{(f_i,f_j)\in\mathcal{L}^2} V_2(f_i, f_j) p_i(f_i) p_j(f_j) \right]. \tag{13}$$

The term $w_{i,j}$ encodes the presence of a discontinuity. If $w_{i,j}$ is constant, then the above equation reverts to the isotropic case. Otherwise, $w_{i,j}$ either enables or disables the penalty function $V_2(f_i, f_j)$. This equation is similar to the anisotropic diffusion equation proposed by Perona and Malik [12].

However, image difference between sites i and j in Perona and Malik's equation is, in our case, replaced by a discrete version: $\sum_{f_j\in\mathcal{L}} V_2(f_i, f_j) p_j(f_j)$. The stopping term $w_{i,j}$ is also the same except that the magnitude of the image gradient is again replaced by a discrete counterpart.

Robust CRL

Robust Continuous Relaxation Labeling. Each iteration of continuous relaxation labeling can be viewed as a consensus-taking process [15]. Neighboring pixels vote on the classification of a central pixel based on their current assignment probabilities $p_j(f_j)$, and their votes are tallied using a weighted sum. The weights used are the same throughout the image; thus, pixels on one side of a region boundary may erroneously vote for pixels on the other side. Anisotropic smoothing of the posterior probabilities can be regarded as implementing a robust voting scheme since votes are tempered by $w_{i,j}$ which estimates the presence of a discontinuity. The connection between anisotropic diffusion on continuous-valued images and robust estimation was recently demonstrated by Black *et. al.* [4].

Isotropic vs. Anisotropic MAP

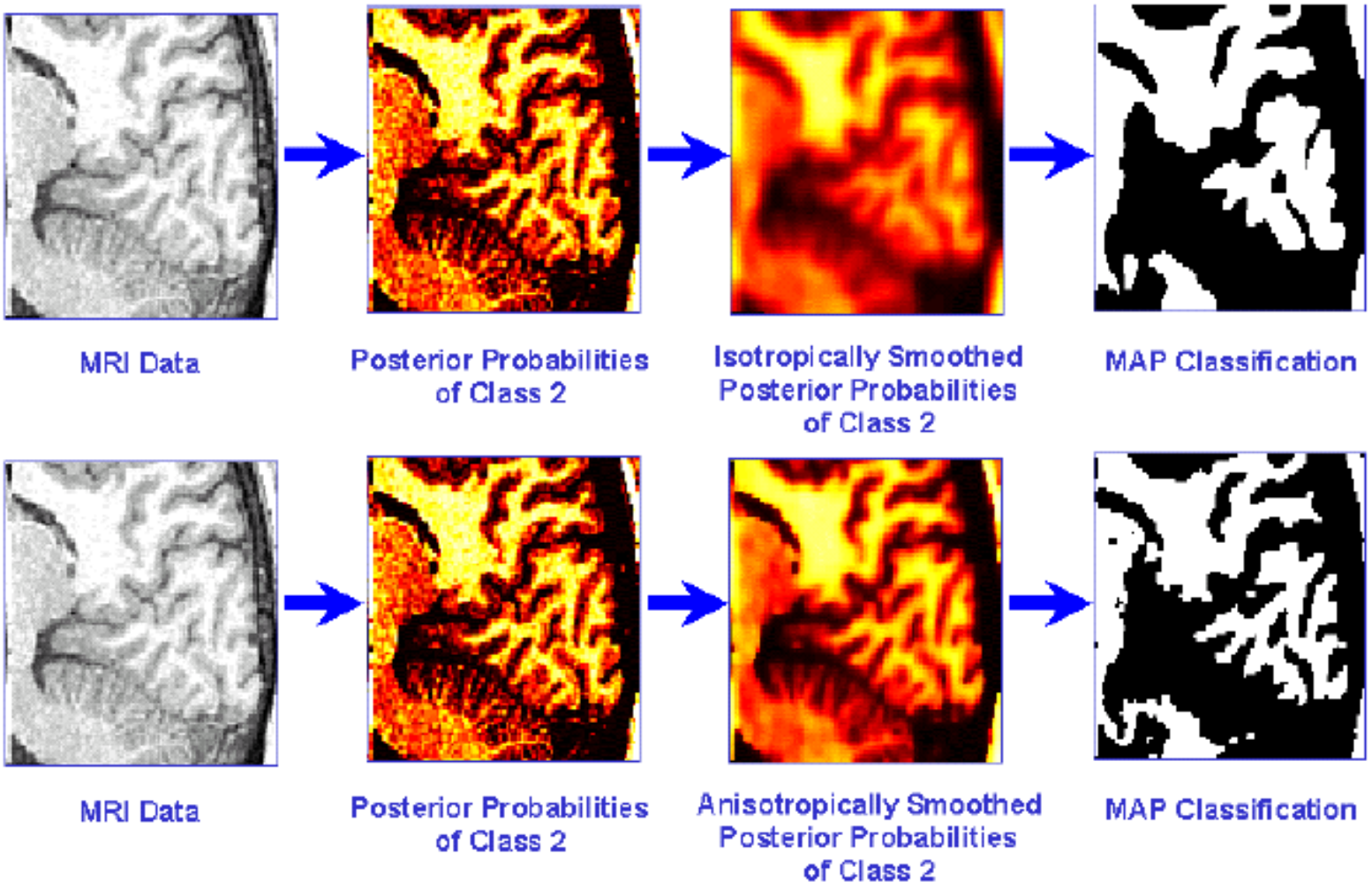

White Matter: Diffusion Tensor Imaging-I

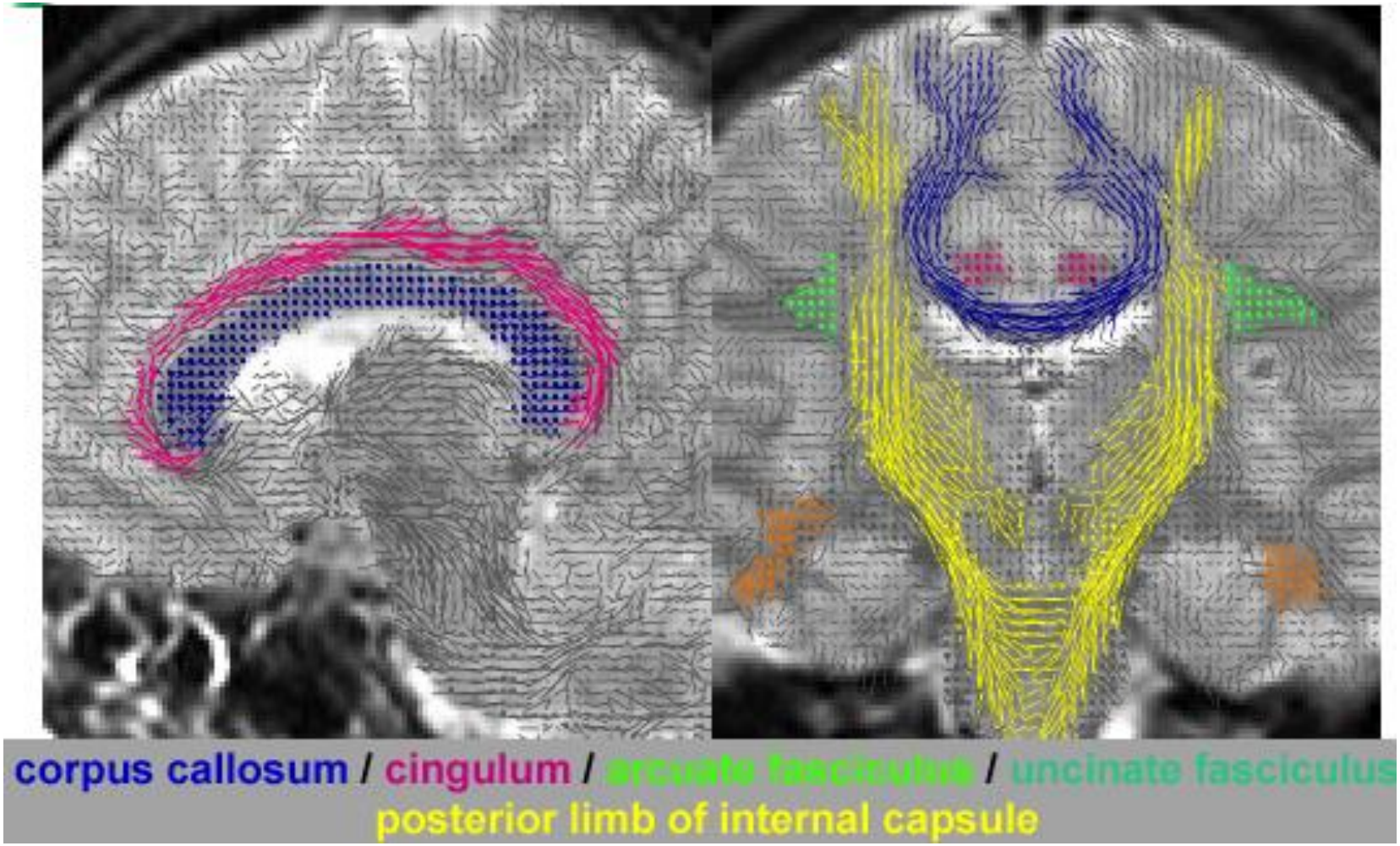

Diffusion Tensor Imaging-II

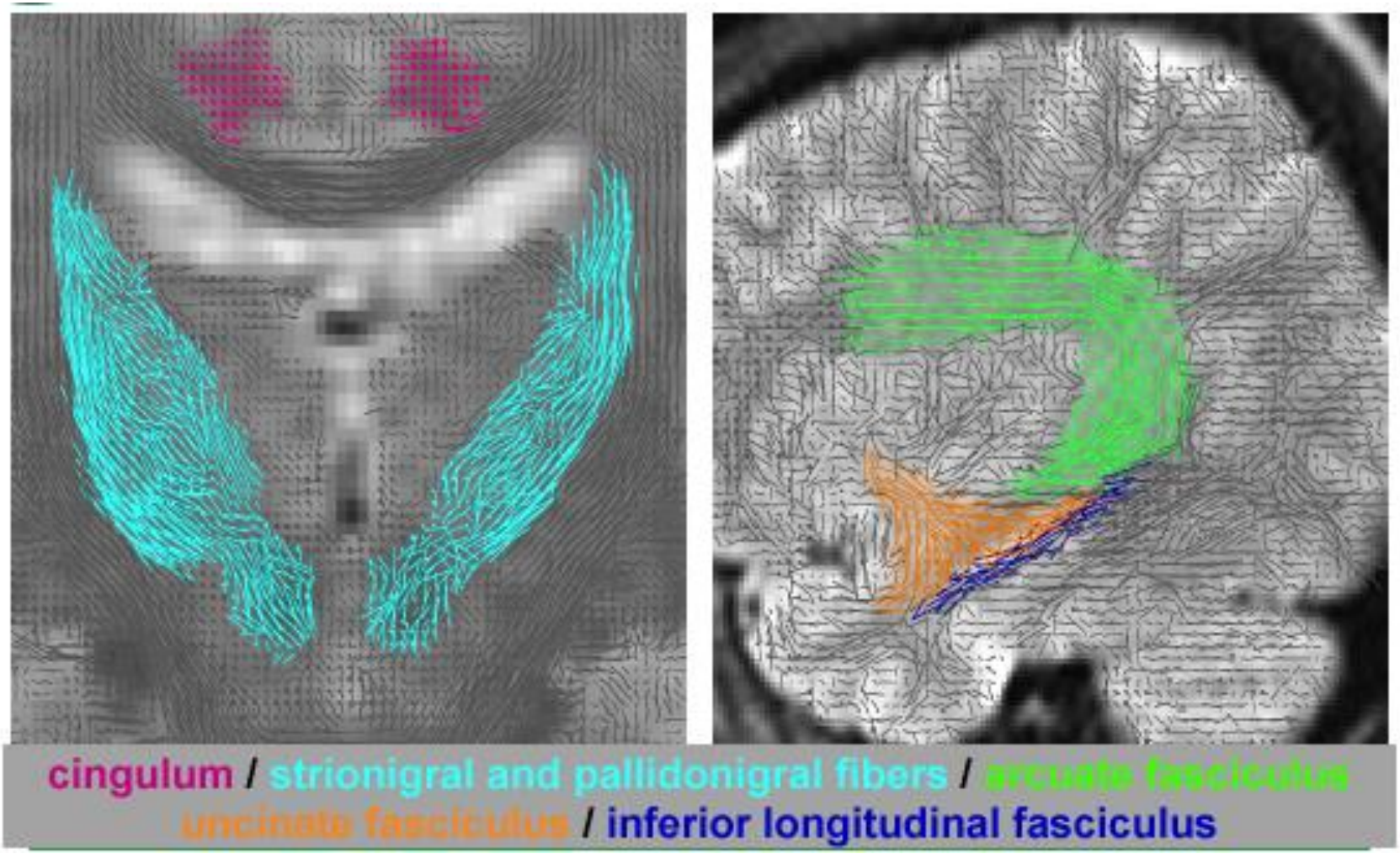

Diffusion Tensor Imaging-III

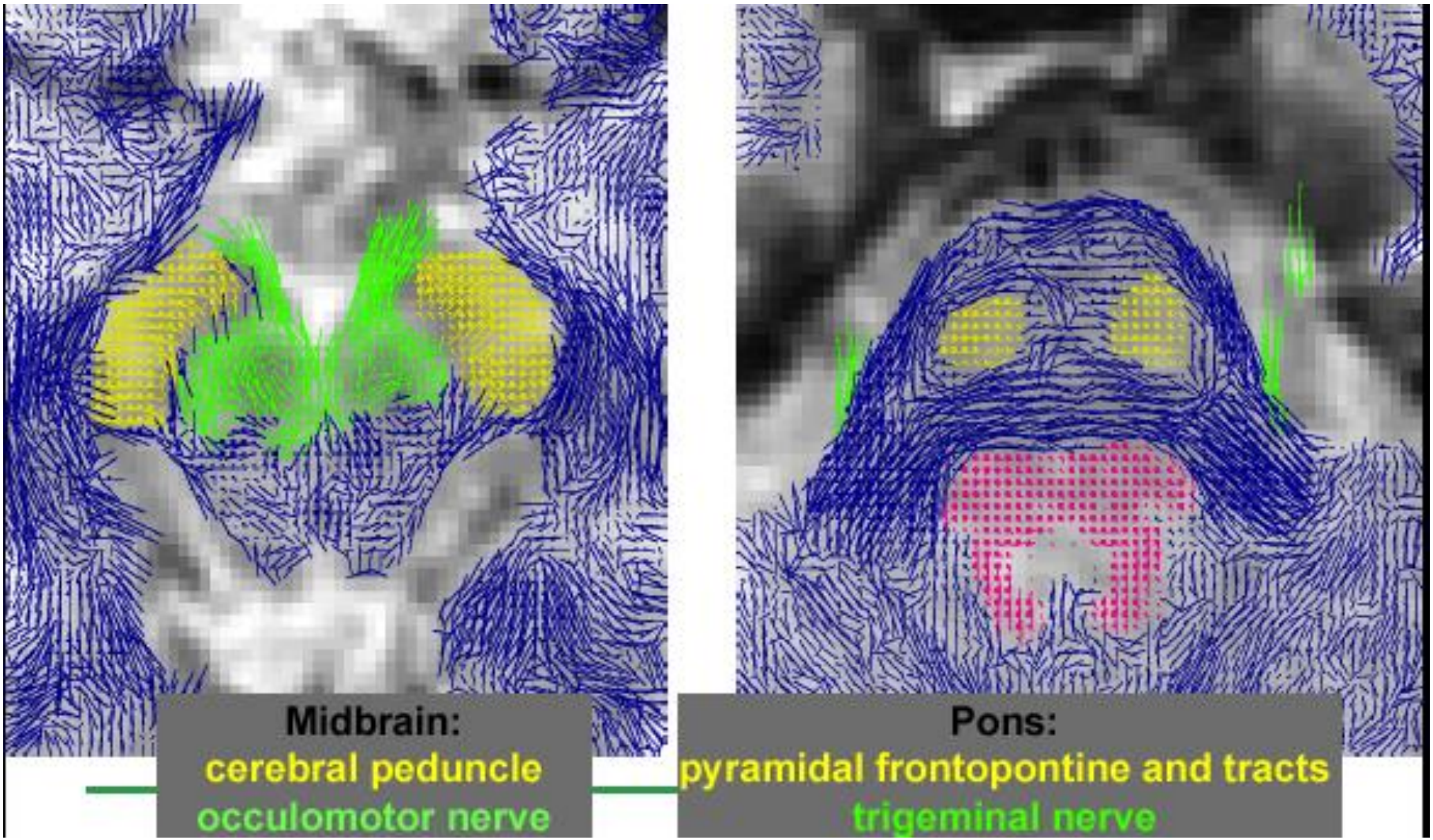

Diffusion Tensor Imaging-IV

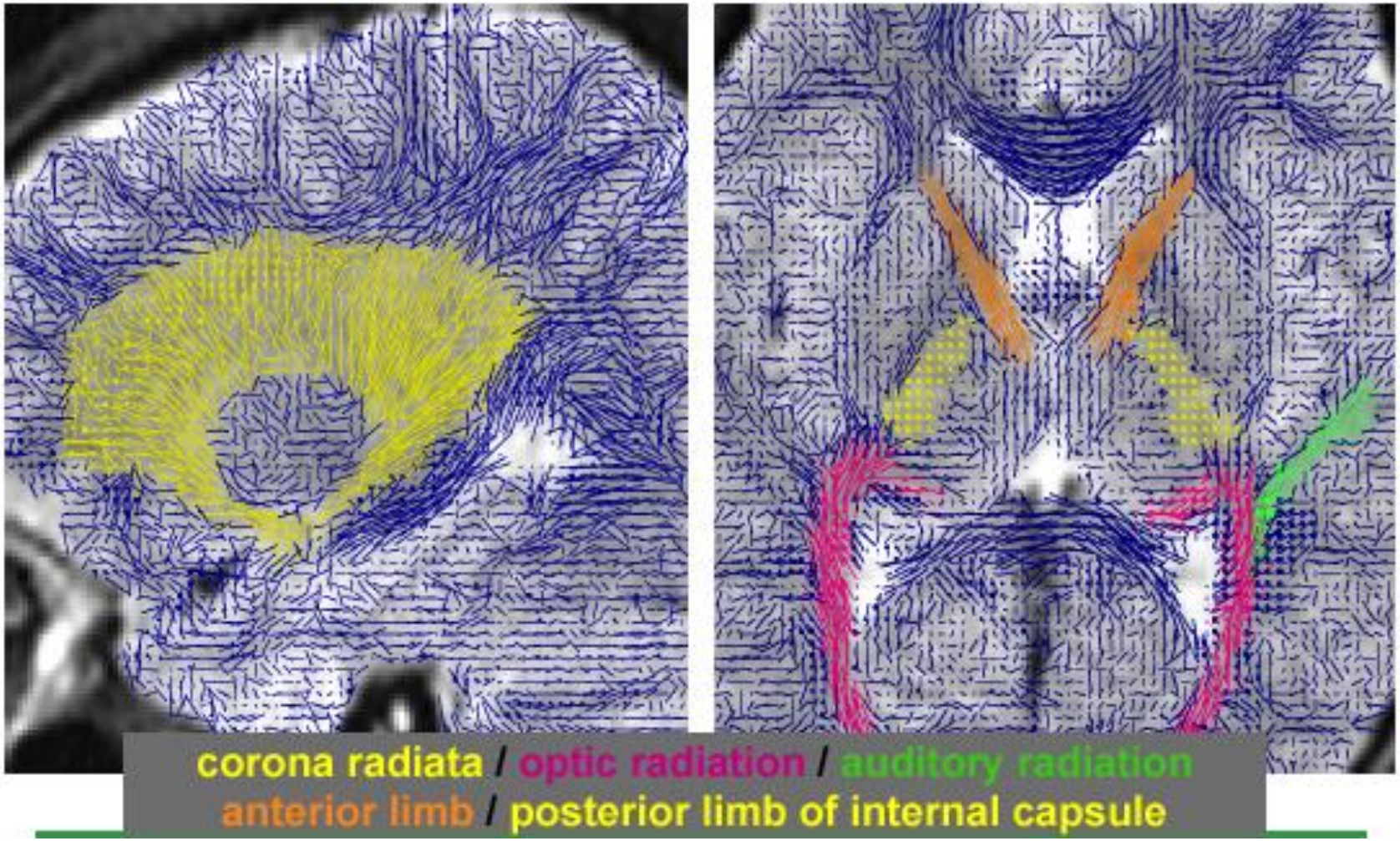

White Matter

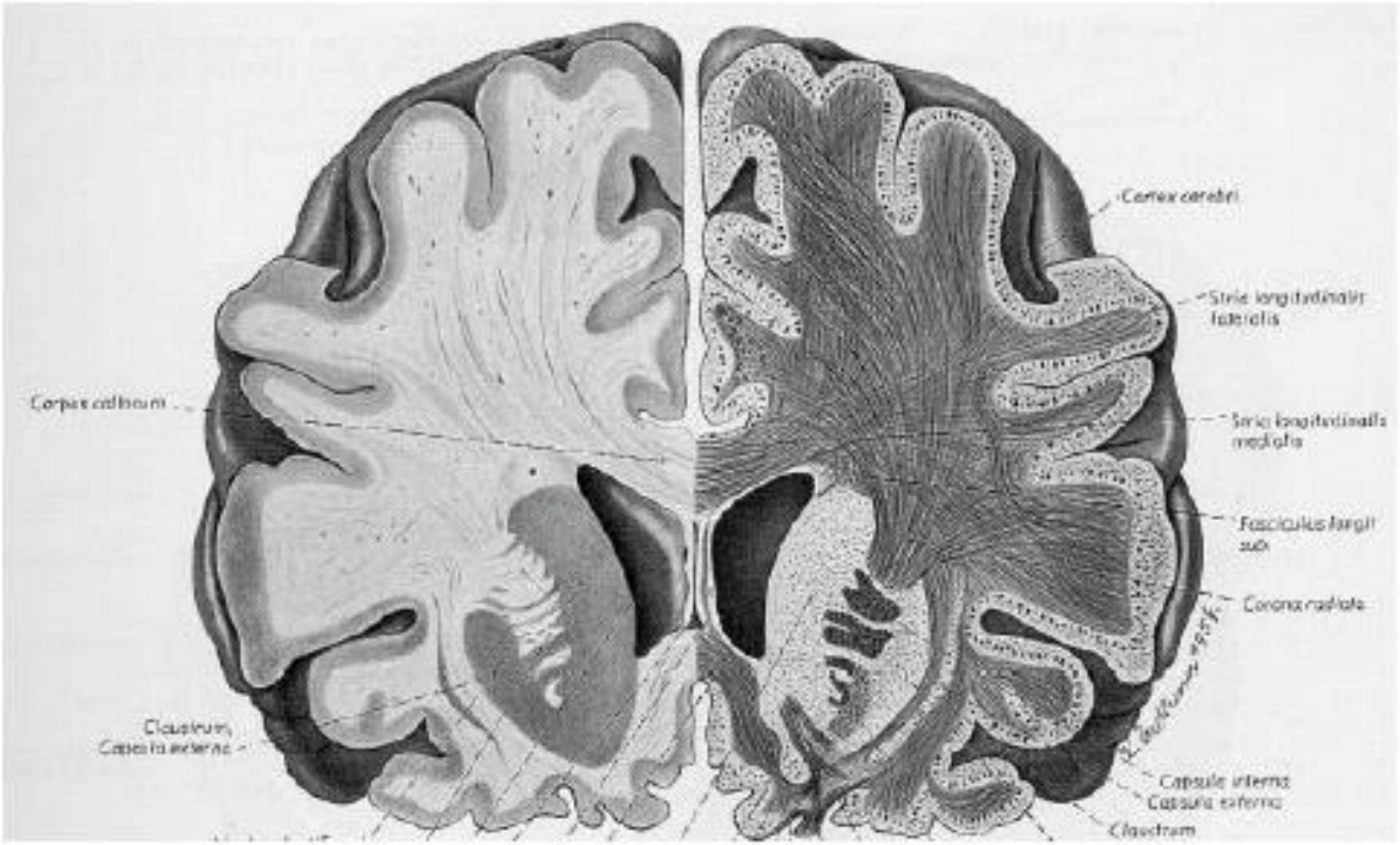

DT-MRI Tractography

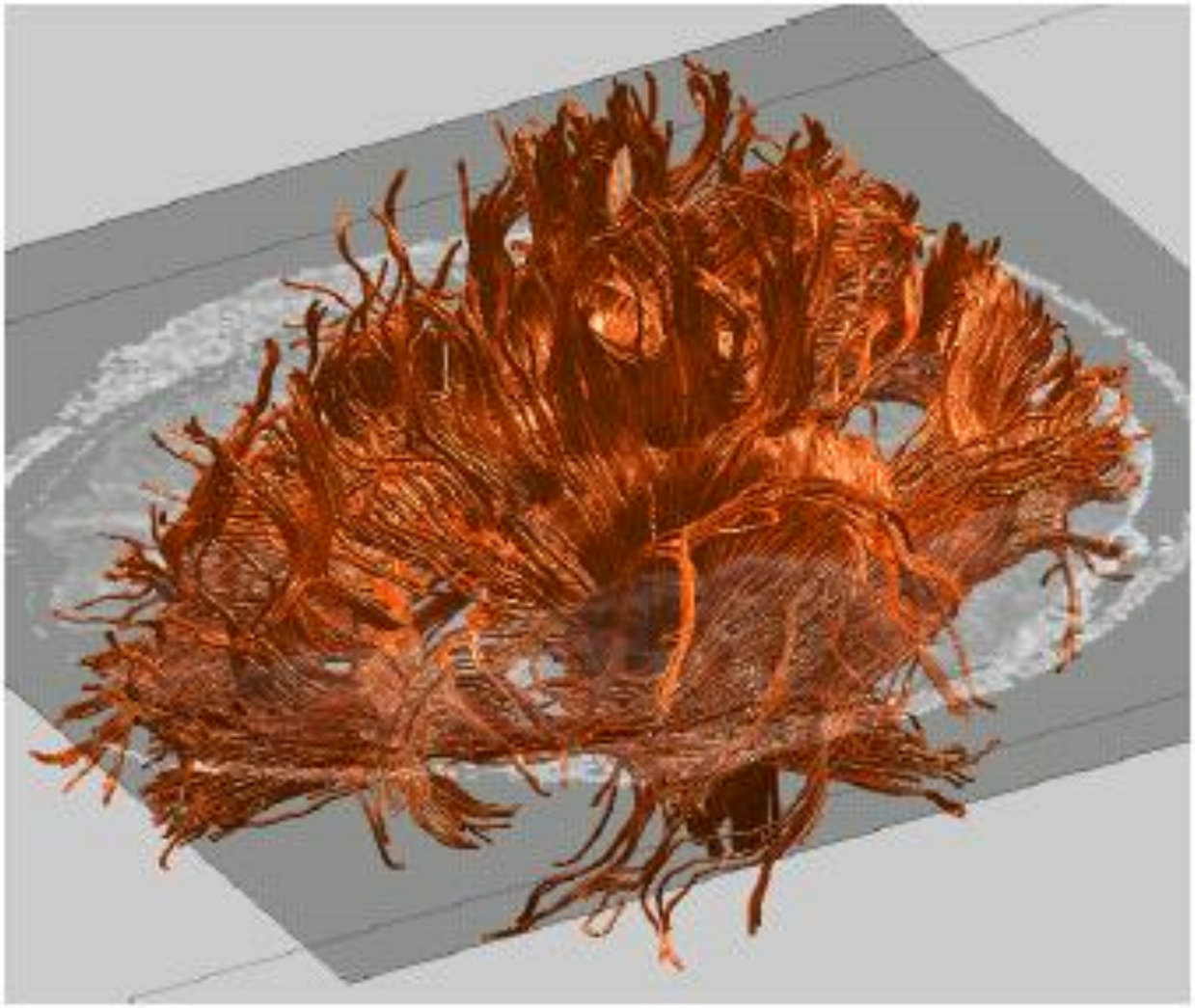

Distance-Based Connectivity

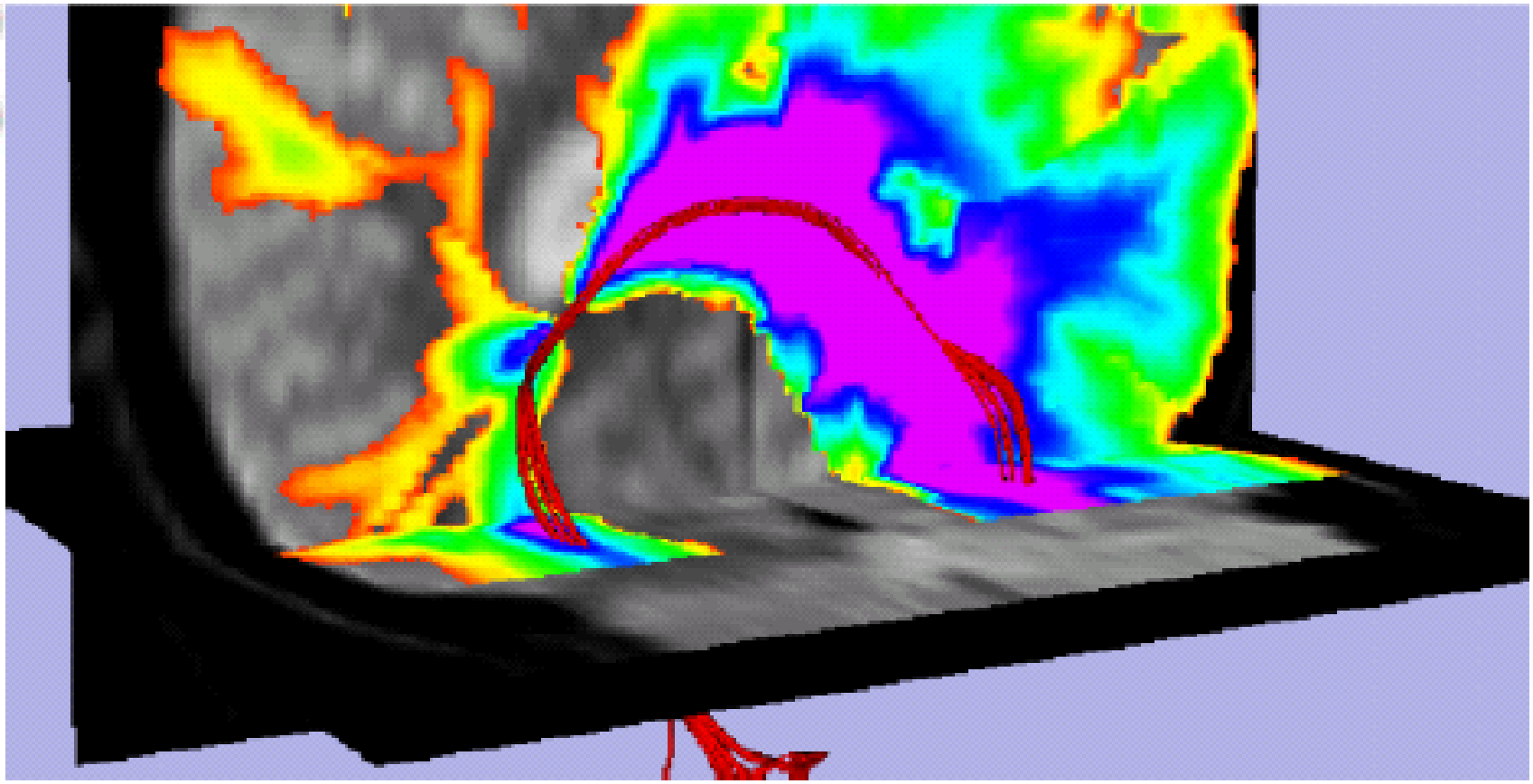

- Traditional DT-tractography is "one to one"
- Distance based connectivity an efficient way of calculating "one to many"

Anisotropic Heat Modelling

Anisotropic heat modelling attractive concept when working with regions (gray matter structure, fMRI activations)

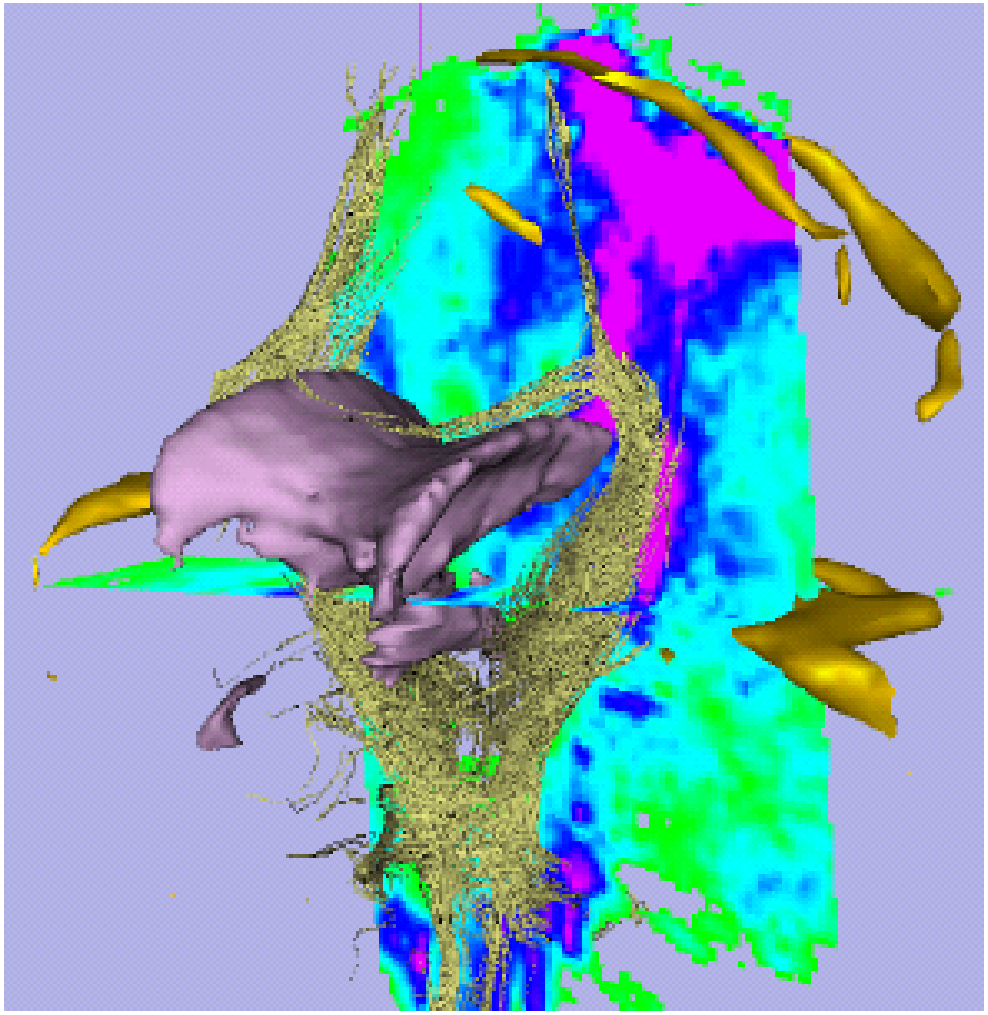

Merging BWH and MGH information: Cortical thickness from FreeSurfer (MGH) and DT-MRI Tractorgraphy in 3D Slicer

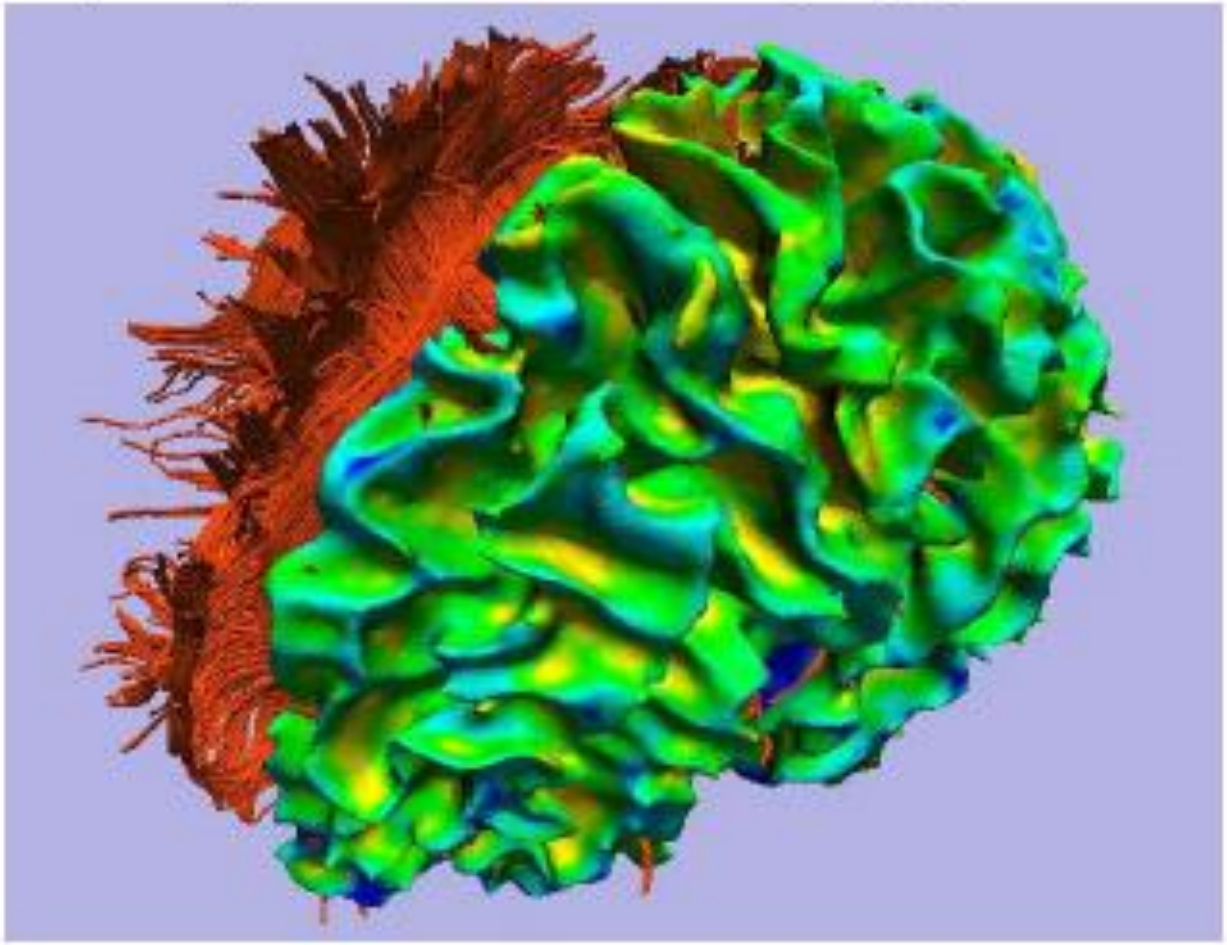

DT-MRI Registration - Atlas

One brain

Average of 10 brains

Fiber Bundle Color Coding

Laplacian Eigenmaps:
Map the three smoothest eigenvectors to colors Red,Green, and Blue

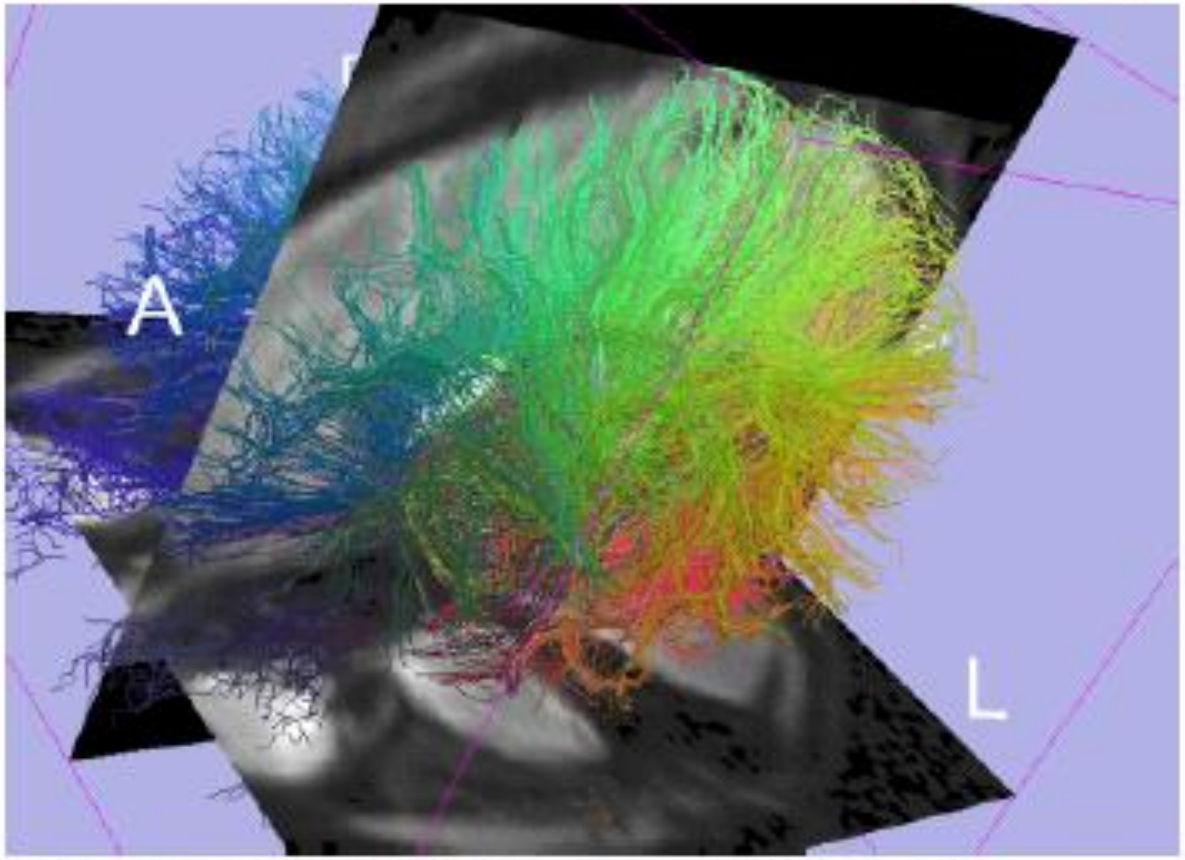

The Laplacian of the graph obtained from the points approximates the Laplace-Beltrami operator defined on the manifold providing "optimal embedding" in the lower dimensional space.

Brain Atlas

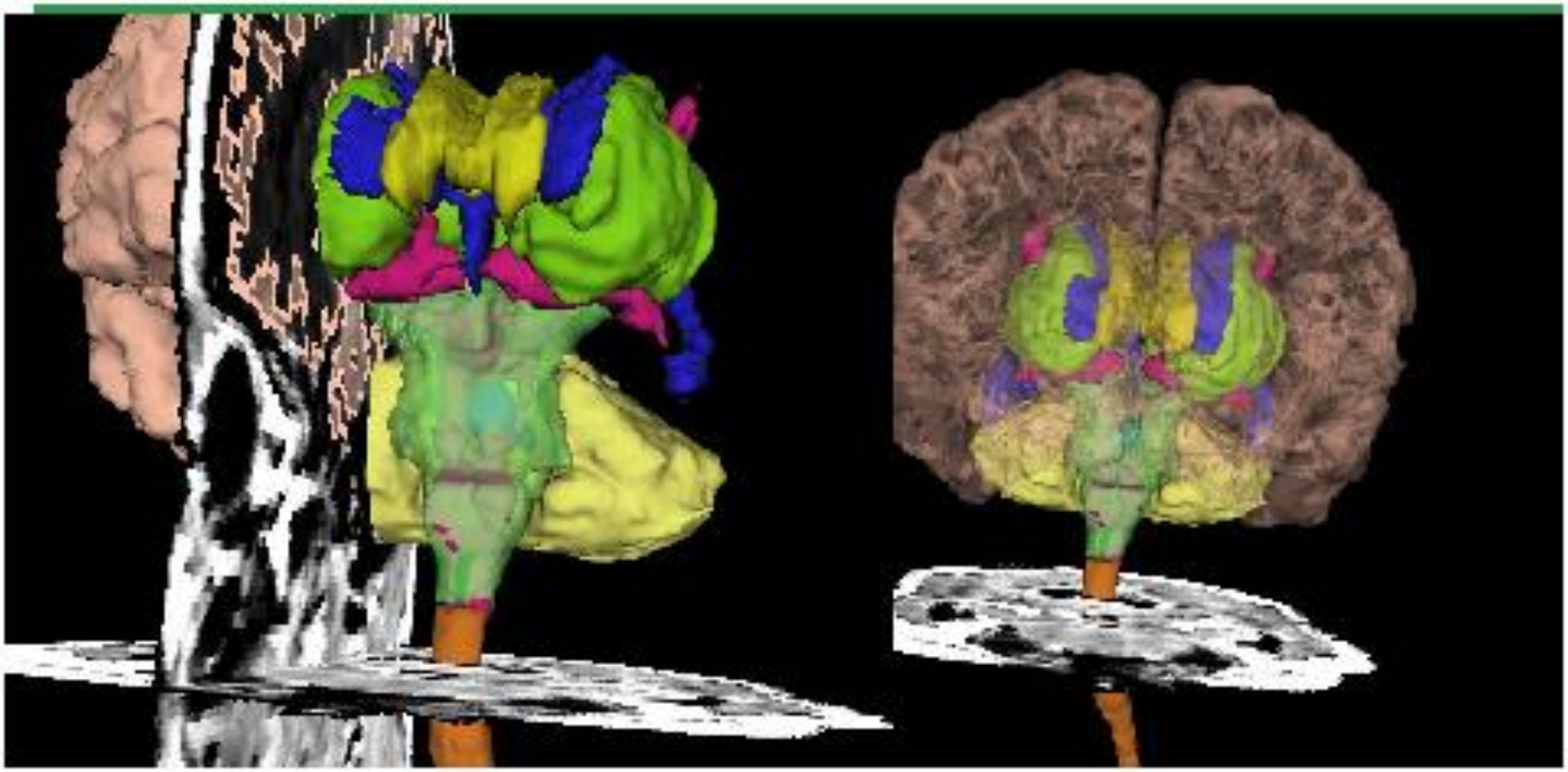

fMRI and DTI for IGS

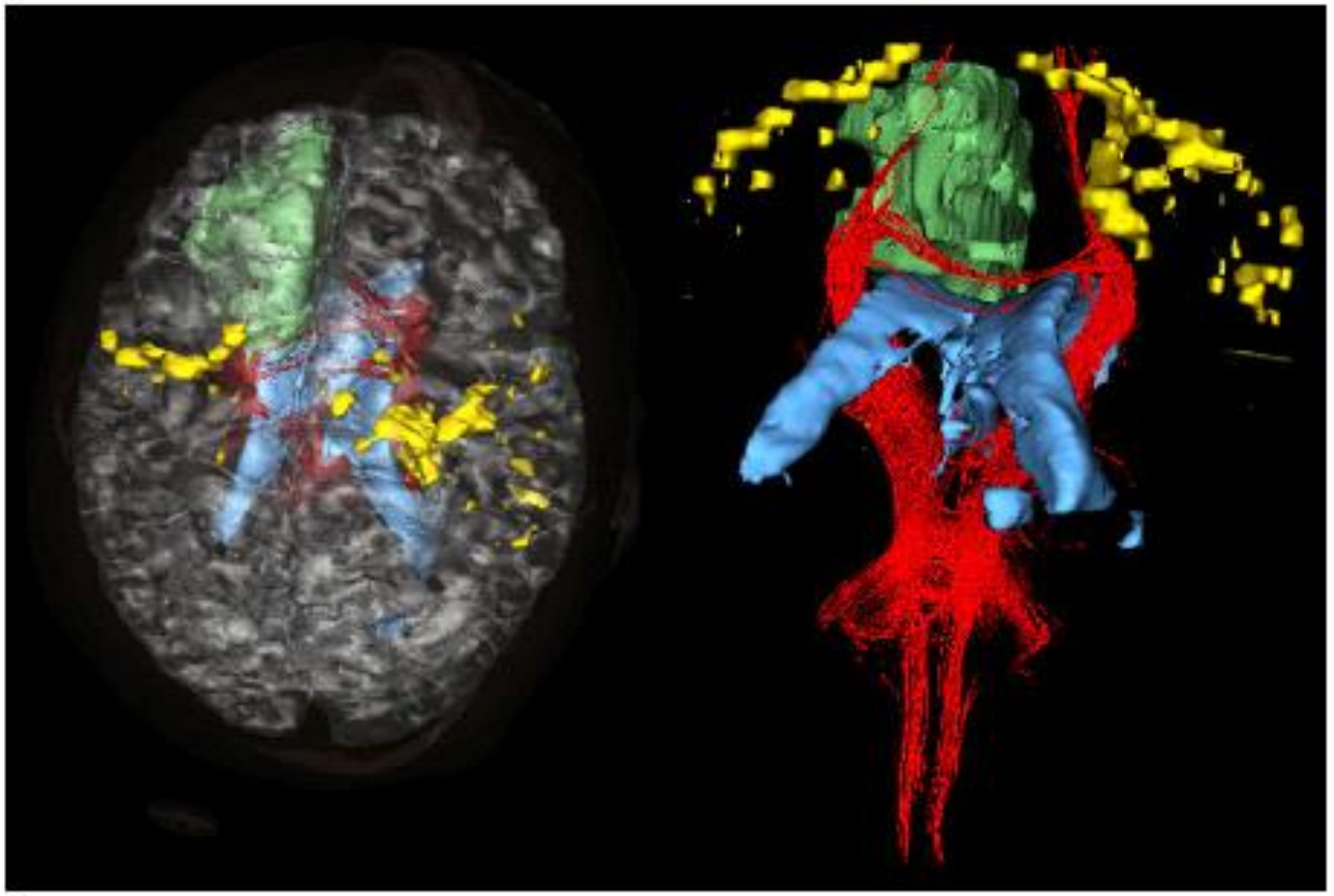

Figure 8.4.6-1. Retrospective Example of fMRI for Neurosurgical Application
62-year-old female patient with left frontal hyperintense non-enhancing mass lesion
Skin, Brain, Ventricles (blue) and Tumor (green) models from conventional MRI; fMRI activations (yellow) from pre-operative finger-taping experiment. Fiber tract indications (red) from Diffusion Tensor MRI.
Imaging suggests that the tumor is in front of motor strip with involvement of supplementary motor area, with fibers from SMA piercing tumor in its posterior aspect.

Data Fusion

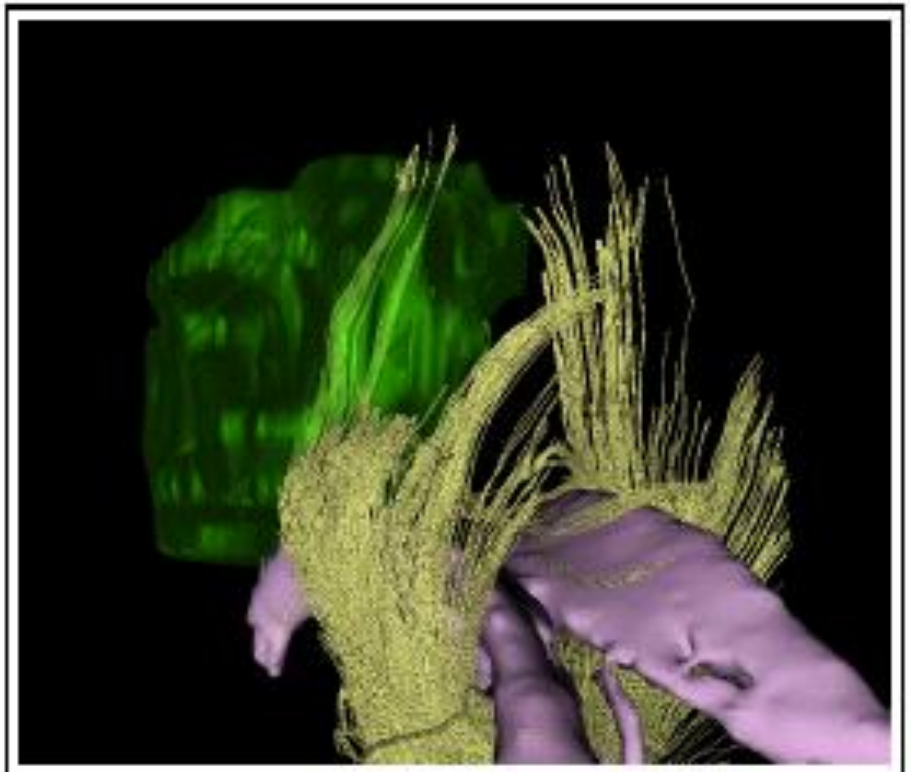

Figure 8.4.3-4. Results from DT-MRI tractography
Tractography results in the cortico-spinal tract are shown in gold. Note that some of the tract is passing through the tumor (green).

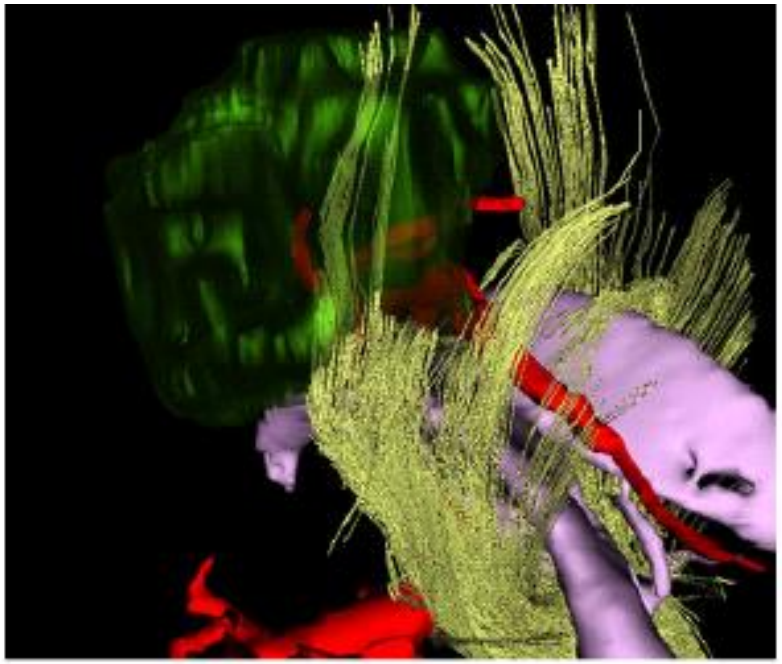

Figure 8.4.4-4. Case 1
Left postero-lateral view of a three-dimensional reconstruction of the tumor (transparent green), lateral ventricles (pink), cerebral arteries (red) and white matter tracts adjacent to the tumor (yellow) in the same case as in Figures 2 and 3. A 3D-SPGR dataset was used for the tumor and ventricle reconstruction and MR angiography was used to create the vessel 3D-model. The same line scan diffusion dataset as in Figure 8.4.4-3 was used for the three-dimensional reconstruction of the fiber tracts.

More Data Fusion

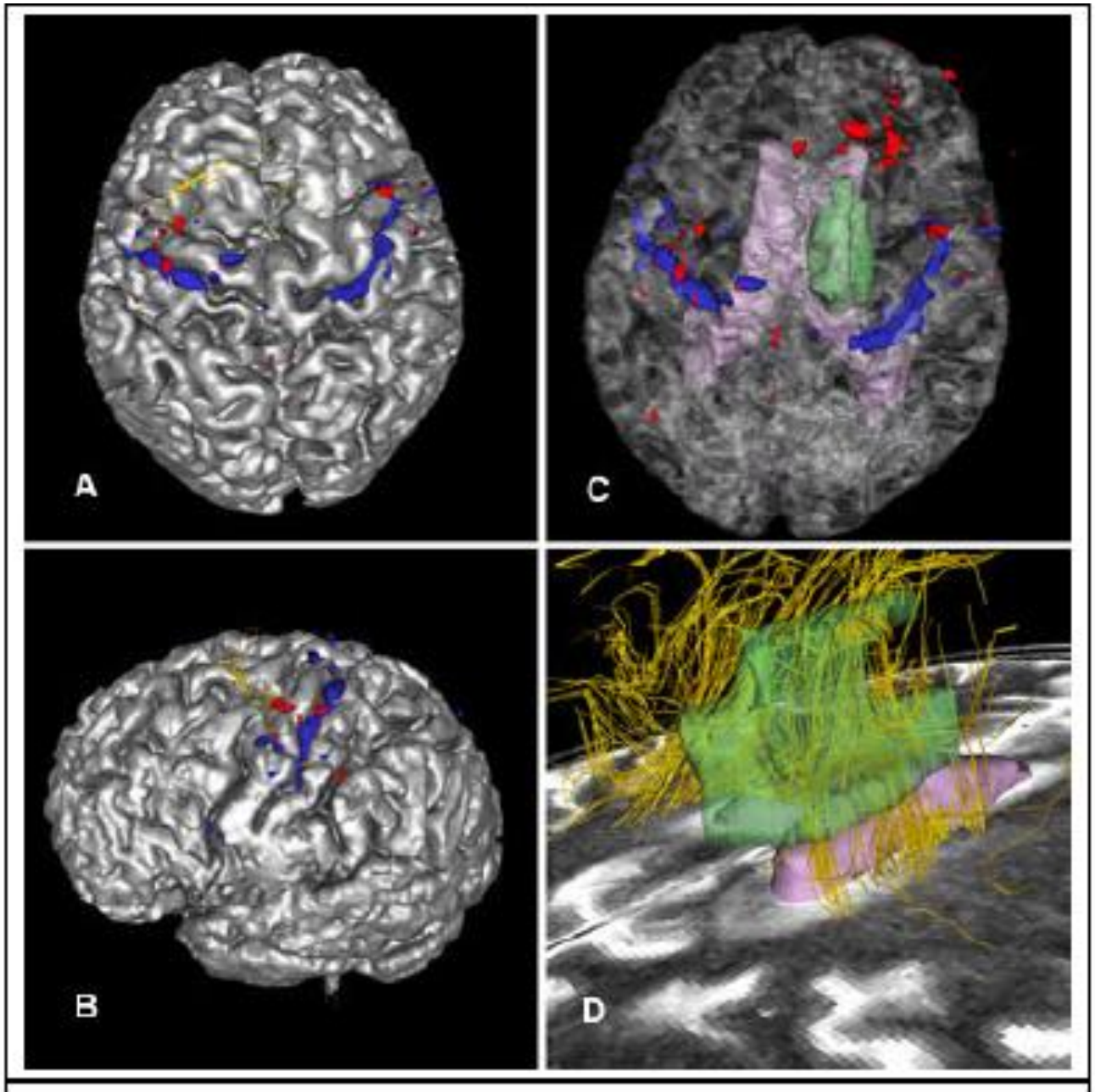

Registration and Surface Warping

Surface Deformations and Flattening

- Conformal and Area-Preserving Maps
  - Optical Flow
- Gives Parametrization of Surface
  - Registration
- Shows Details Hidden in Surface Folds
- Path Planning
  - Fly-Throughs
- Medical Research
  - Brain, Colon, Bronchial Pathologies
  - Functional MR and Neural Activity
- Computer Graphics and Visualization
  - Texture Mapping

Mathematical Theory of Surface Mapping

- **Conformal Mapping:**
  - One-one
  - Angle Preserving
  - Fundamental Form $(E,F,G) \rightarrow \rho(E,F,G)$
- **Examples of Conformal Mappings:**
  - One-one Holomorphic Functions
  - Spherical Projection
- **Uniformization Theorem:**
  - Existence of Conformal Mappings
  - Uniqueness of Mapping

Deriving the Mapping Equation

Let p be a point on the surface Σ. Let

$$z : \Sigma \rightarrow S^2$$

be a conformal equivalence sending p to the North Pole.

Introduce **Conformal Coordinates** (u, v) near p, with $u = v = 0$ at p.

In these coordinates, $ds^2 = \lambda(u,v)^2 \left(du^2 + dv^2 \right)$

We can ensure that $\lambda(p) = 1$.

In these coordinates, the Laplace Beltrami operator takes the form

$$\Delta = \frac{1}{\lambda(u,v)^2} \left(\frac{\partial^2}{\partial u^2} + \frac{\partial^2}{\partial v^2} \right).$$

Deriving the Equation-Continued

Set $w = u + iv$. The mapping $z = z(w)$ has a simple pole at $w = 0$, i.e. at p .

Near p , we have a Laurent series $z(w) = \frac{A}{w} + B + C + Dw^2 + \ldots$

Apply Δ to get $\Delta z = A\Delta\left(\frac{1}{w}\right)$.

Taking $A = \frac{1}{2\pi}$,

$$\begin{aligned}
\Delta z &= \frac{1}{2\pi}\Delta\left(\frac{1}{w}\right) \\
&= \frac{1}{2\pi}\Delta\left(\frac{\partial}{\partial u} - i\frac{\partial}{\partial v}\right)\log|w| \\
&= \frac{1}{2\pi}\left(\frac{\partial}{\partial u} - i\frac{\partial}{\partial v}\right)\Delta\log|w| \\
&= \frac{1}{2\pi}\left(\frac{\partial}{\partial u} - i\frac{\partial}{\partial v}\right)(2\,\pi\,\delta_p)
\end{aligned}$$

The Mapping Equation

$$\Delta z = \left(\frac{\partial}{\partial u} - i \frac{\partial}{\partial v} \right) \delta_p .$$

Simply a second order linear PDE. Solvable by standard methods.

Finite Elements-I

Σ is a triangulated surface. Start with

$$\Delta z = \left(\frac{\partial}{\partial u} - i \frac{\partial}{\partial v} \right) \delta_p$$

Multiply by an arbitrary smooth f and integrate by parts. For all f we want:

$$\iint_\Sigma \nabla z \cdot \nabla f \; dS = \iint_\Sigma \left(\frac{\partial}{\partial u} - i \frac{\partial}{\partial v} \right) \delta_p \; f \; dS$$

$$= \frac{\partial f}{\partial u}(p) - i \frac{\partial f}{\partial v}(p)$$

Let $z,\ f \in PL(\Sigma)$, the space of piecewise linear functions.

Finite Elements-II

For each vertex $P \in \Sigma$, let ϕ_p be the continuous function such that:

$$\begin{cases} \phi_P(P) = 1 \\ \phi_P(Q) = 0, Q \neq P, Q \text{ a vertex}, \\ \phi_P \text{ is linear on each triangle.} \end{cases}$$

These functions form a basis for the finite dimensional space $PL(\Sigma)$.

Then $z = \Sigma_P \, z_P \phi_P$.
And we want, for all Q ,

$$\Sigma_P z_P \int\int \nabla \phi_P \cdot \nabla Q dS = \frac{\partial \phi_Q}{\partial u}(p) - \frac{\partial \phi_Q}{\partial v}(p)$$

This is simply a matrix equation.

Finite Elements-III

Set $D = \left(D_{PQ} \right)$, $D_{PQ} = \int\int \nabla \phi_P \cdot \nabla \phi_Q dS$.

Define vectors

$$a = \left(a_Q \right) = \left(\frac{\partial \phi_Q}{\partial u}(p) \right),$$

$$b = \left(b_Q \right) = \left(\frac{\partial \phi_Q}{\partial v}(p) \right).$$

Our equation becomes simply $Dz = a - ib$.

$$D_{PQ} = -\frac{1}{2}\{\cot \angle R + \cot \angle S\},$$

$$D_{PP} = -\Sigma_{P \neq Q} D_{PQ}.$$

Need formulas for a, b.

Finite Elements-IV

Suppose the point p lies on a triangle with vertices ABC.

Since $a = \left(a_Q \right) = \left(\frac{\partial \phi_Q}{\partial u}(p) \right)$,

and $b = \left(b_Q \right) = \left(\frac{\partial \phi_Q}{\partial v}(p) \right)$,

we have $a_Q - ib_Q = 0$ if $Q \notin \{A, B, C\}$.

Finite Elements-V

If $Q \in \{A, B, C\}$, then considering that ϕ_Q is linear on ABC:

$$a_Q - ib_Q := \begin{cases} \dfrac{-1}{\|B-A\|} + i\dfrac{1-\theta}{\|C-E\|} & Q = A, \\ \dfrac{1}{\|B-A\|} + i\dfrac{\theta}{\|C-E\|} & Q = B, \\ i\dfrac{-1}{\|C-E\|} & Q = C, \end{cases}$$

$$\theta = \frac{\langle C-A, B-A \rangle}{\|B-A\|^2}$$

Finite Elements-VI

If we set $z = x + iy$, then our system $Dz = a - ib$ becomes $Dx = a$ and $Dy - b$.

D is sparse, real, symmetric and positive semi-definite. Its kernel is the space of constant vectors, and it is positive definite on the space orthogonal to its kernel.

These properties of D allow us to use the conjugate gradient method to solve the system.

Summary of Flattening

Flattening:
Calculate the elements of the matrices $D, a,$ and b.

Use the conjugate gradient method to solve $Dx = a$ and $Dy = -b$.
The resulting $z = x + iy$ is the conformal mapping to the complex plane.

Compose z with inverse stereo projection to get a conformal map to the unit sphere.

Cortical Surface Flattening-Normal Brain

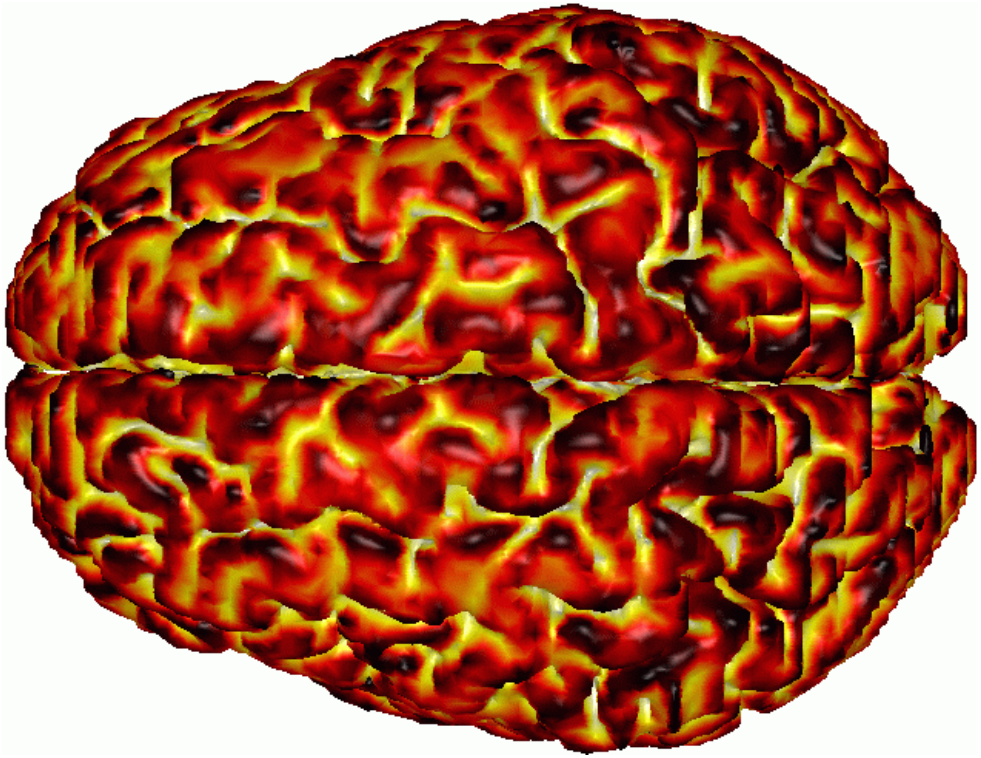

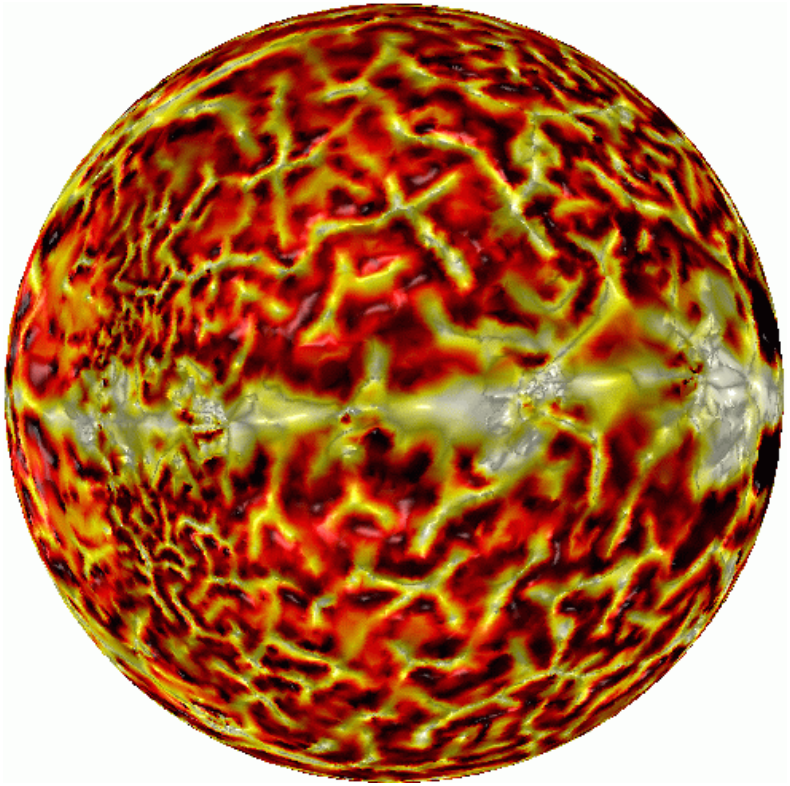

White Matter Segmentation and Flattening

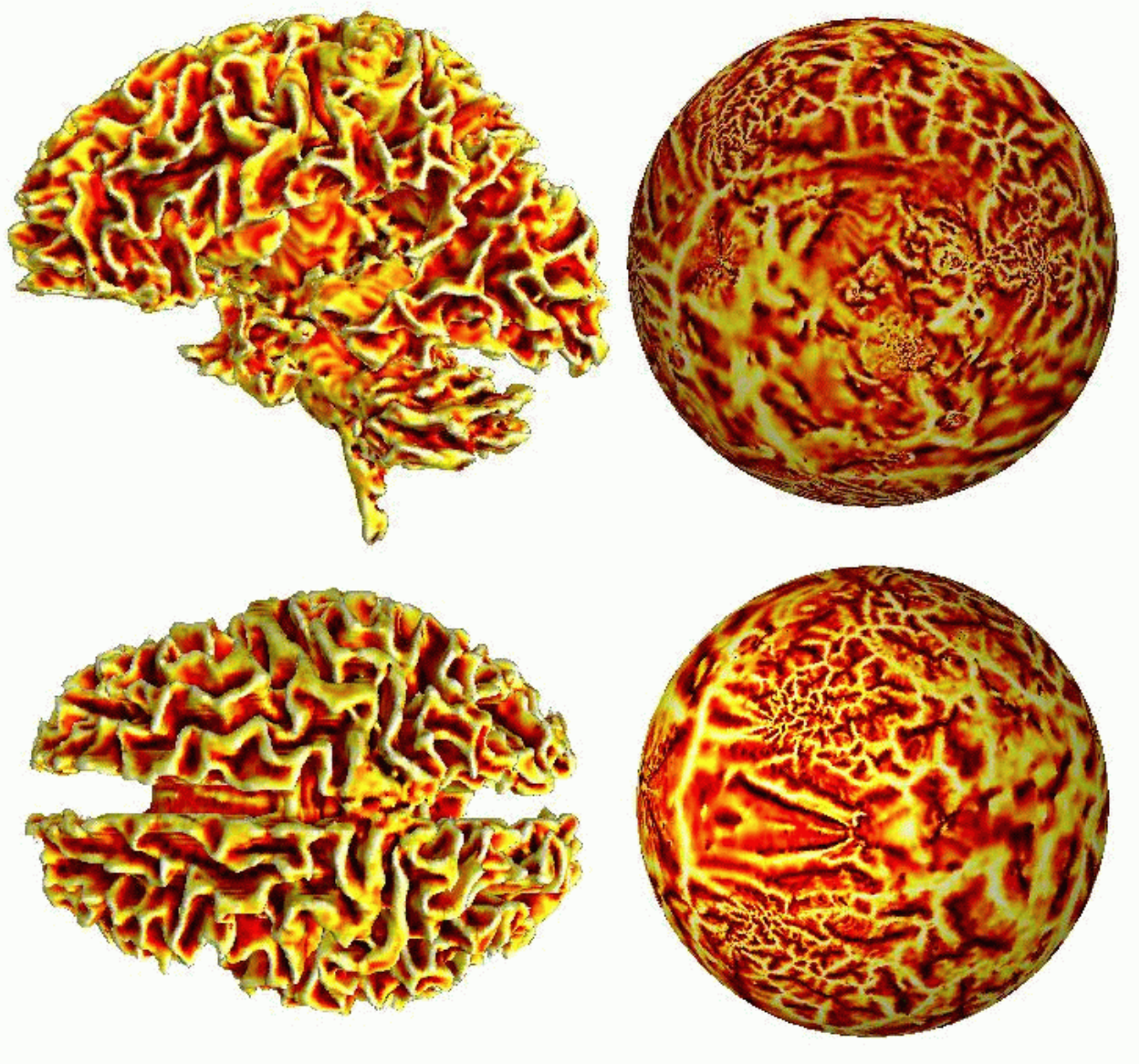

Conformal Mapping of Neonate Cortex

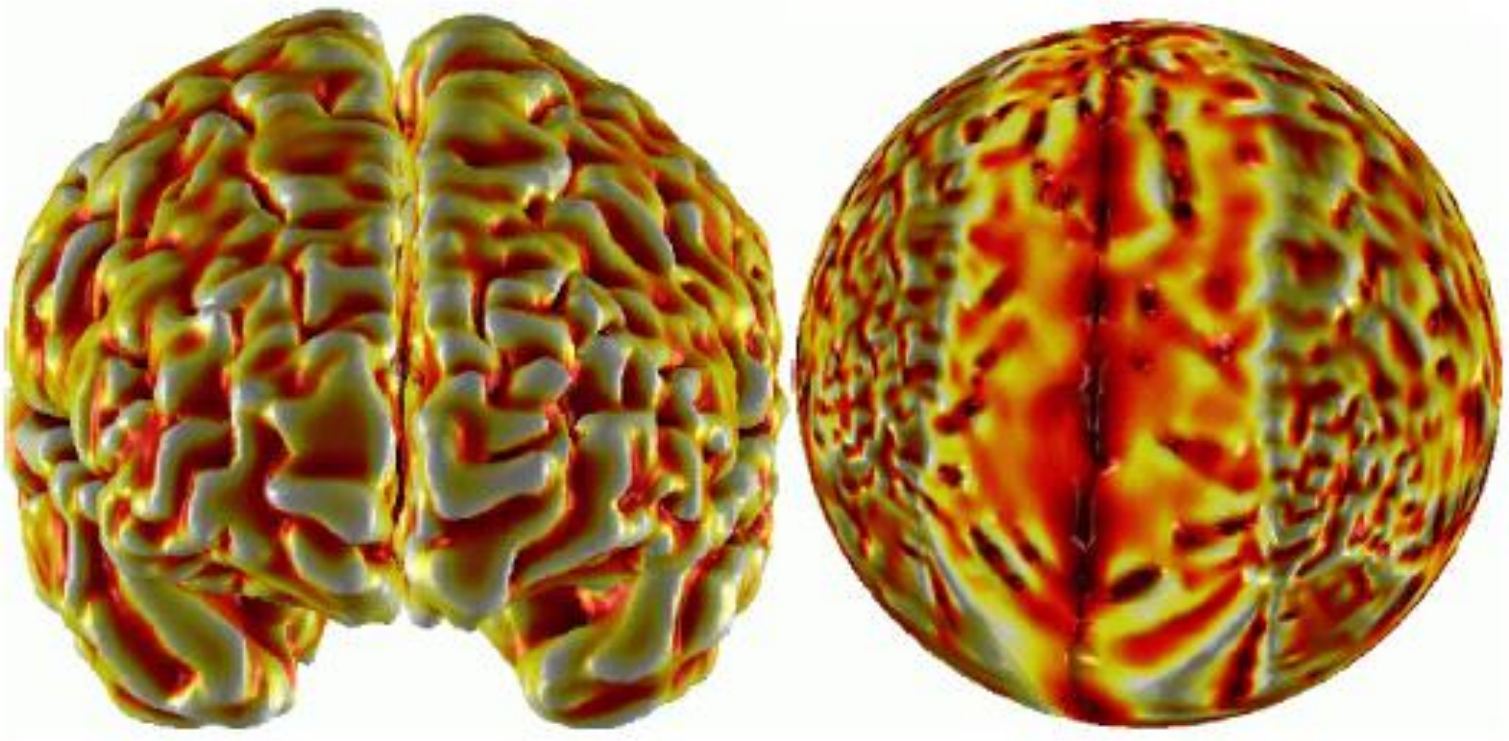

Figure 8.4.5-12
Conformal mapping of the neonate cortical surface to the sphere. The shading scheme represents mean curvature.

Coordinate System on Cortical Surface

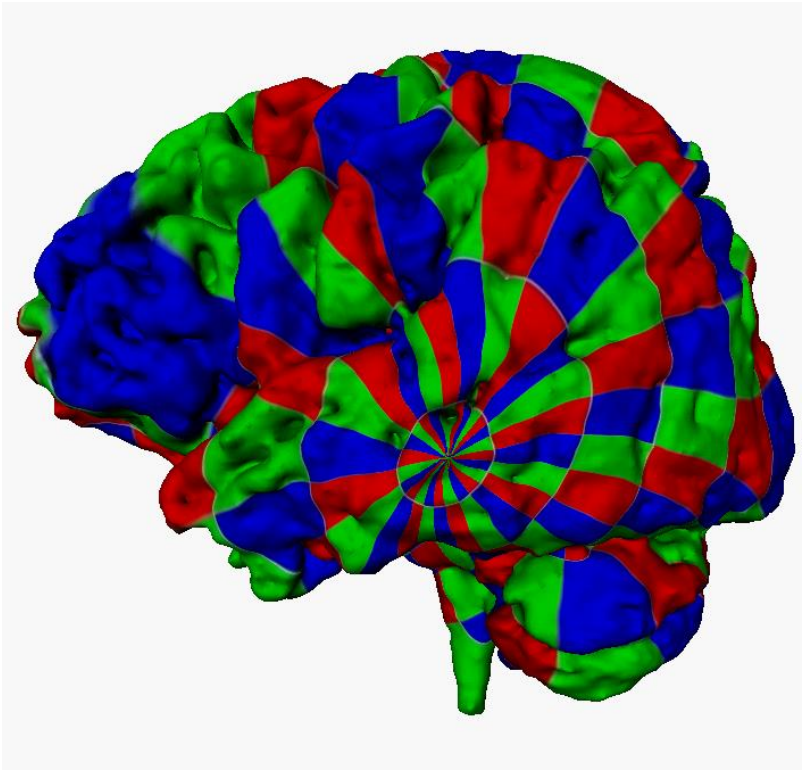

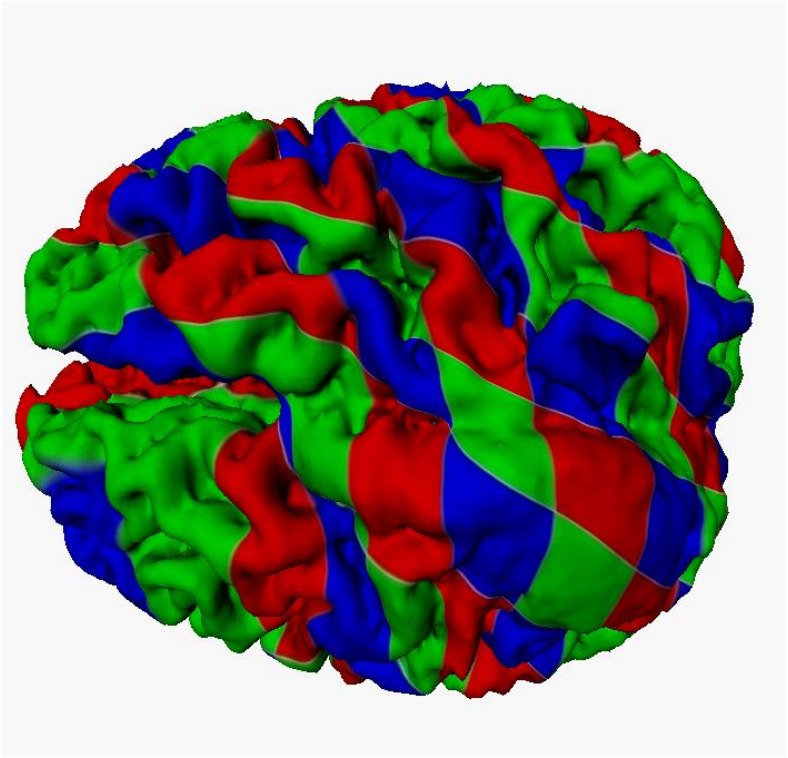

Principal Lines of Curvature on Brain Surface-I

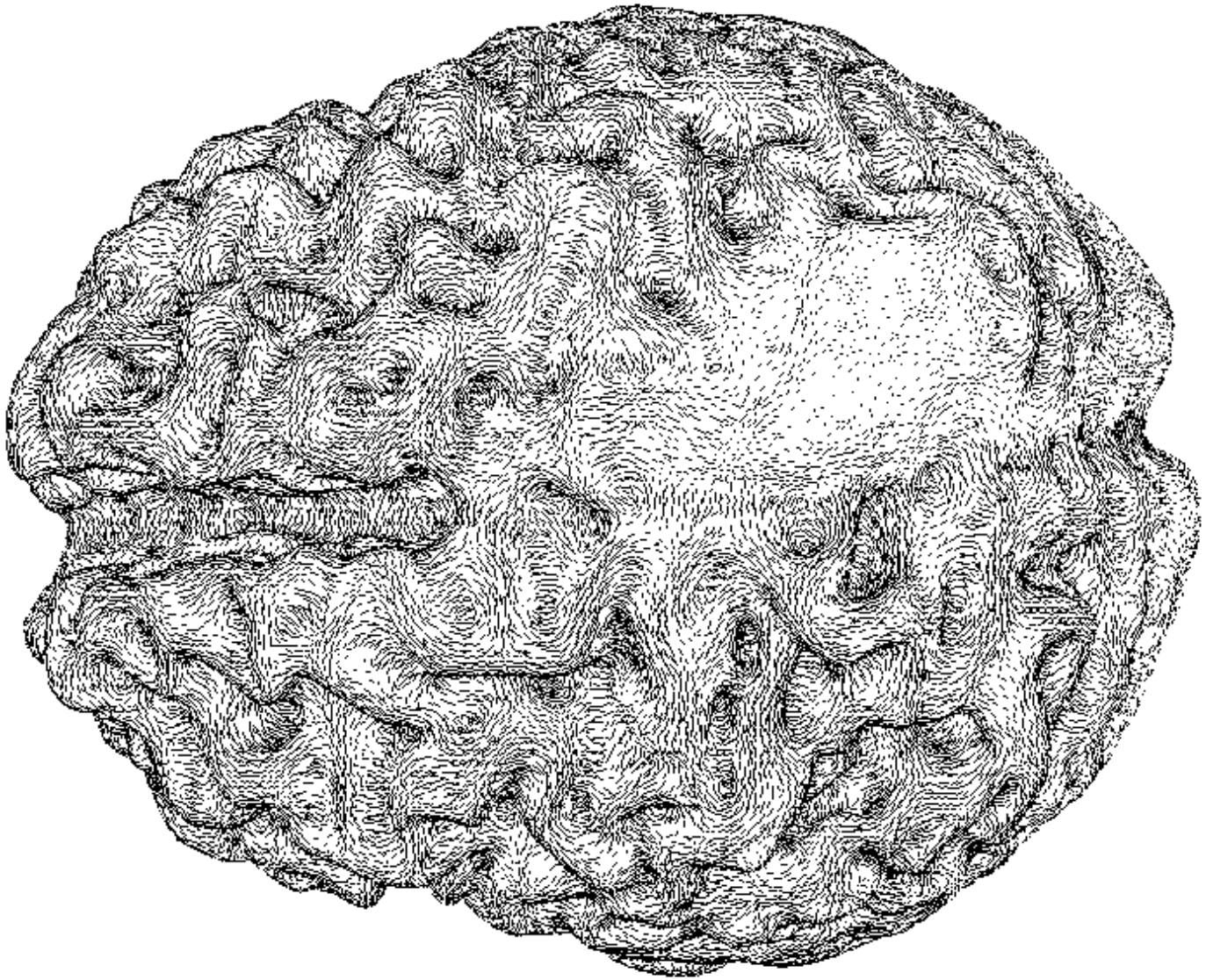

Principal Lines of Curvatures on the Brain-II

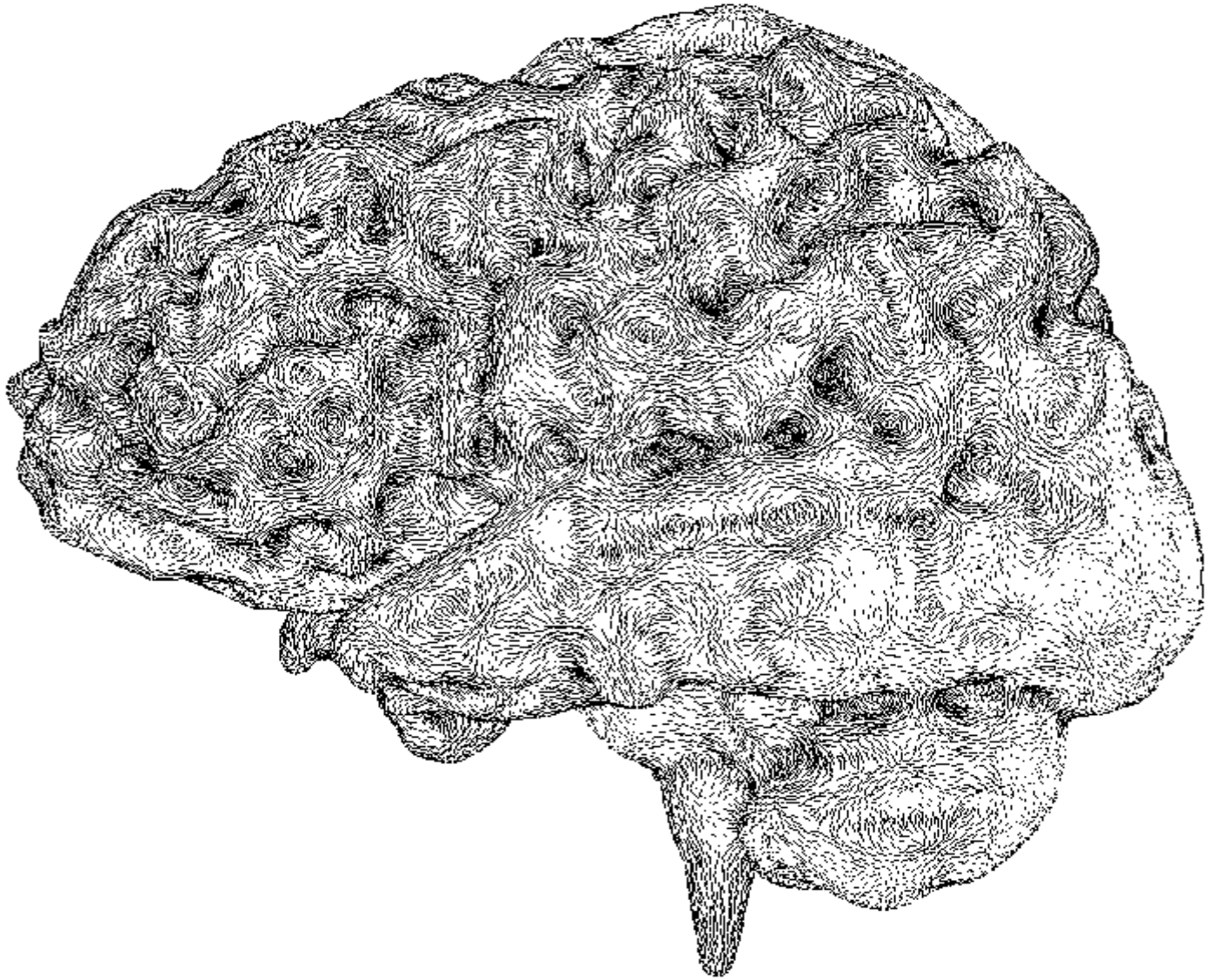

Bladder Flattening

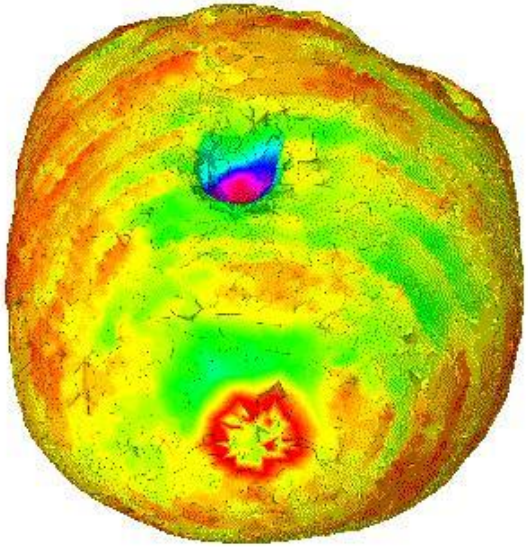

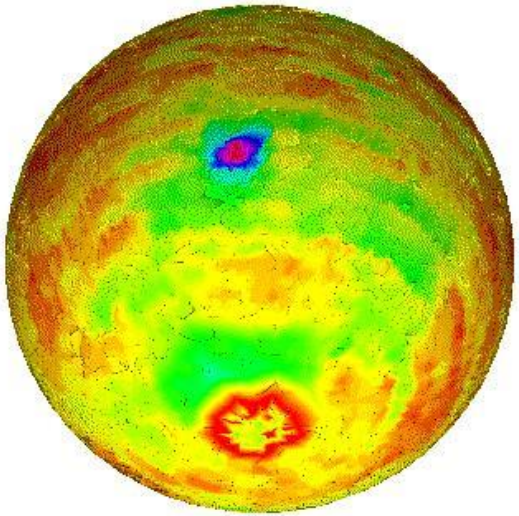

3D Ultrasound Cardiac Heart Map

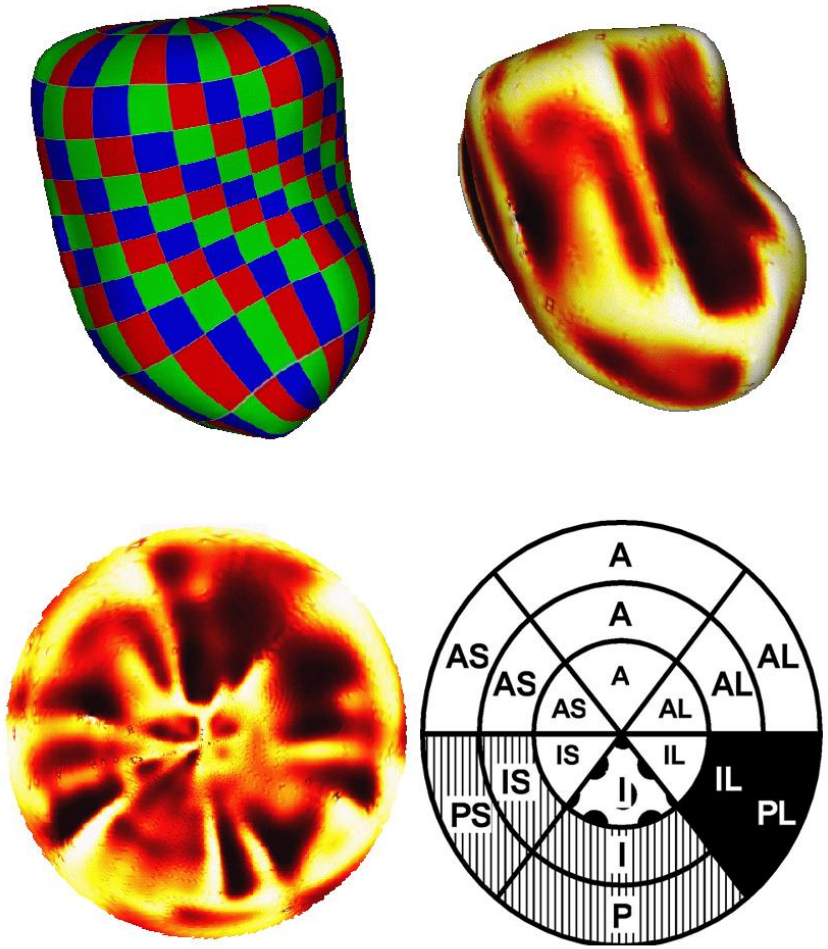

Flattening a Tube

(1) Solve

$$\Delta u = 0 \quad on \quad \Sigma \setminus \left(\sigma_0 \cup \sigma_1 \right)$$

$$u = 0 \quad on \quad \sigma_0$$

$$u = 1 \quad on \quad \sigma_1$$

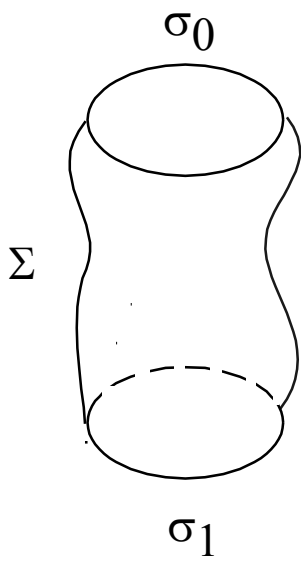

(2) Make a cut from σ_0 to σ_1 .

Make sure u is increasing along the cut.

Flattening a Tube-Continued

(3) Calculate v on the boundary loop

$$\sigma_0 \to cut \to \sigma_1 \to cut \to \sigma_0$$

by integration

$$v(\xi) = \int^{\xi} \frac{\partial v}{\partial s} ds = \int^{\xi} \frac{\partial u}{\partial n} ds$$

(4) Solve Dirichlet problem using boundary values of v.

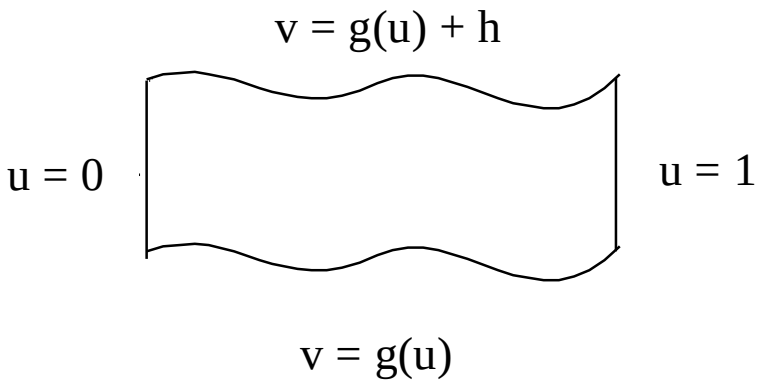

If you want, scale so $h = 2\pi$, take e^{u+iv} to get an annulus.

Flattening Without Distortion-I

In practice, once the tubular surface has been flattened into a rectangular shape, it will need to be visually inspected for pathologies. We present a simple technique by which the entire colon surface can be presented to the viewer as a sequence of images or cine. In addition, this method allows the viewer to examine each surface point without distortion at some time in the cine. Here, we will say a mapping is without distortion at a point if it preserves the intrinsic distance there.

It is well known that a surface cannot in general be flattened onto the plane without some distortion somewhere. However, it may be possible to achieve a surface flattening which is free of distortion along some curve. A simple example of this is the familiar Mercator projection of the earth, in which the equator appears without distortion. In our case, the distortion free curve will be a level set of the harmonic function (essentially a loop around the tubular colon surface), and will correspond to the vertical line through the center of a frame in the cine. This line is orthogonal to the "path of flight" so that every point of the colon surface is exhibited at some time without distortion.

Flattening Without Distortion-II

Suppose we have conformally flattened the colon surface onto a rectangle

$$R = [0, u_{\max}] \times [-\pi, \pi].$$

Let F be the inverse of this mapping, and let $\phi^2 = \phi^2(u,v)$ be the amount by Which F scales a small area near (u,v), i.e. let $\phi > 0$ be the "conformal factor" for F.

Fix $w > 0$, and for each $u_0 \in [0, u_{\max}]$ define a subset $R_0 = ([u_0 - w, u_0 + w] \times [-\pi, \pi]) \cap R$ which will correspond to the contents of a cine frame. We define a mapping

$$(\hat{u}, \hat{v}) = G(u,v) = \left(\int_{u_0}^{u} \phi(\mu, v) d\mu, \int_{0}^{v} \phi(u_0, v) dv \right).$$

Flattening Without Distortion-III

We have

$$dG(u,v)=\begin{pmatrix}\hat{u}_u & \hat{u}_v\\ \hat{v}_u & \hat{v}_v\end{pmatrix}=\begin{pmatrix}\phi(u,v) & \int_{u_0}^{u}\phi_v(\mu,v)d\mu\\ 0 & \phi(u_0,v)\end{pmatrix},$$

$$dG(u_0,v)=\phi(u_0,v)\times\begin{pmatrix}1 & 0\\ 0 & 1\end{pmatrix}.$$

This implies that composition of the flattening map with G sends level set loop $\{u=u_0\}$ on the surface to the vertical line $\{\hat{u}=0\}$ in the $\hat{u}-\hat{v}$ plane without distortion. In addition, it follows from the formula for dG that lengths measured in the $\hat{u}$ direction accurately reflect the lengths of corresponding curves on the surface.

Introduction: Colon Cancer

- US: 3rd most common diagnosed cancer
- US: 3rd most frequent cause of death
- US: 56.000 deaths every year

- Most of the colorectal cancers arise from preexistent adenomatous polyps

- Landis S, Murray T, Bolden S, Wingo Ph.Cancer Statitics 1999. Ca Cancer J Clin. 1999; 49:8-31.

Problems of CT Colonography

- Proper preparation of bowel
- How to ensure complete inspection

→ Nondistorting colon flattening program

Colon Segmentation and Flattening

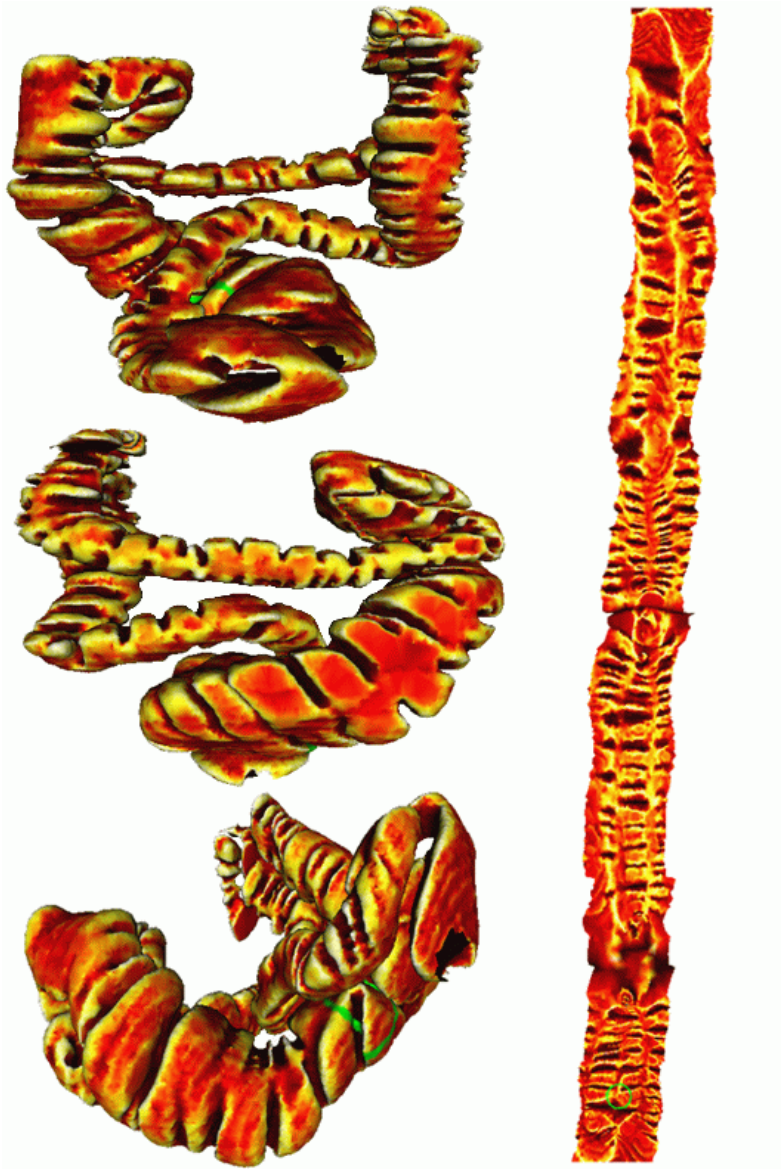

Nondistorting colon flattening

- Simulating pathologist' approach
- No Navigation is needed
- Entire surface is visualized

Nondistorting Colon Flattening

- Using CT colonography data
- Standard protocol for CT colonography
- 43 patients (28 m, 15 f)
- Mean age 70.2 years (from 50 to 82)

Flattened Colon

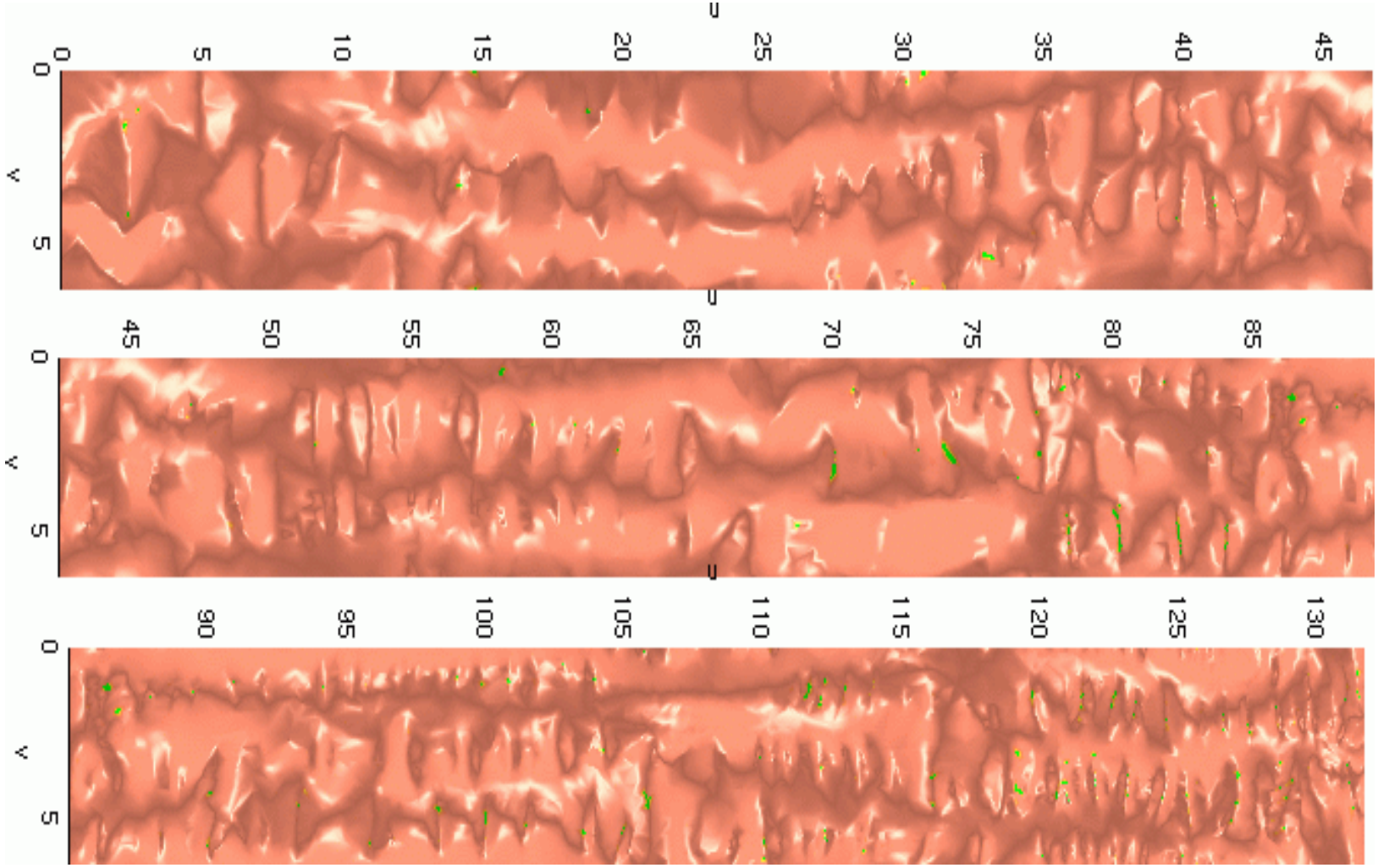

Colon Fly-Through Without Distortion

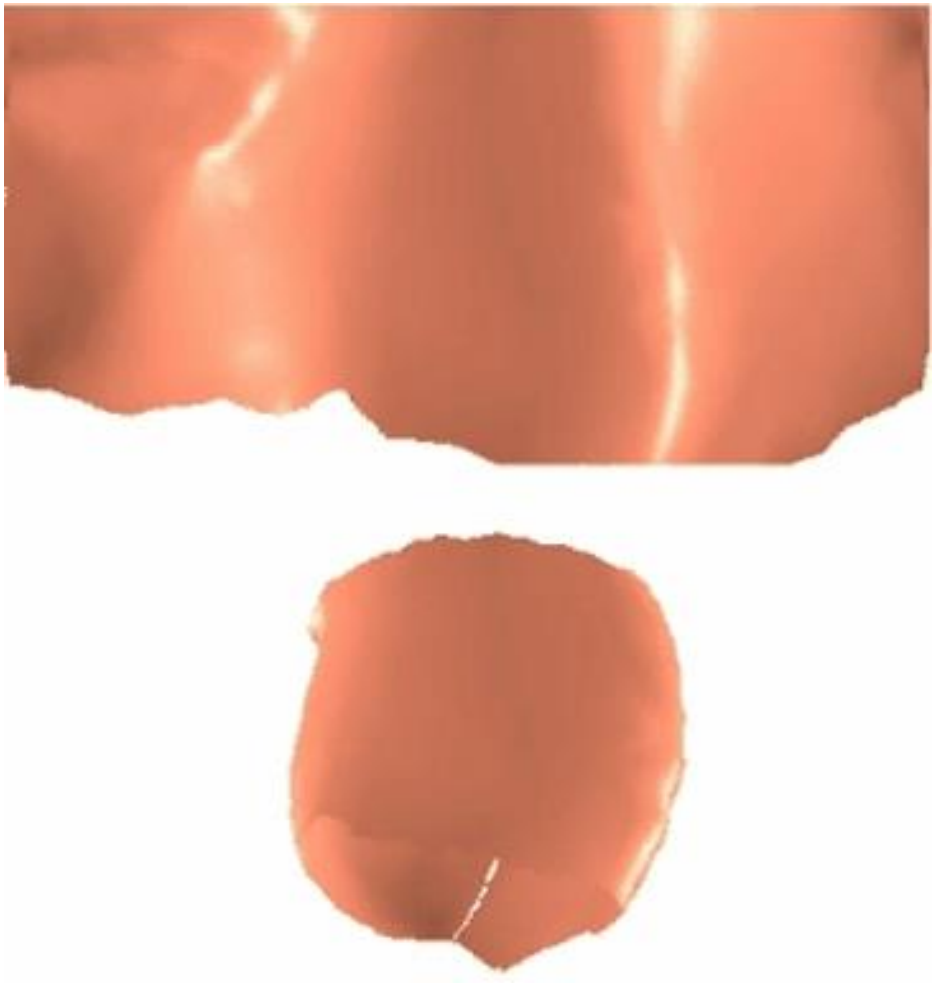

Polyps Rendering

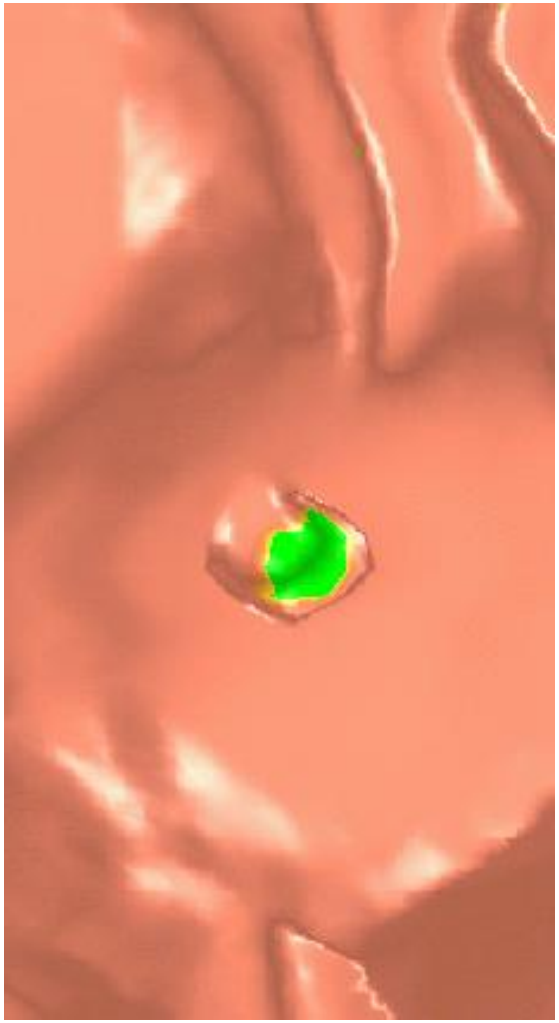

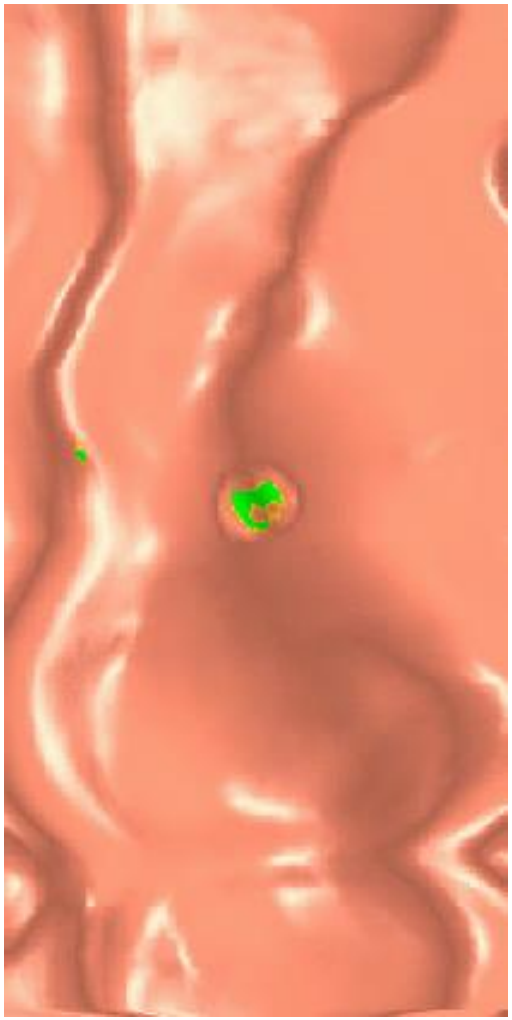

Finding Polyps on Original Images

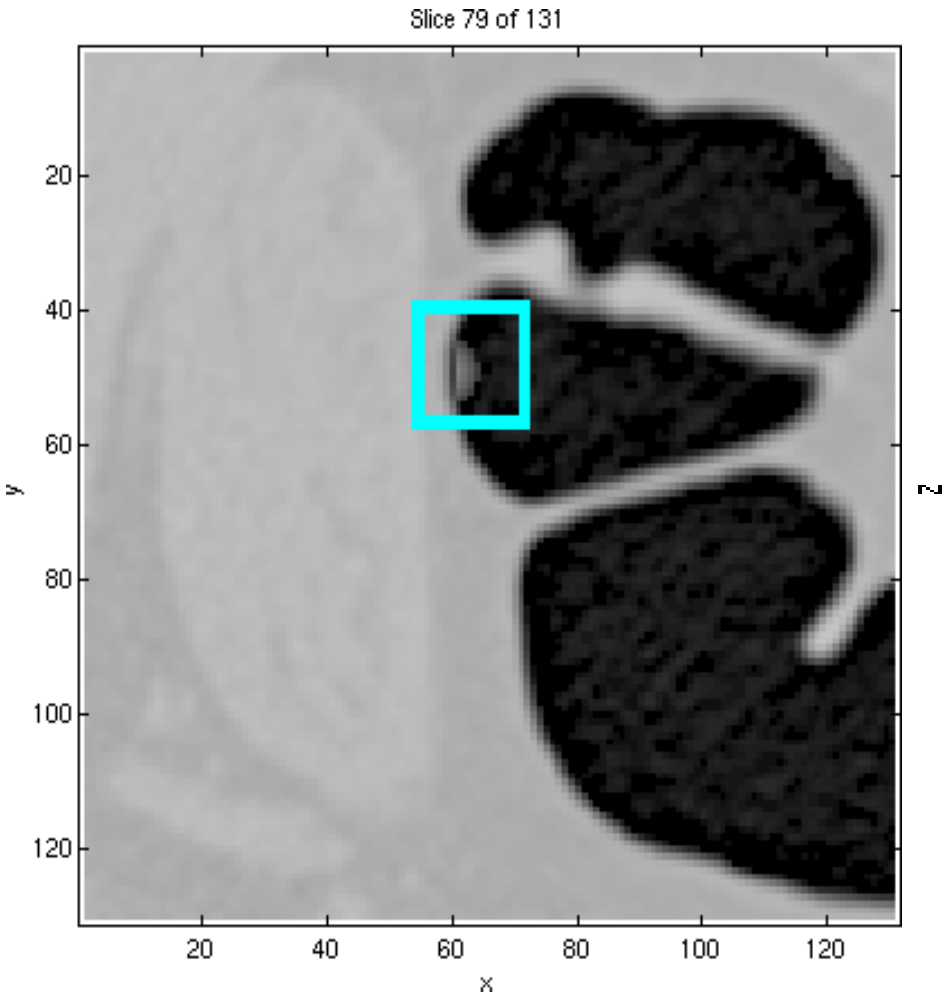

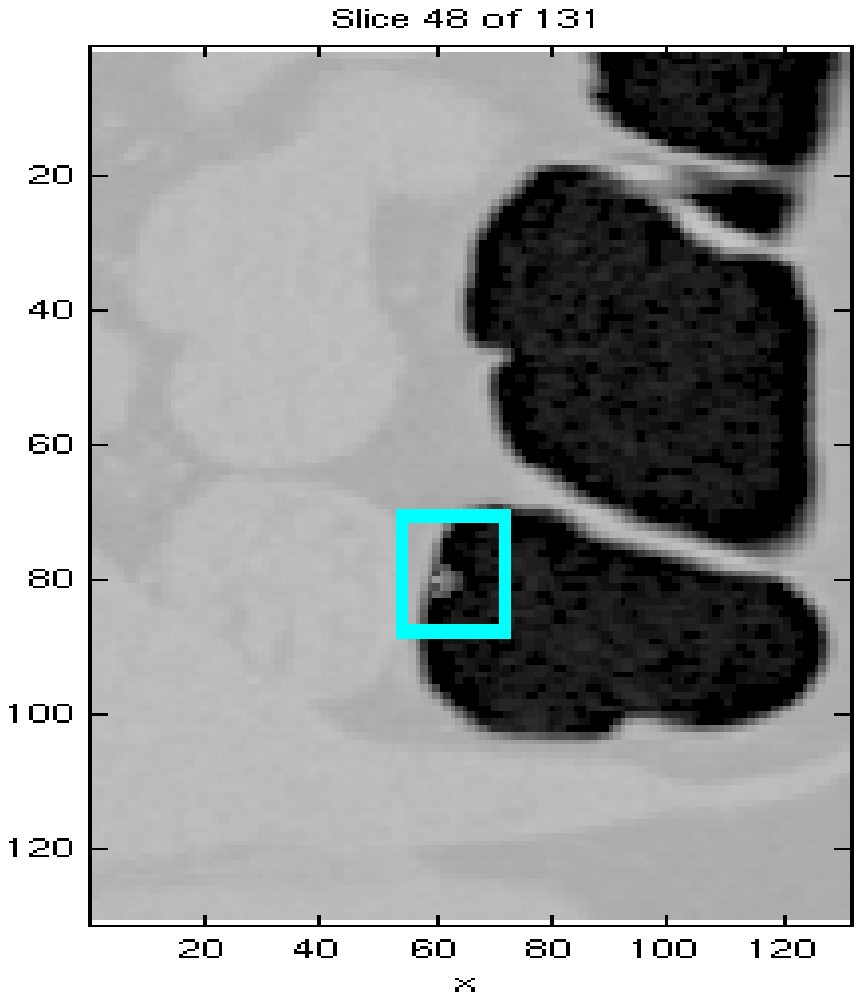

Polyp Detection

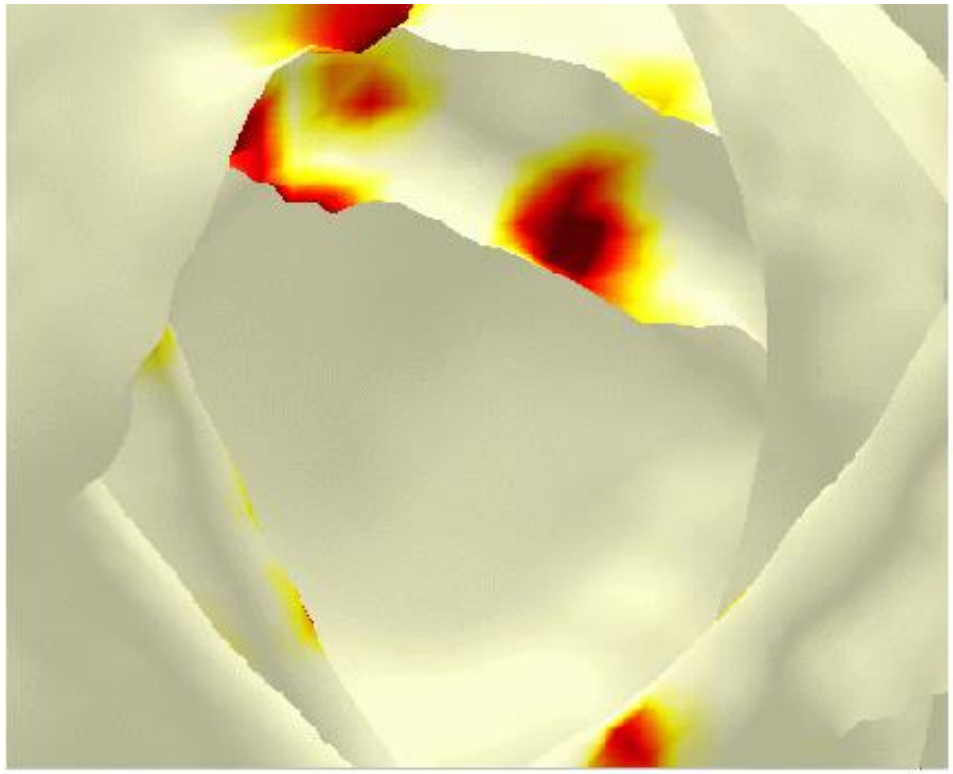

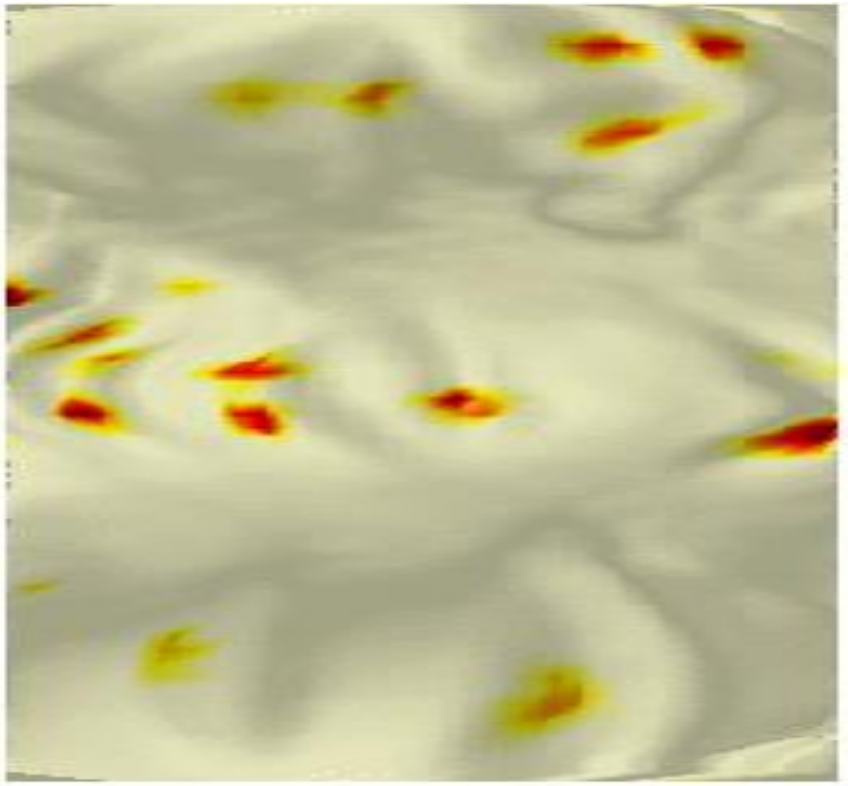

Polyp Highlighted

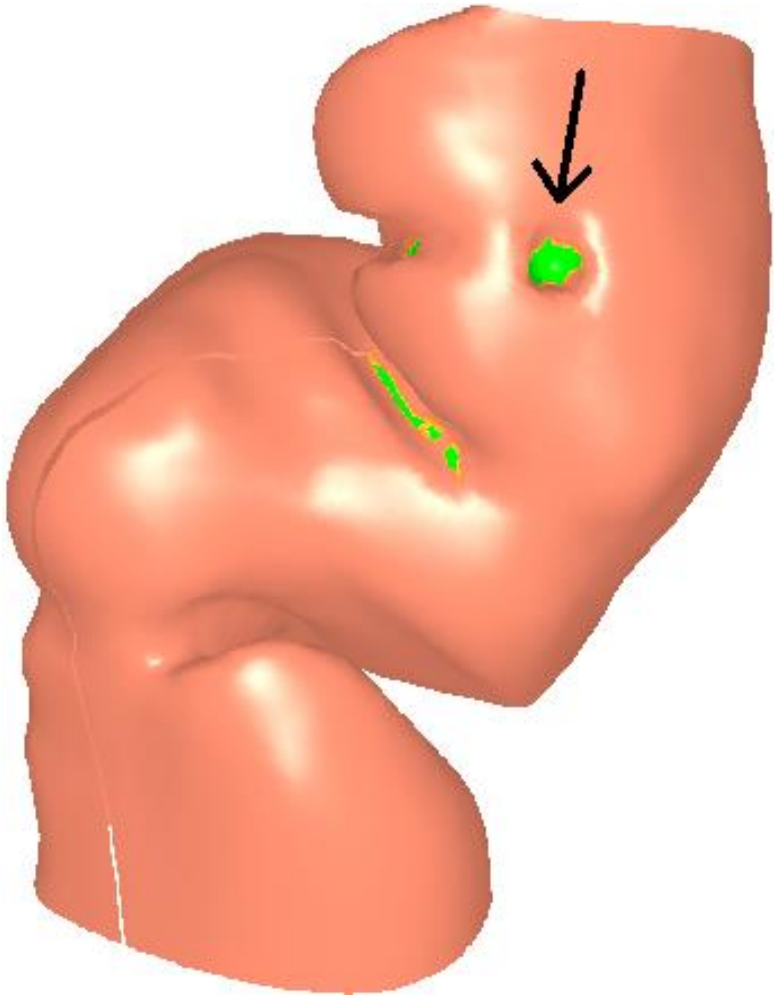

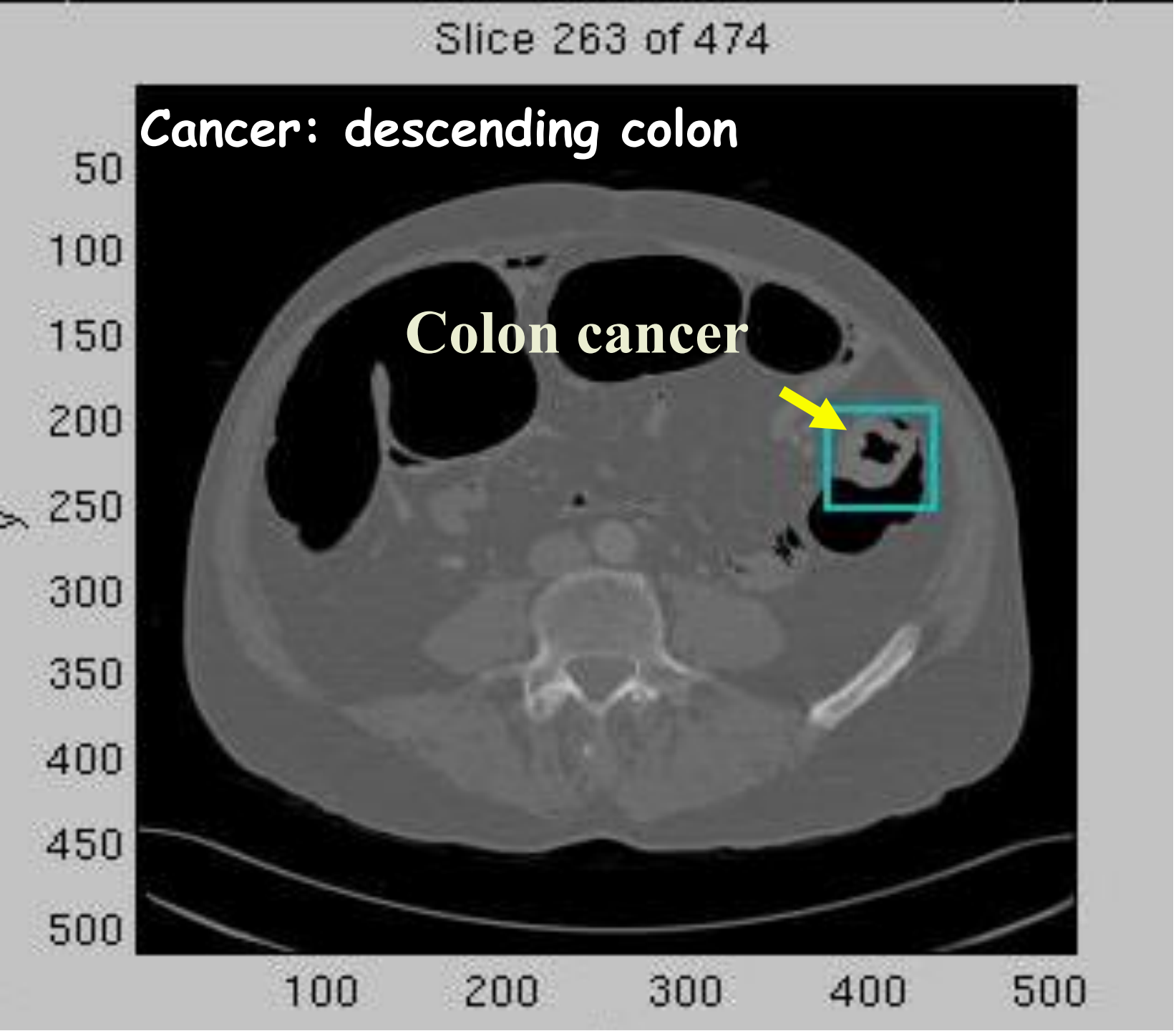
Slice 263 of 474
Cancer: descending colon
Colon cancer
50
100
150
200
250
300
350
400
450
500
100
200
300
400
500

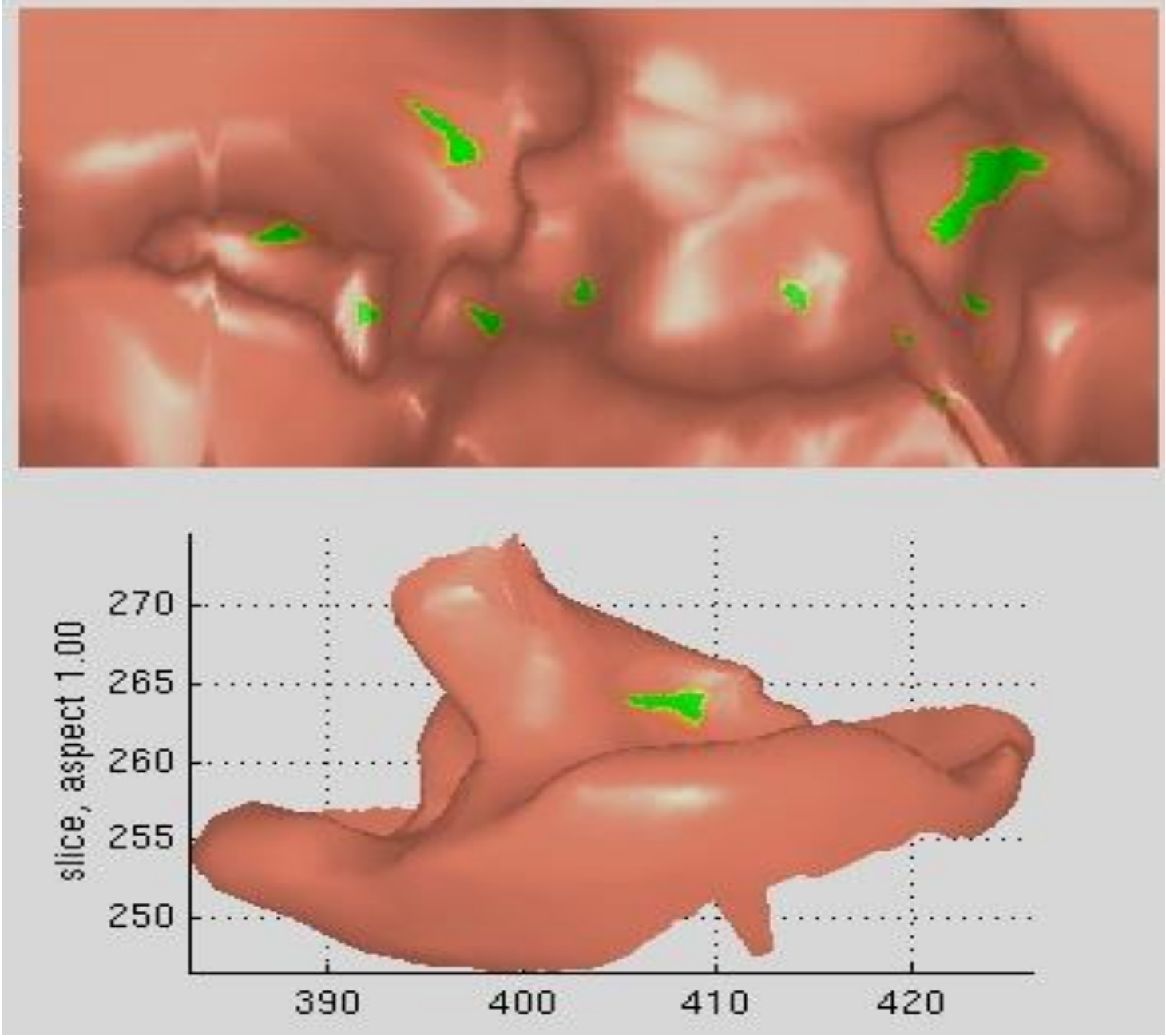

Cancer: Descending Colon

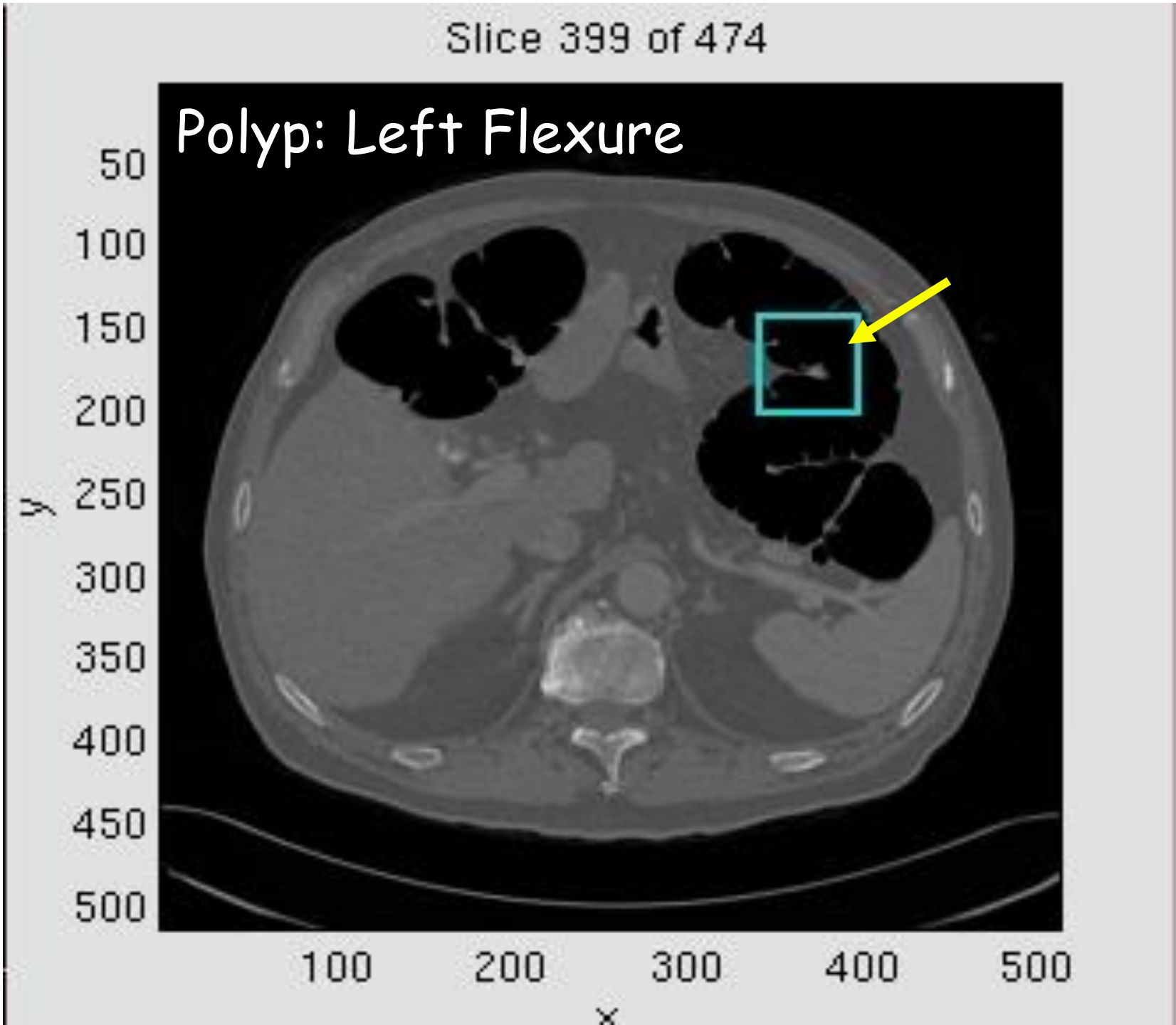
Slice 399 of 474
Polyp: Left Flexure
50
100
150
200
250
300
350
400
450
500
y
100
200
300
400
500
x

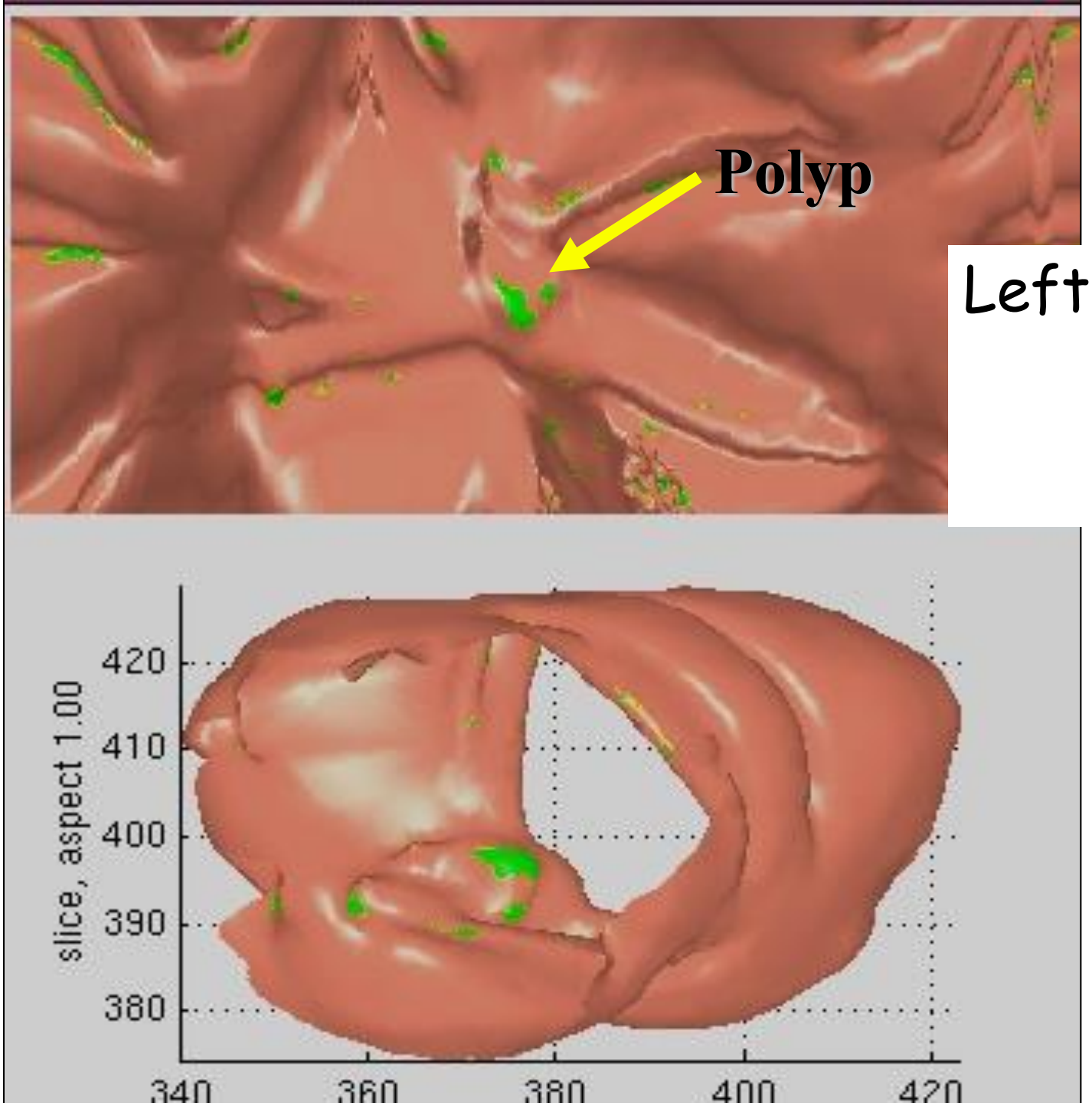
Polyp
Left Flexur
slice, aspect 1.00
420
410
400
390
380
340
360
380
400
420

Polyp: Transverse Colon

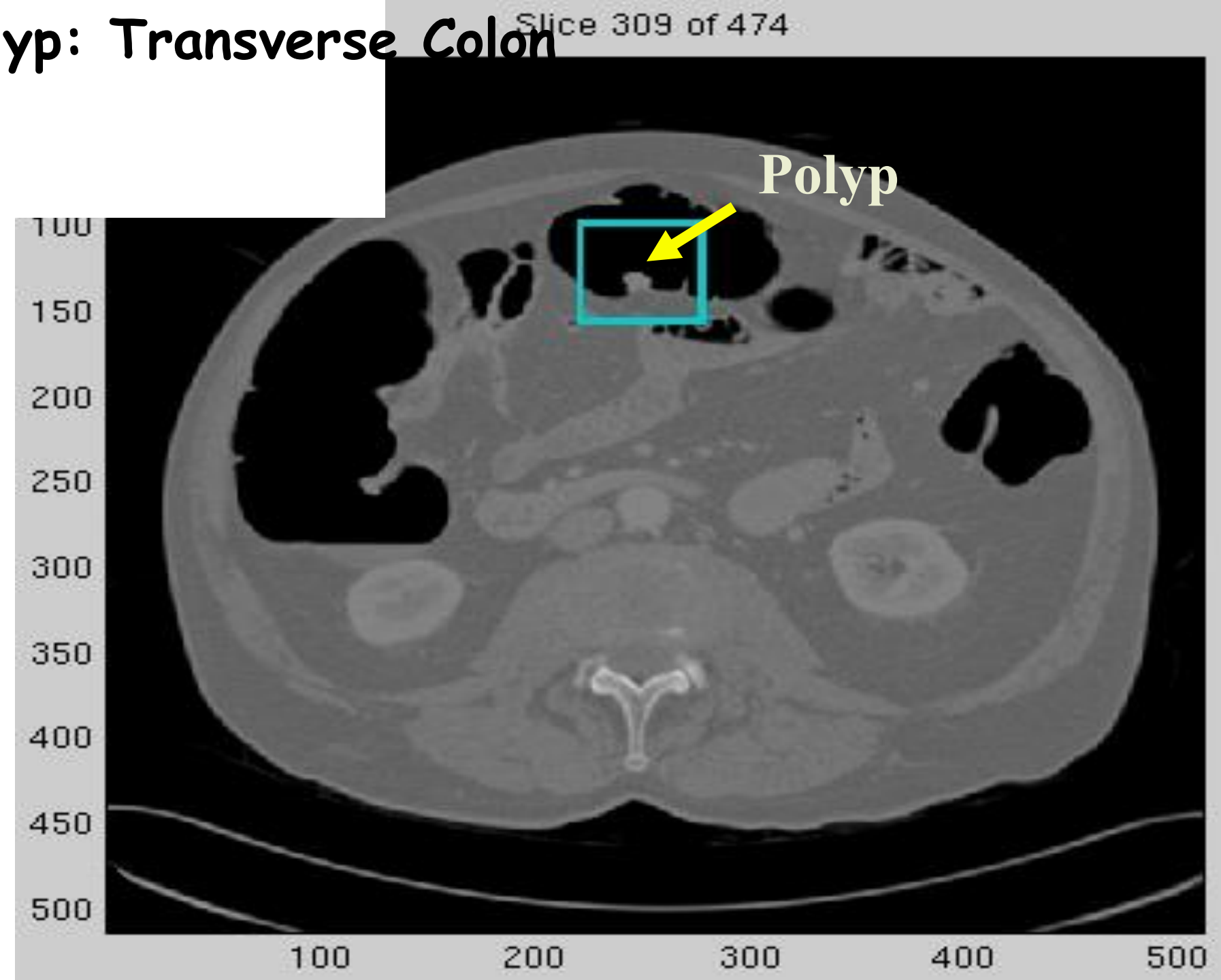

Polyp: Transverse Colon

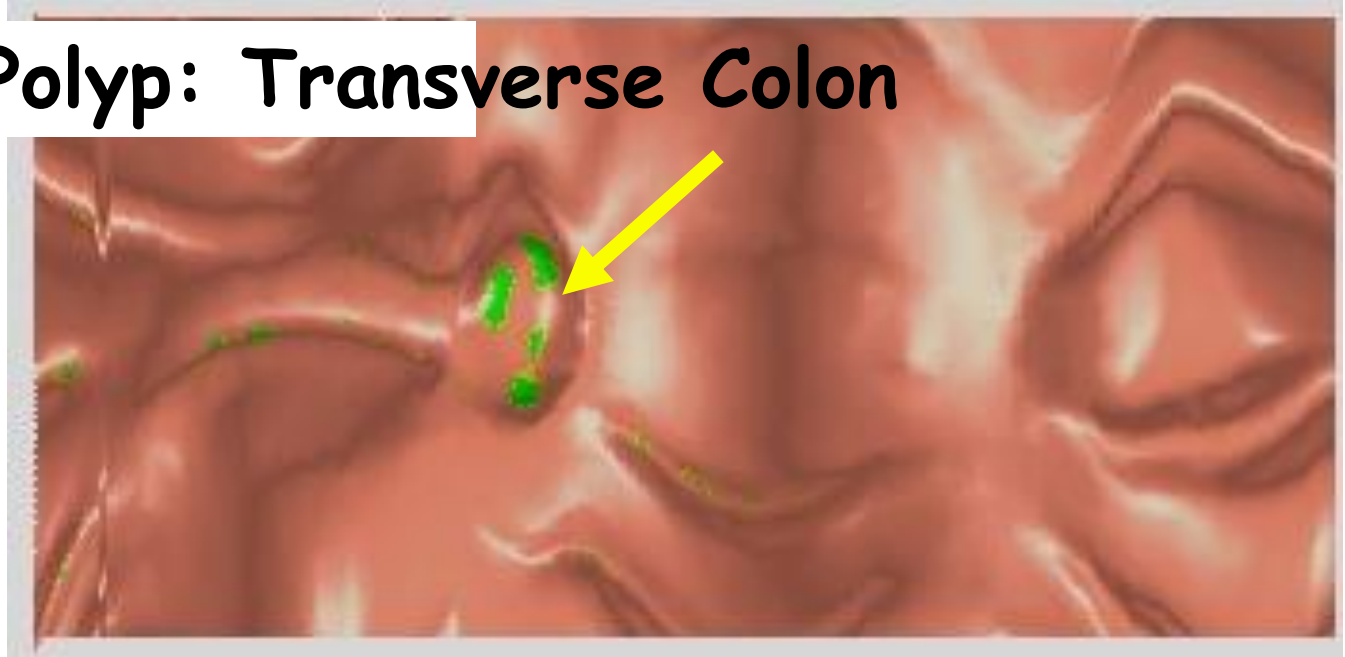

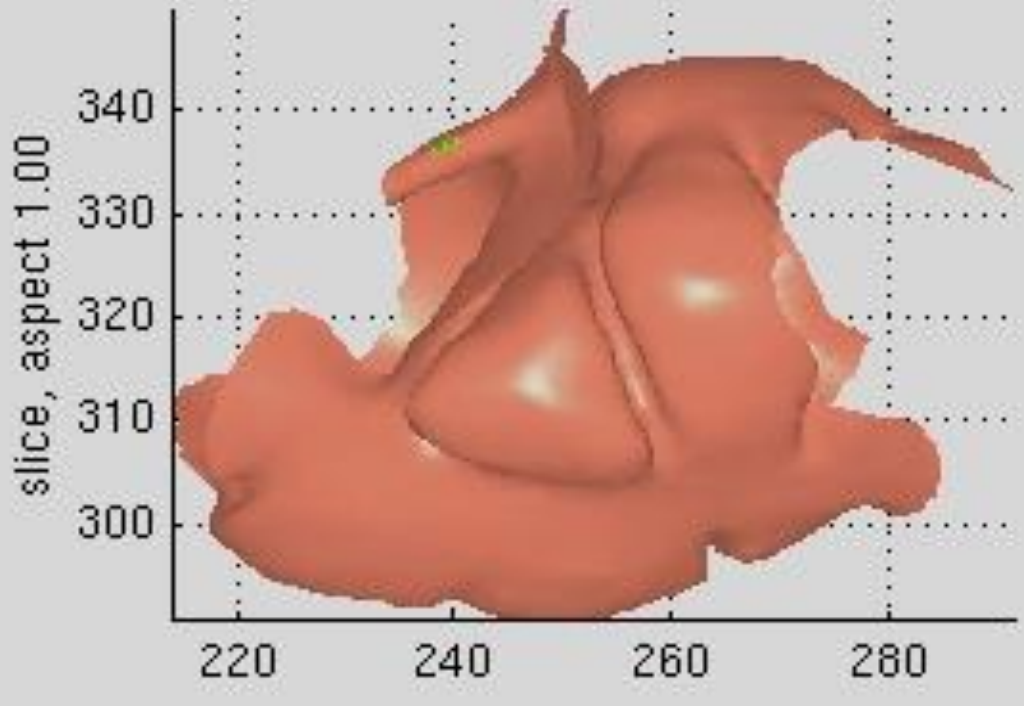

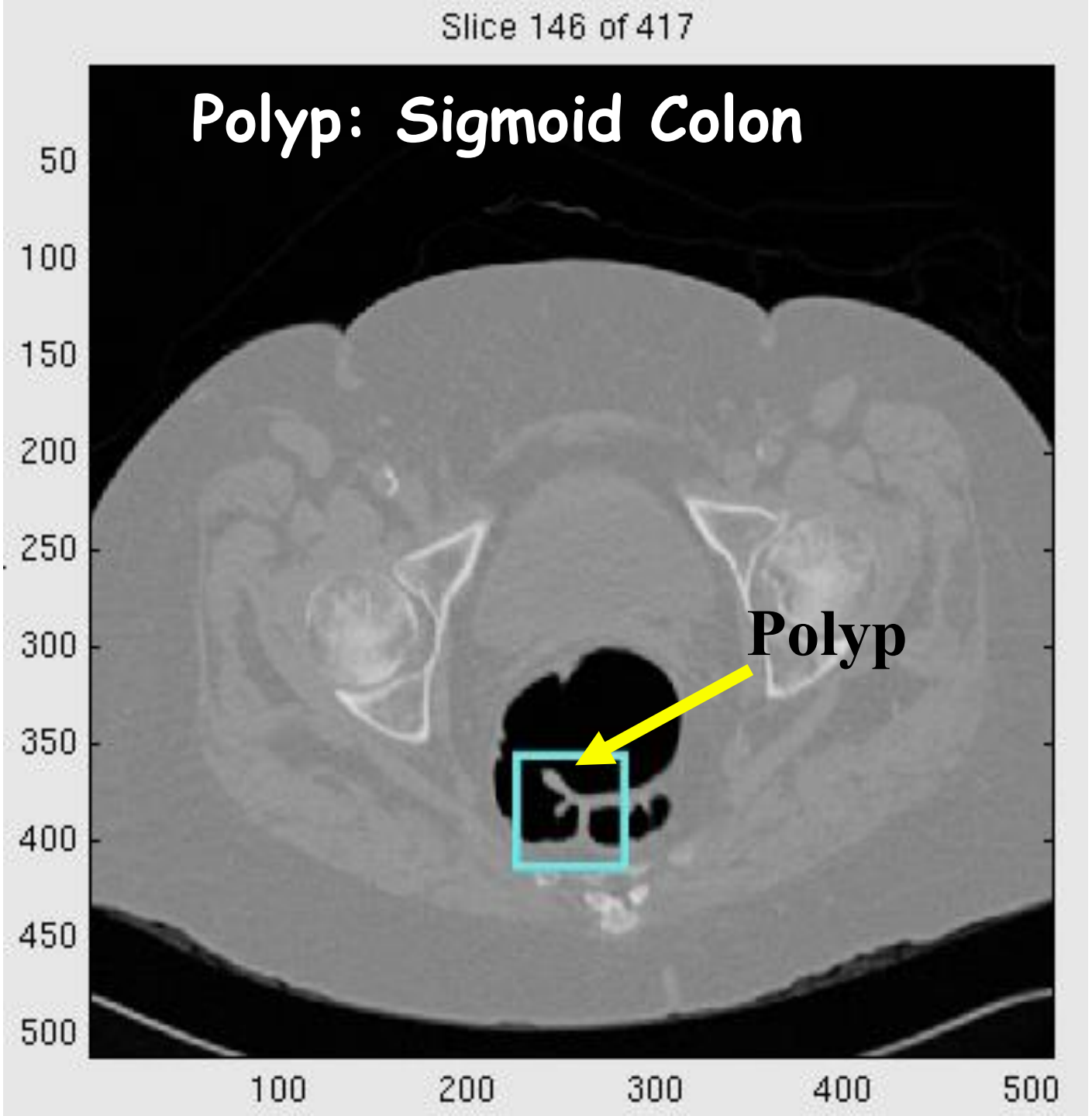
Slice 146 of 417
Polyp: Sigmoid Colon
Polyp
50
100
150
200
250
300
350
400
450
500
100
200
300
400
500

Polyp: Sigmoid Colon

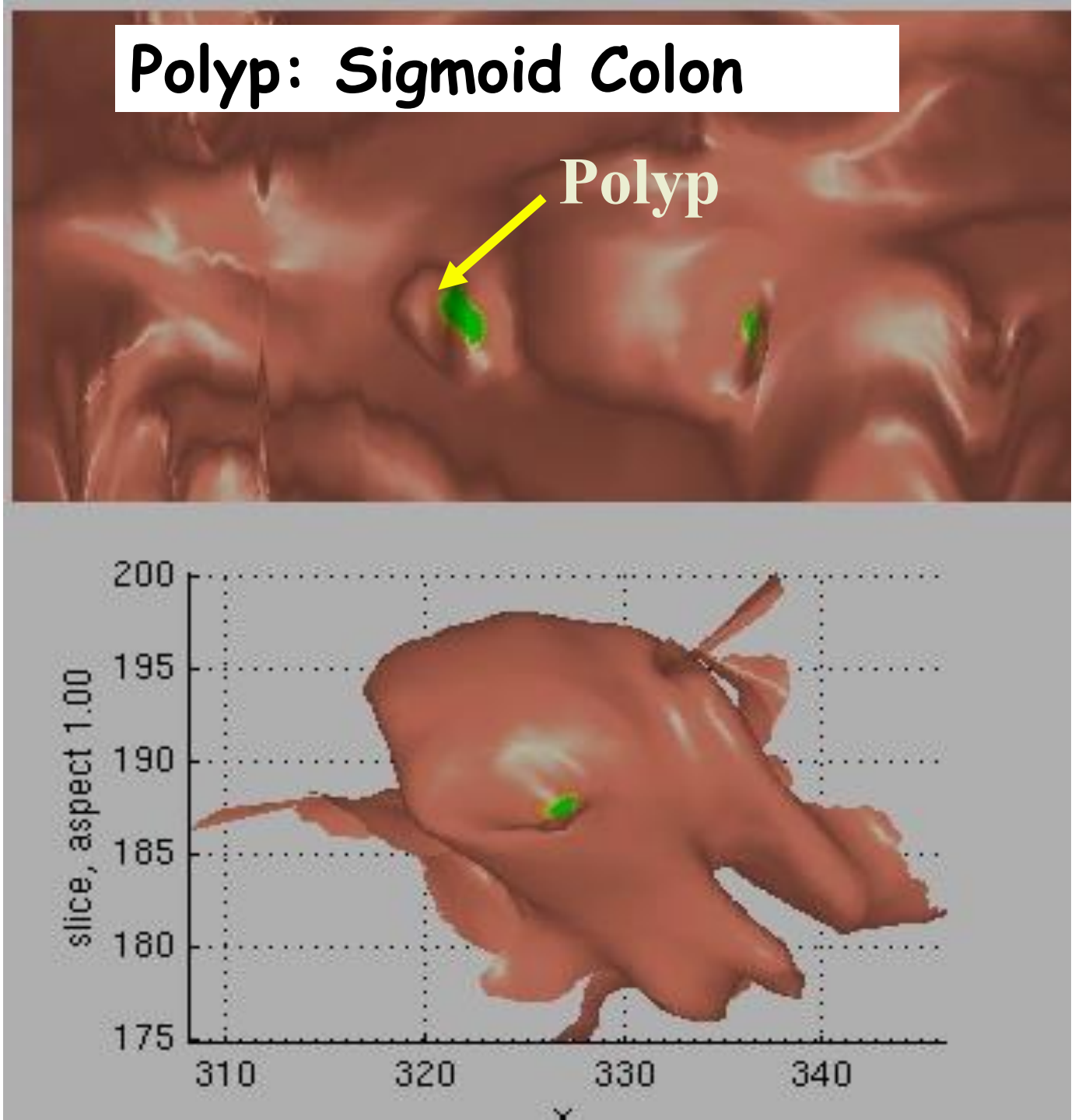

Path-Planning Deluxe

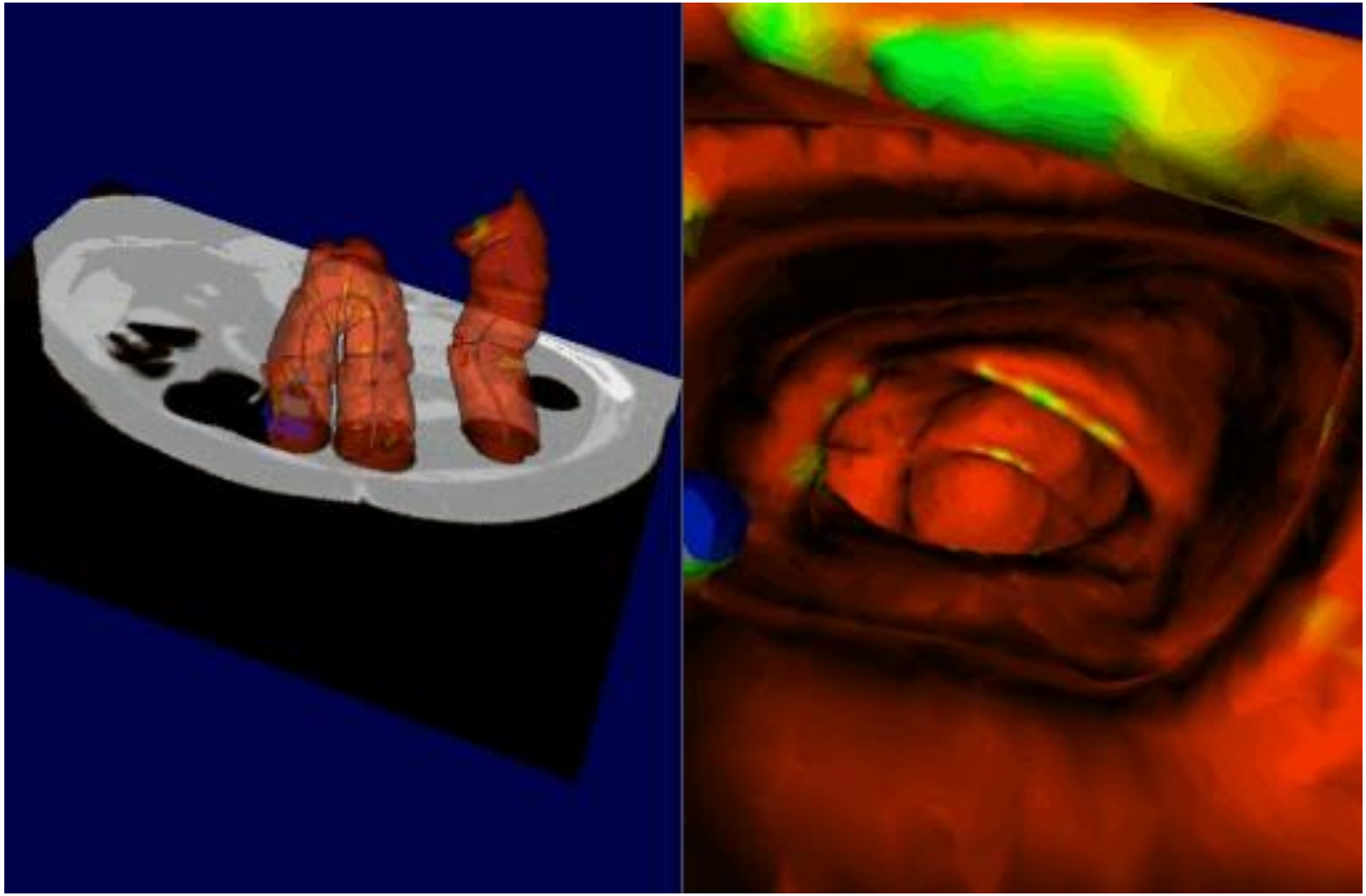

Simultaneous Fly-Through

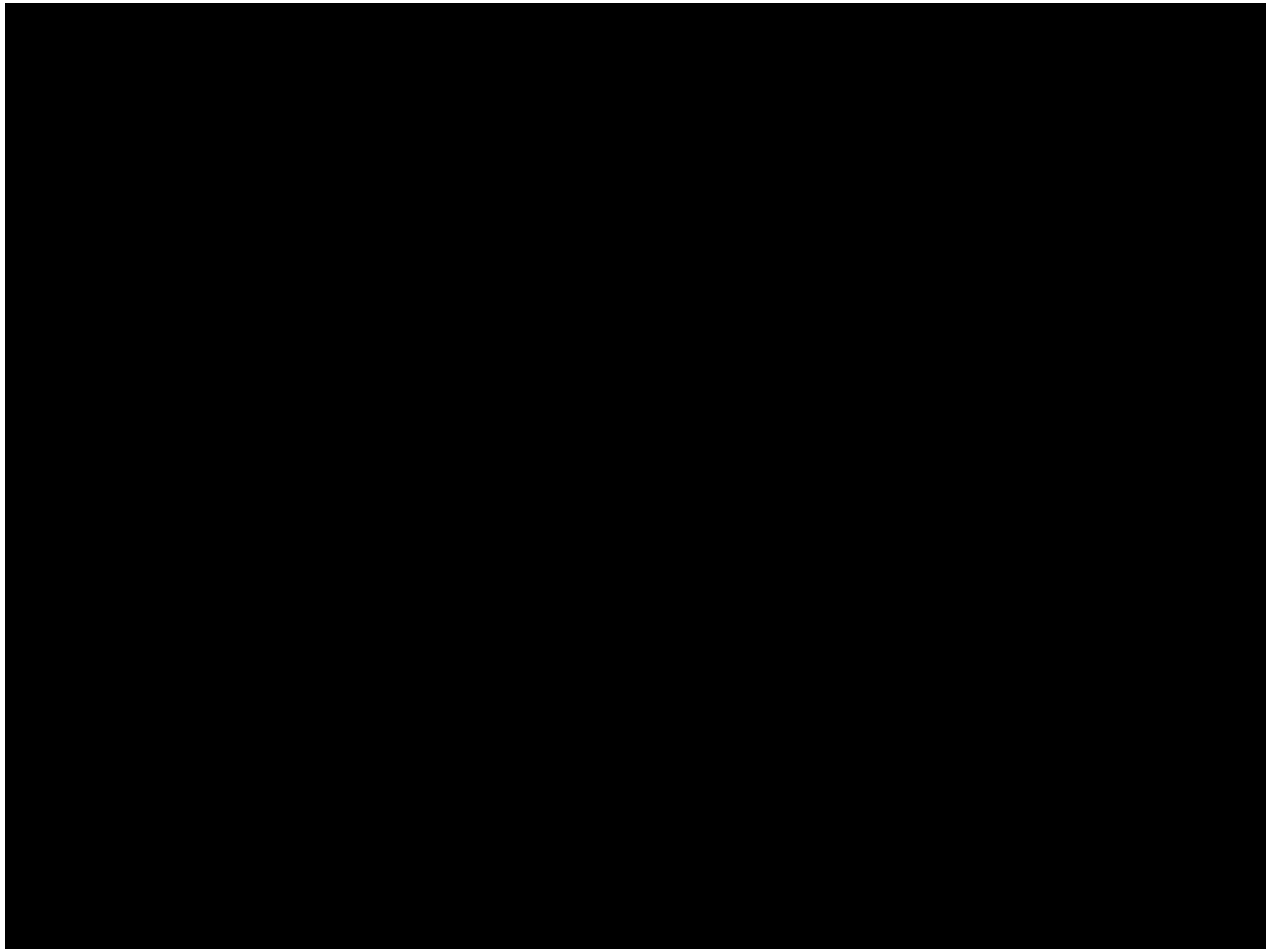

Coronary Vessels-Rendering

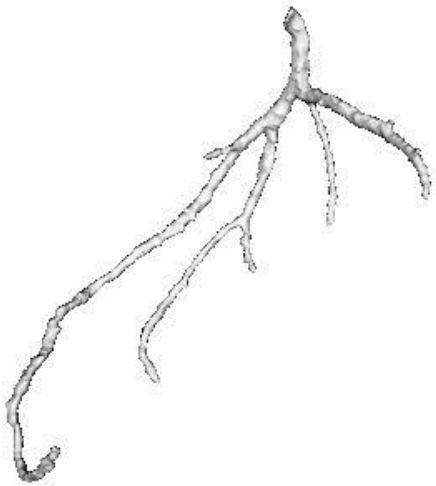

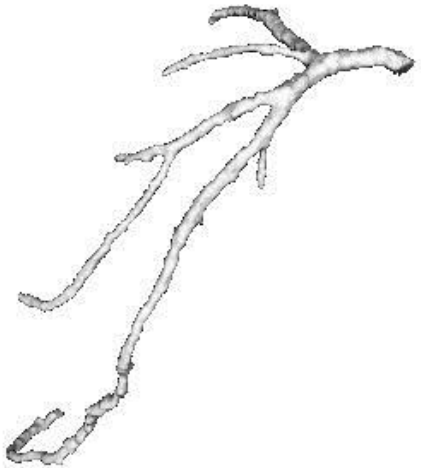

Coronary Vessels: Fly-Through

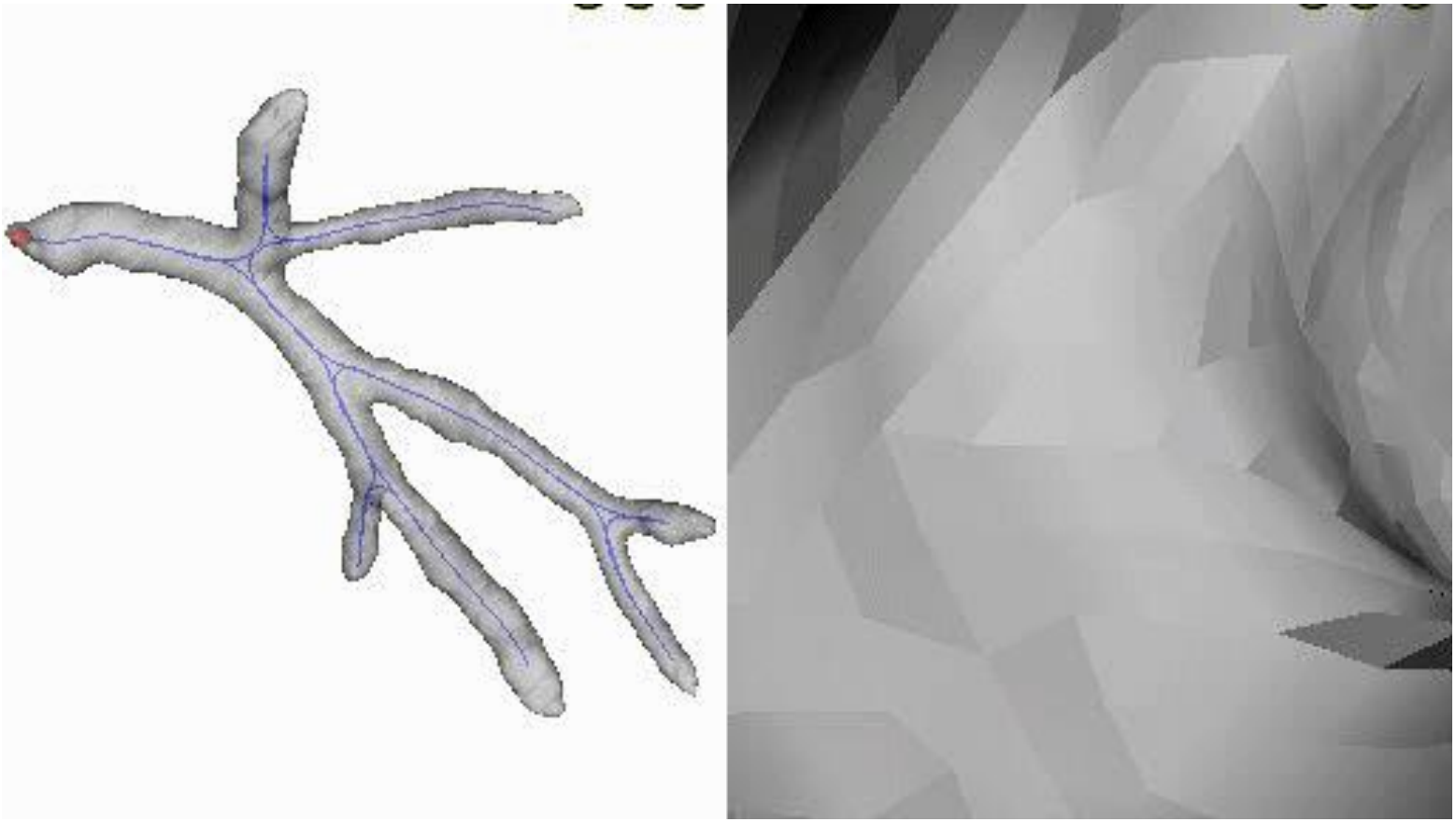

Area-Preserving Flows-I

Let M be a closed, connected n-dimensional manifold. **Volume form:**

$$\tau = g(x)\,dx\,,\ dx = dx_1 \wedge \ldots \wedge dx_n,$$
$$g(x) > 0$$

Theorem (Moser):

M, N compact manifolds with volume forms τ and σ. Assume that M and N are diffeomorphic. If

$$\int_M \tau = \int_N \sigma\,,$$

then there exists a diffeomorphism of M into N taking τ into σ.

Area-Preserving Flows-II

- The basic idea of the proof of the theorem is the contruction of an orientation-preserving automorphism homotopic to the identity.

- As a corollary, we get that given M and N any two diffeomorphic surfaces with the same total area, there exists are area-preserving diffeomorphism.
  - This can be constructed explicitly via a PDE.

Area-Preserving Flows for the Sphere-I

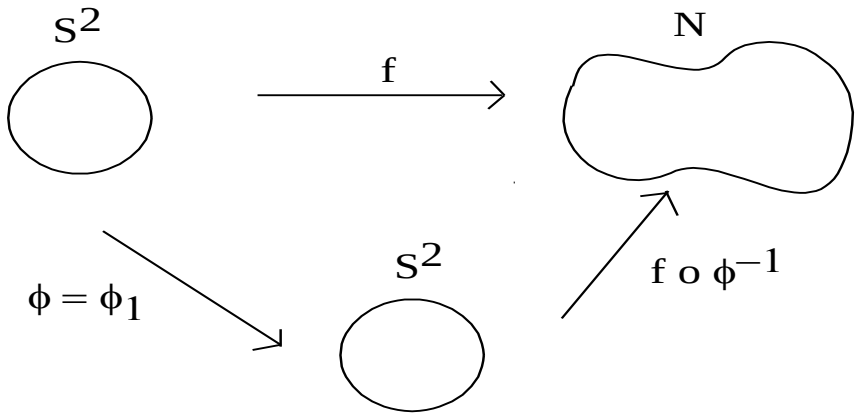

Find a one-parameter family of vector fields $u_t, t \in [0,1]$ **and solve the ODE**

$$\frac{d}{dt}\phi_t = u_t \circ \phi_t$$

to get a family of diffeomorphisms ϕ_t **such that**

$$\phi_0 = id$$

and

$$\det\left(D\,\phi_t\right)\left((1-t)\det(\ Df\ ) + t\right) = \det(\ Df\ )\ .$$

Area-Preserving Flows for the Sphere-II

To find u_t **, solve**

$$\Delta\theta = 1 - \det(Df),$$

then

$$u_t = \frac{-\nabla\theta}{(1-t)\det(Df) + t}$$

Area-Preserving Flows of Minimal Distortion

Let M and N be two compact surfaces with Riemannian metrics h and g respectively, and let ϕ be an area preserving map. This means if Ω_g and Ω_h are the area forms then

$$\phi^*(\Omega_g) = \Omega_h.$$

Many other area preserving maps from $M \longrightarrow N$ (just compose ϕ with any other area preserving map). Which one has the smallest distortion?

Minimize the Dirichlet integral with respect to area-preserving maps:

$$J(\phi) = 1/2 \int_M |D\phi|^2 \ \Omega_h$$

This leads to explicit gradient descent equations. Method will be discussed when we describe Monge-Kantorovich algorithms.

Registration and Mass Transport

Image registration is the process of establishing a common geometric frame of reference from two or more data sets from the same or different imaging modalities taken at different times.

Multimodal registration proceeds in several steps. First, each image or data set to be matched should be individually calibrated, corrected from imaging distortions, cleaned from noise and imaging artifacts. Next, a measure of dissimilarity between the data sets must be established, so we can quantify how close an image is from another after transformations are applied to them. Similarity measures include the proximity of redefined landmarks, the distance between contours, the difference between pixel intensity values. One can extract individual features that to be matched in each data set. Once features have been extracted from each image, they must be paired to each other. Then, a the similarity measure between the paired features is formulated can be formulated as an optimization problem.

We can use Monge-Kantorovich for the similarity measure in this procedure.

Mass Transportation Problems

- Original transport problem was proposed by Gaspar Monge in 1781, and asks to move a pile of soil or rubble to an excavation with the least amount of work.
- Modern measure-theoretic formulation given by Kantorovich in 1942. Problem is therefore known as *Monge-Kantorovich Problem (MKP).*
- Many problems in various fields can be formulated in term of MKP: statistical physics, functional analysis, astrophysics, reliability theory, quality control, meteorology, transportation, econometrics, expert systems, queuing theory, hybrid systems, and nonlinear control.

Monge-Kantorovich Mass Transfer Problem-I

We consider two density functions

$$\int \mu_0(x)\ dx = \int \mu_T(x)\ dx$$

We want

$$M: \mathbf{R}^d \to \mathbf{R}^d$$

which for all bounded subsets $A \subset \mathbf{R}^d$

$$\int_{x \in A} \mu_T(x)\ dx = \int_{M(x) \in A} \mu_0(x)\ dx$$

For M smooth and 1-1, we have (Jacobian equation)

$$\det(\nabla M(x))\ \mu_T(M(x)) = \mu_0(x)$$

We call such a map M ***mass preserving (MP).***

MK Mass Transfer Problem-II

Jacobian problem has many solutions. Want **optimal** one (**Lp-Kantorovich-Wasserstein metric**)

$$d_p(\mu_0, \mu_1)^p := \inf_M \int |M(x) - x|^p \mu_0(x) dx$$

Optimal map (when it exists) chooses a map with preferred geometry (like the Riemann Mapping Theorem) in the plane.

Algorithm for Optimal Transport-I

Subdomains with smooth boundaries and positive densities:

$$\Omega_0, \Omega_1 \subset \mathbf{R}^d$$

$$\int_{\Omega_0} \mu_0 = \int_{\Omega_1} \mu_1$$

We consider diffeomorphisms which map one density to the other:

$$\mu_o = \det(D\tilde{u})\mu_1 \circ \tilde{u}$$

We call this the ***mass preservation*** *(MP)* property. We let *u* be a initial MP mapping.

Algorithm for Optimal Transport-II

We consider a one-parameter family of MP maps derived as follows:

$$\tilde{u} := u \circ s^{-1},\ s = s(\cdot\,, t),\ \mu_0 = \det(Ds)\mu_0 \circ s$$

Notice that from the MP property of the mapping s, and definition of the family,

$$\tilde{u}_t = -\frac{1}{\mu_0} D\tilde{u} \cdot \zeta,\ \ \zeta = \mu_0\, s_t \circ s^{-1}$$

$$\operatorname{div} \zeta = 0$$

Algorithm for Optimal Transport-III

We consider a functional of the following form which we infimize with respect to the maps $\tilde{u}$:

$$M(t) = \int_{\Omega_0} \Phi(\tilde{u}(x,t) - x)\mu_0(x)\ dx$$

$$= \int \Phi(u(y) - s(y,t))\mu_0(y)\ dy,\ \ x = s(y,t),\ \ s^*(\mu_0(x)dx) = \mu_0(y)dy$$

Taking the first variation:

$$M'(t) = -\int \langle \Phi'(u-s),\ \ s_t \rangle \mu_0 dy$$

$$= -\int \langle \Phi'(\tilde{u}(x,t) - x),\ \ \mu_0 s_t \circ s^{-1} \rangle\ \ dx$$

$$= -\int_{\Omega_0} \langle \Phi'(\tilde{u}(x,t) - x),\ \ \zeta \rangle\ \ dx$$

Algorithm for Optimal Transport-IV

First Choice:

$$\zeta = \Phi'(\tilde{u} - x) + \nabla p$$

$$\text{div } \zeta = 0$$

$$\zeta|_{\partial\Omega_0} \text{ tangential to } \partial\Omega_0$$

This leads to following system of equations:

$$\tilde{u}_t = -1/\mu_0 D\tilde{u} \cdot (\Phi'(\tilde{u} - x) + \nabla p)$$

$$\Delta p + \text{div } (\Phi'(\tilde{u} - x)) = 0, \text{ on } \Omega_0$$

$$\frac{\partial p}{\partial \vec{n}} + \vec{n} \cdot \Phi'(\tilde{u} - x) = 0, \text{ on } \partial\Omega_0$$

Algorithm for Optimal Transport-V

This equation can be written in the *non-local* form:

$$\frac{\partial \tilde{u}}{\partial t} = -\frac{1}{\mu_0} D\tilde{u} \cdot (I - \nabla \Delta^{-1} \nabla \cdot) \Phi'(\tilde{u} - x)$$

At optimality, it is known that

$$\Phi'(\tilde{u} - x) \stackrel{\alpha}{=} \nabla \alpha$$

where α is a function. Notice therefore for an optimal solution, we have that the non-local equation becomes

$$\frac{\partial \tilde{u}}{\partial t} = 0$$

Solution of L2 M-K and Polar Factorization

For the L2 Monge-Kantorovich problem, we take

$$\Phi(x) = \frac{|x|^2}{2}$$

This leads to the following "non-local" gradient descent equation:

$$\tilde{u} = -1/\mu_0 D\tilde{u}(\tilde{u} - \nabla\Delta^{-1}\ \operatorname{div}(\tilde{u}))$$

Notice some of the motivation for this approach. We take:

$$\tilde{u} = u \circ s^{-1} = \nabla w + \chi,\ \ \operatorname{div}(\chi) = 0\ \ \textbf{Helmholtz decomp.}$$

The idea is to push the fixed initial u around (considered as a vector field) using the 1-parameter family of MP maps s(x,t), in such a manner as to remove the divergence free part. Thus we get that at optimality

$$u = \nabla w \circ s\ \ \textbf{Polar factorization}$$

Example of Mass Transfer-I

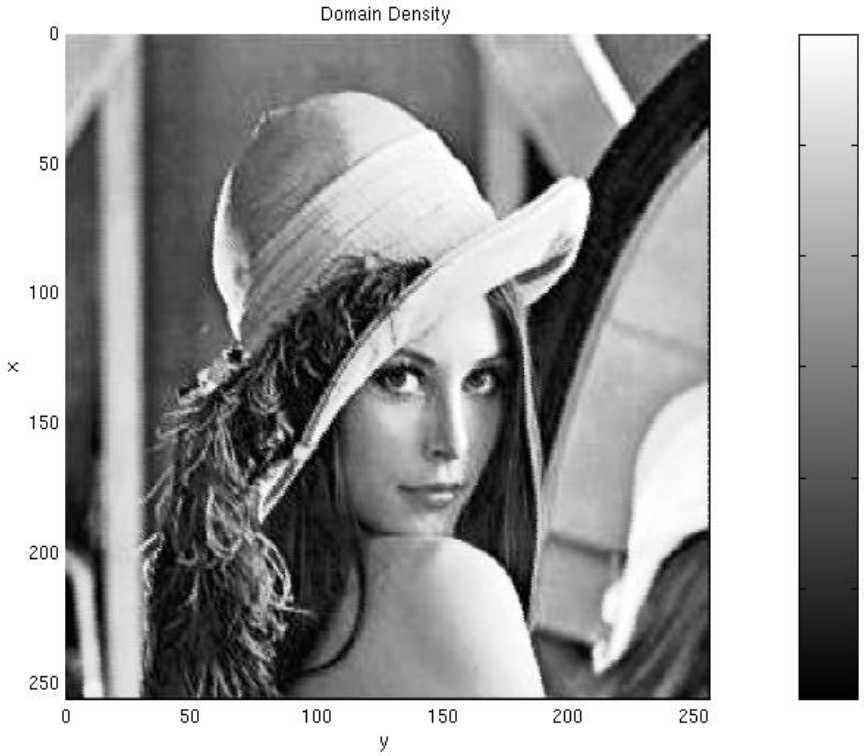

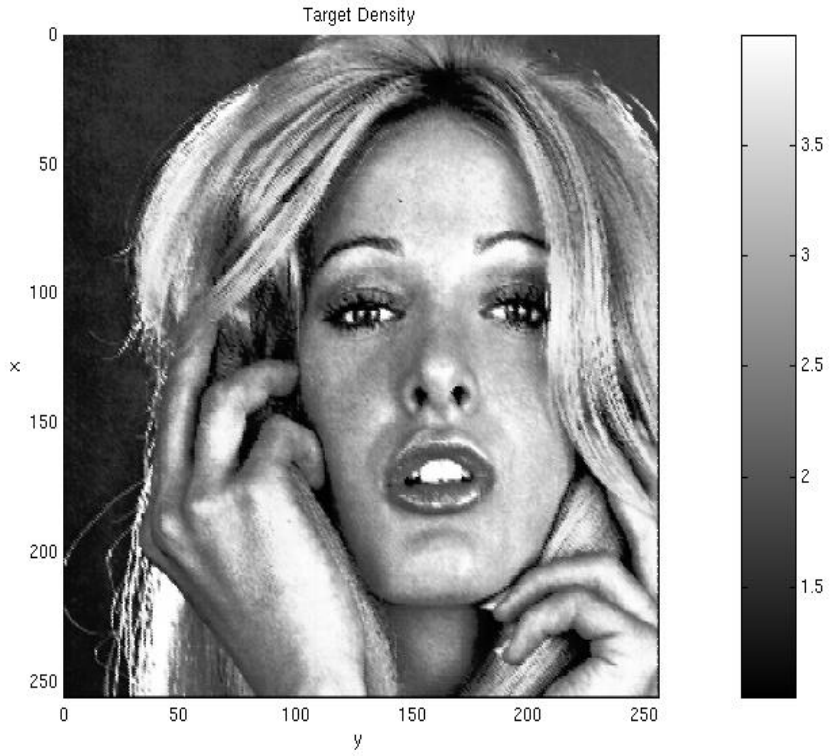

We want to map the Lena image to the Tiffany one.

Example of Mass Transfer-II

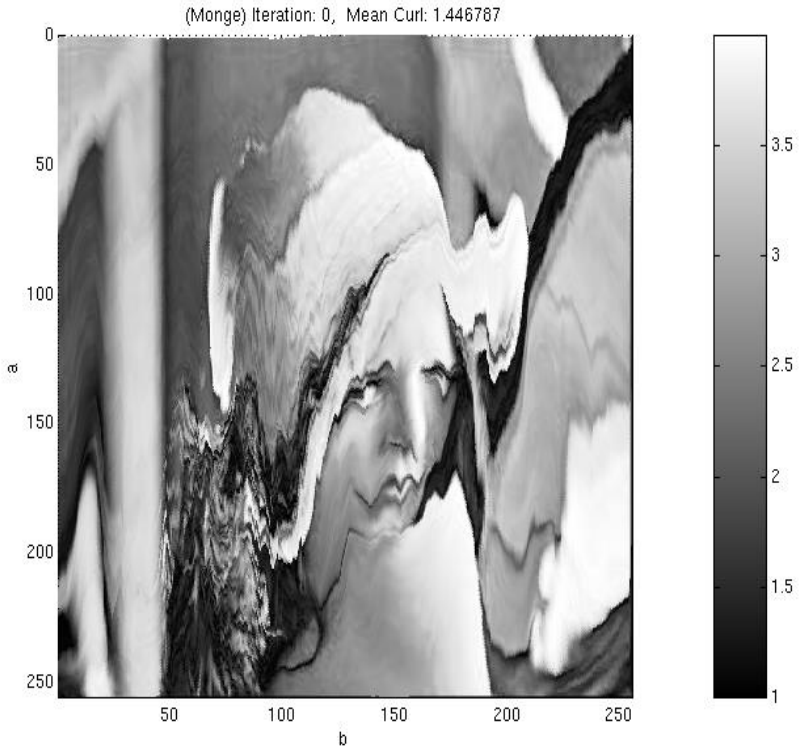

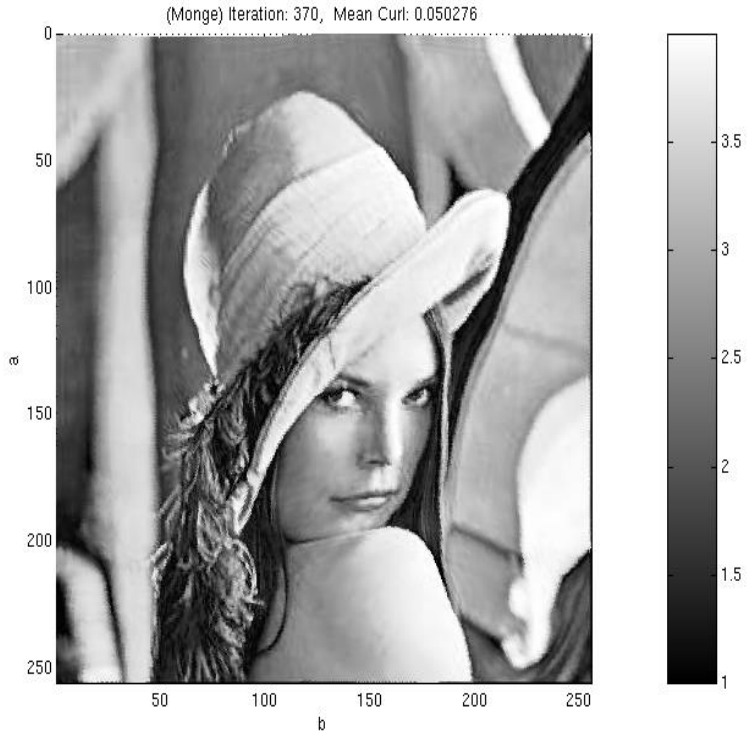

The first image is the initial guess at a mapping. The second is the Monge-Kantorovich improved mapping.

Morphing the Densities-I

$$V(t,x) = x + t(u_{opt}(x) - x)$$

Morphing the Densities-II (Brain Sag)

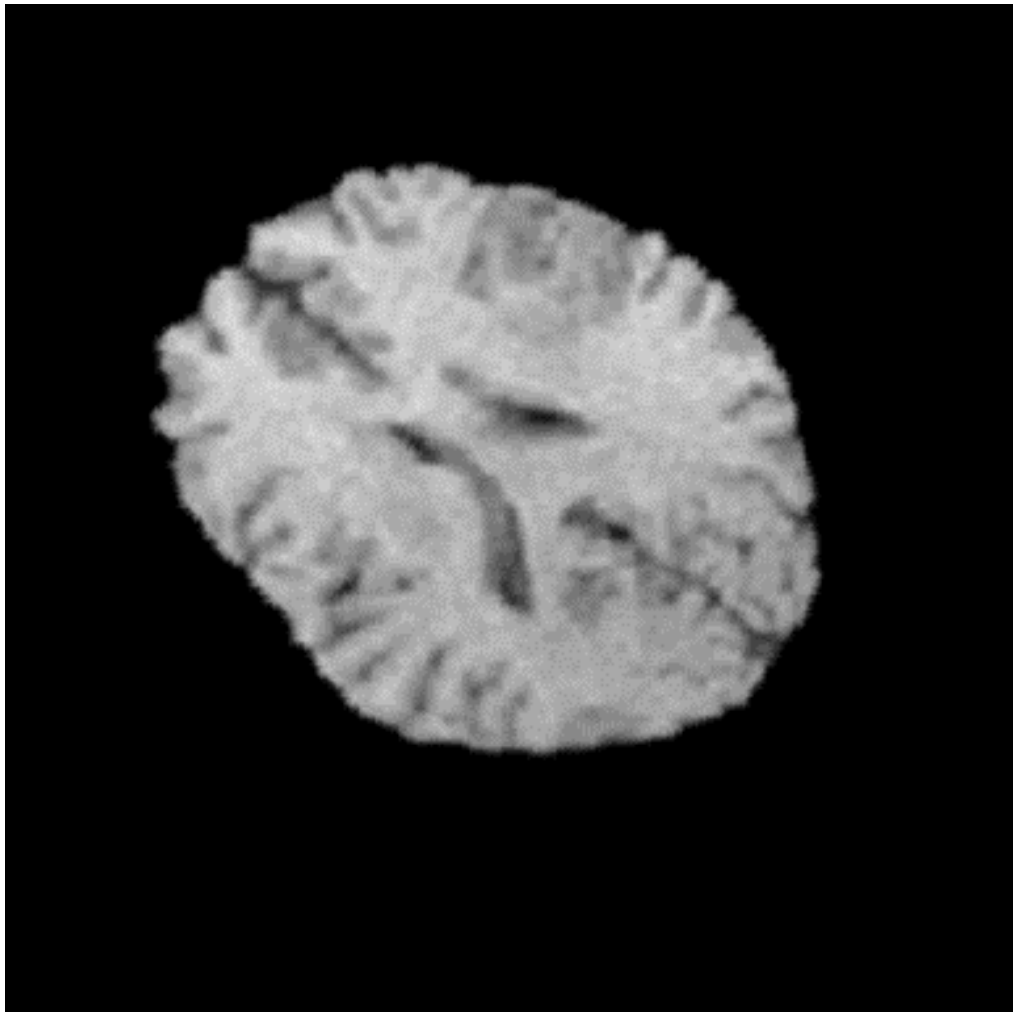

Deformation Map

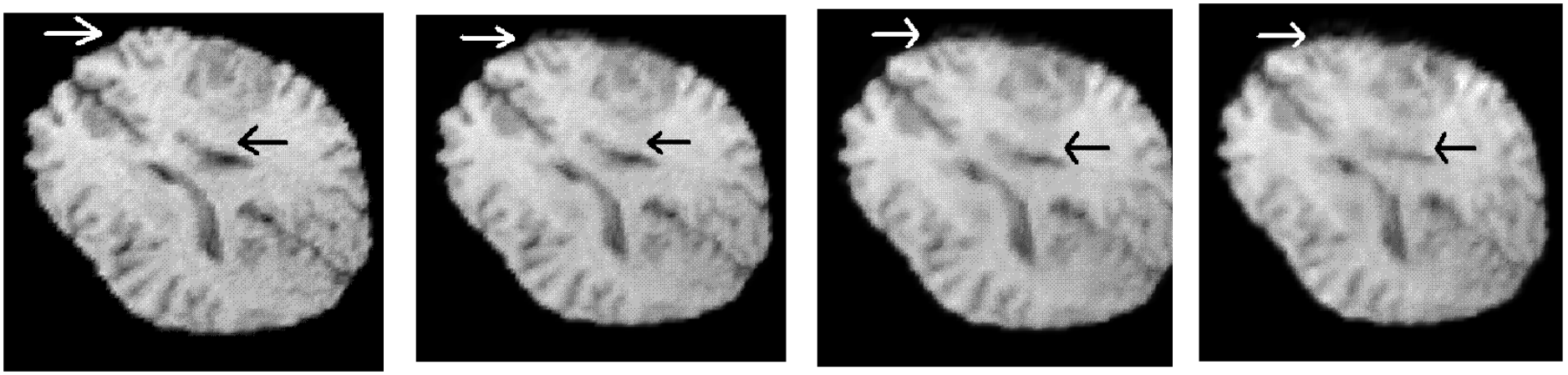

Brain deformation sequence. Two 3D MR data sets were used. First is pre-operative, and second during surgery, after craniotomy and opening of the dura. First image shows planar slice while subsequent images show 2D projections of 3D surfaces which constitute path from original slice. Here time t=0, 0.33, 0.67,and 1.0. Arrows indicate areas of greatest deformation.

Morphing-III

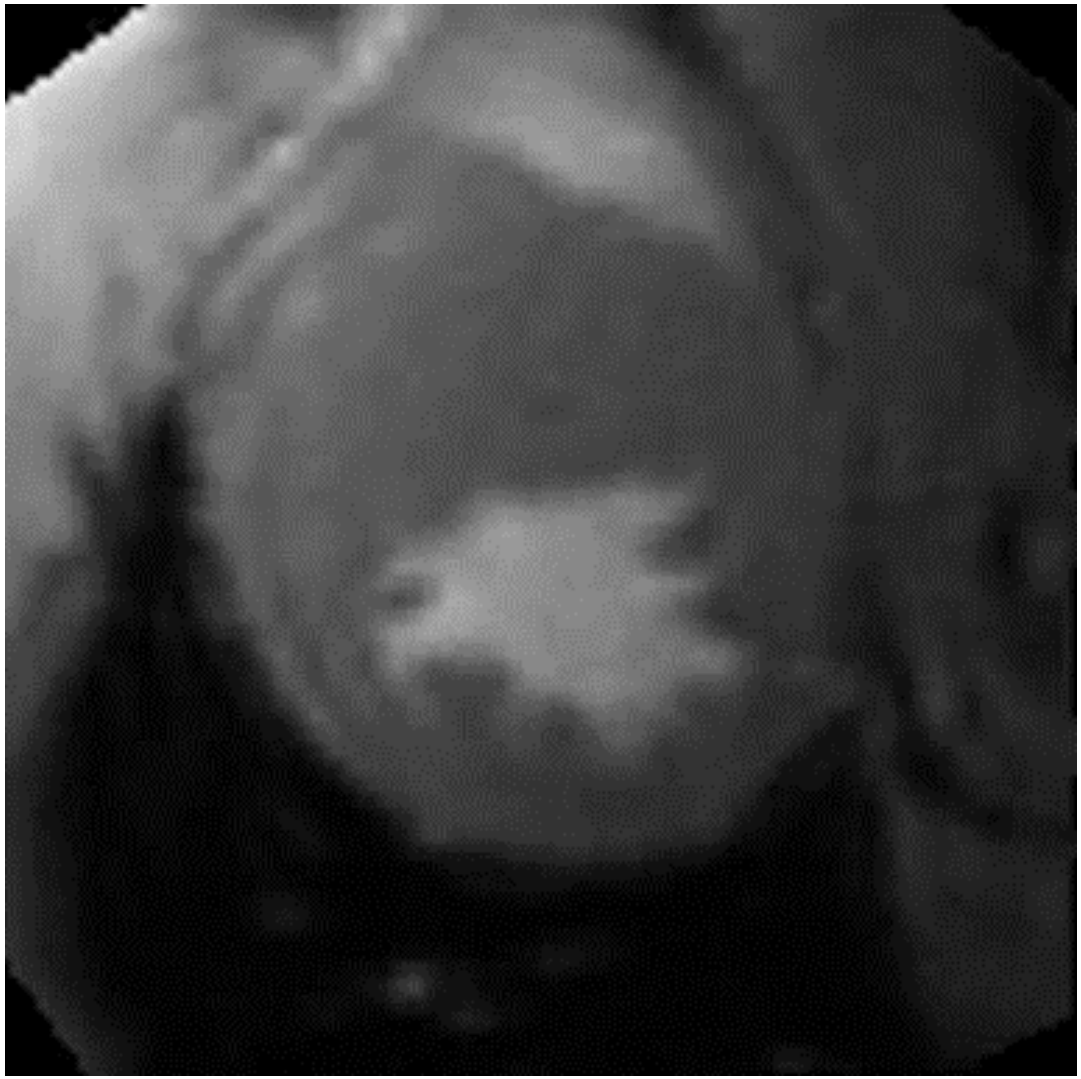

Morphing-IV

Morphing-V

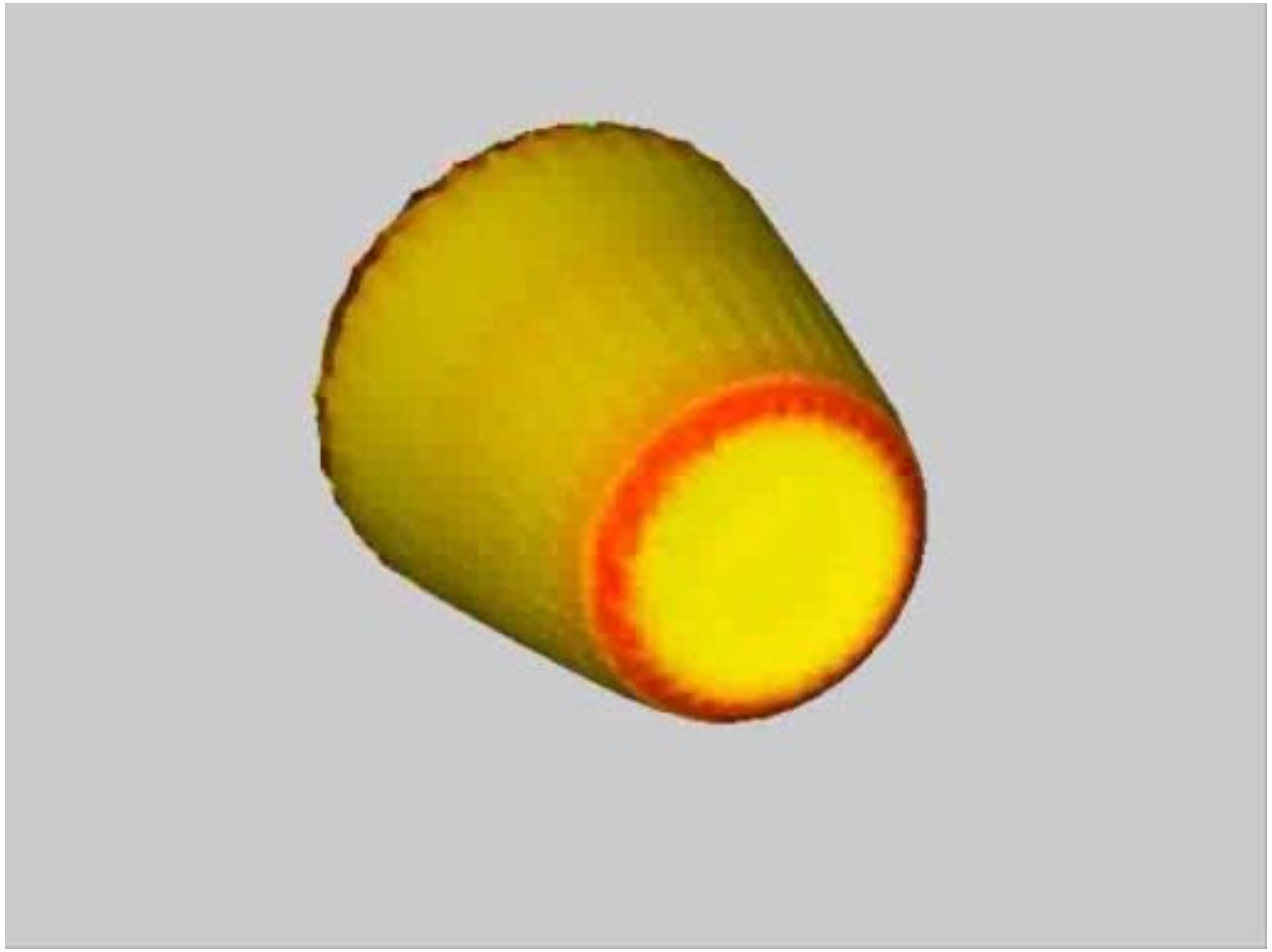

Surface Warping-I

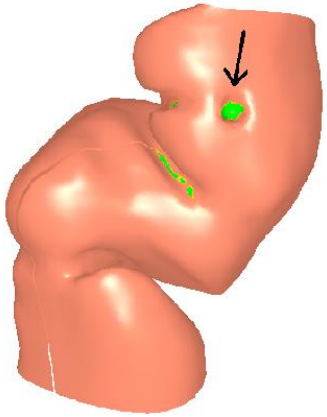

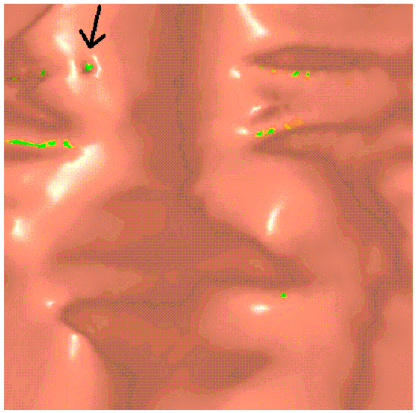

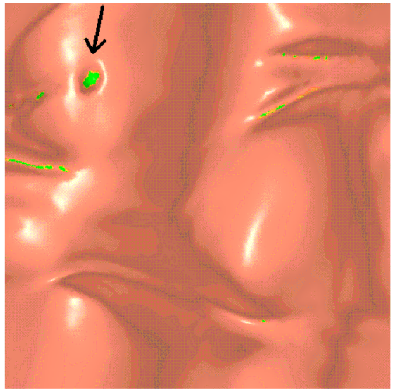

M-K allows one to find area-correcting flattening. After conformally flattening surface, define density mu_0 to be determinant of Jacobian of inverse of flattening map, and mu_1 to be constant. MK optimal map is then area-correcting.

Surface Warping-II

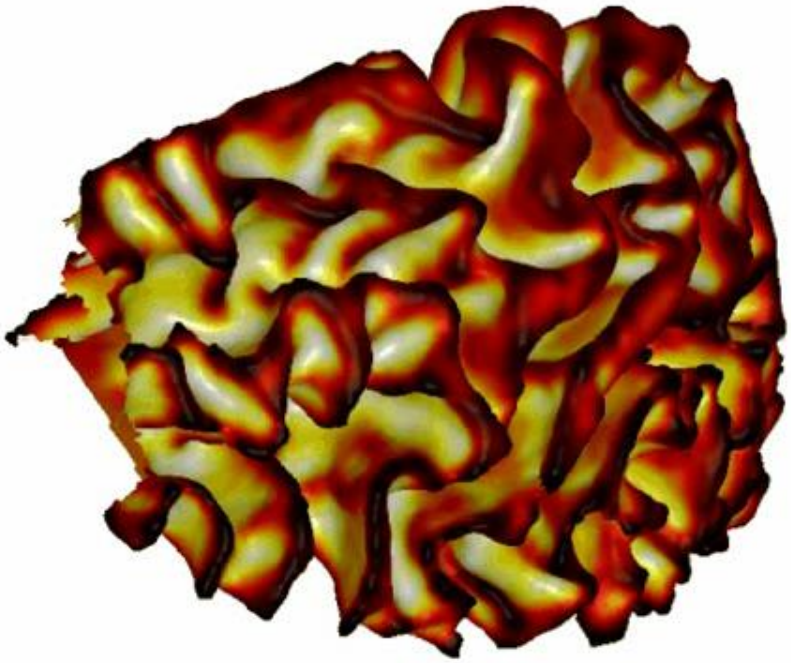

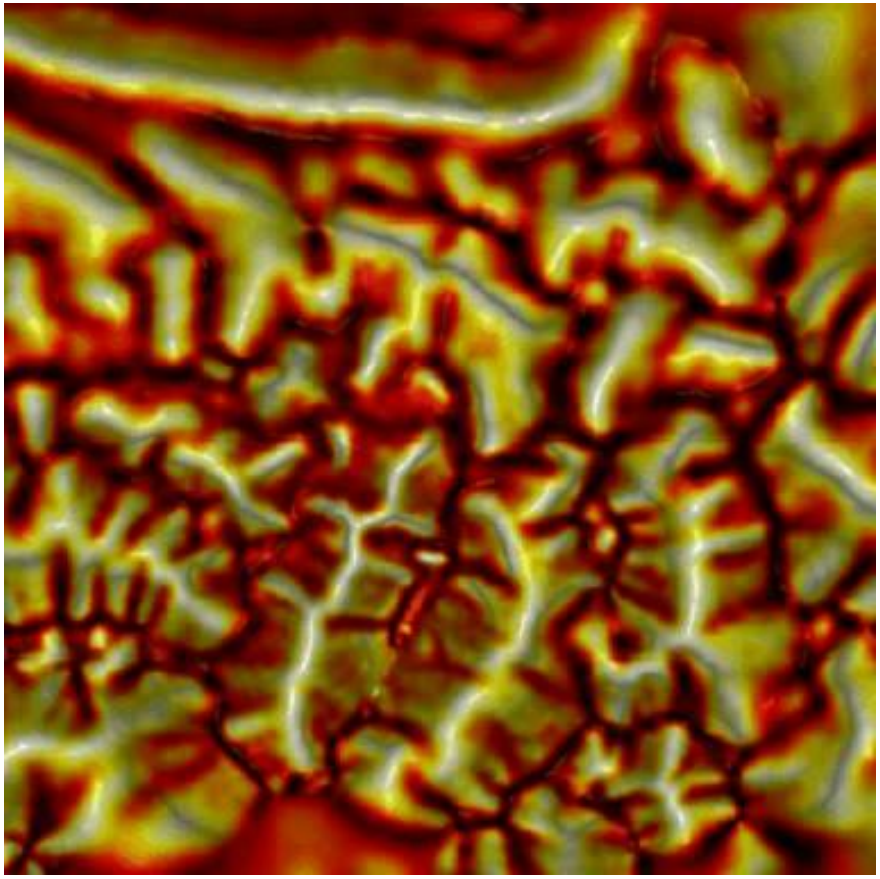

General Set-Up for L2 Mass Transport

Optimal mass transport and area-preserving maps of minimal distortion can be including in the following general framework:

$$\inf_{\tilde{u}\ \mathrm{MP}} \int \Phi(\tilde{u}-x, D(\tilde{u}-x))\mu_0(x)\ \ dx$$

Here Φ is a positive definite quadratic form. The case of interest is:

$$\Phi = 1/2|\tilde{u}-x|^2 + \alpha^2|D(\tilde{u}-x)|^2$$

Second term also acts as "smoothness term" in the M-K problem.

Mass Transfer and Interpolation

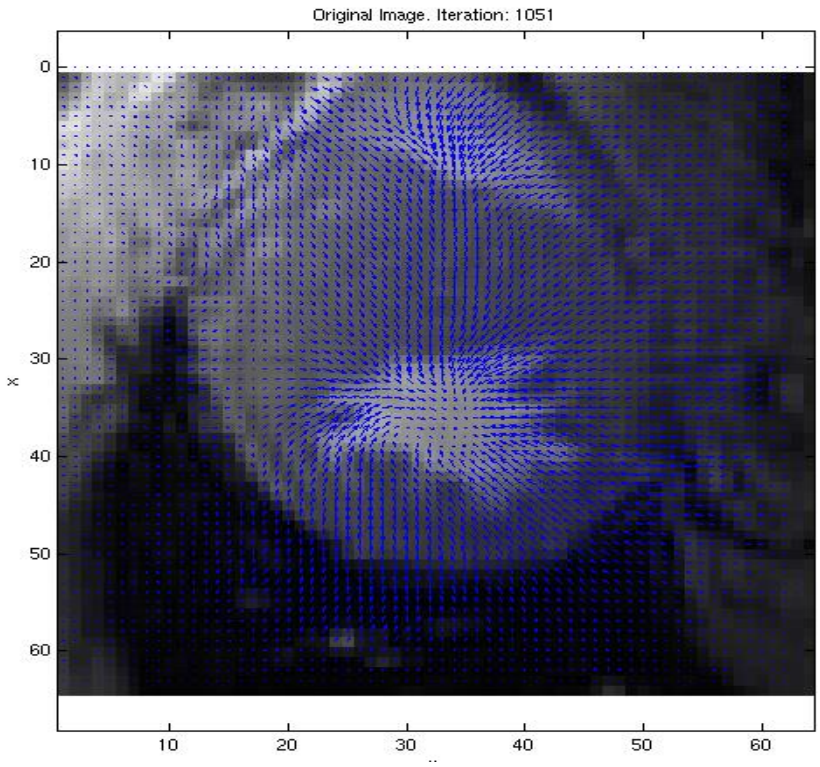

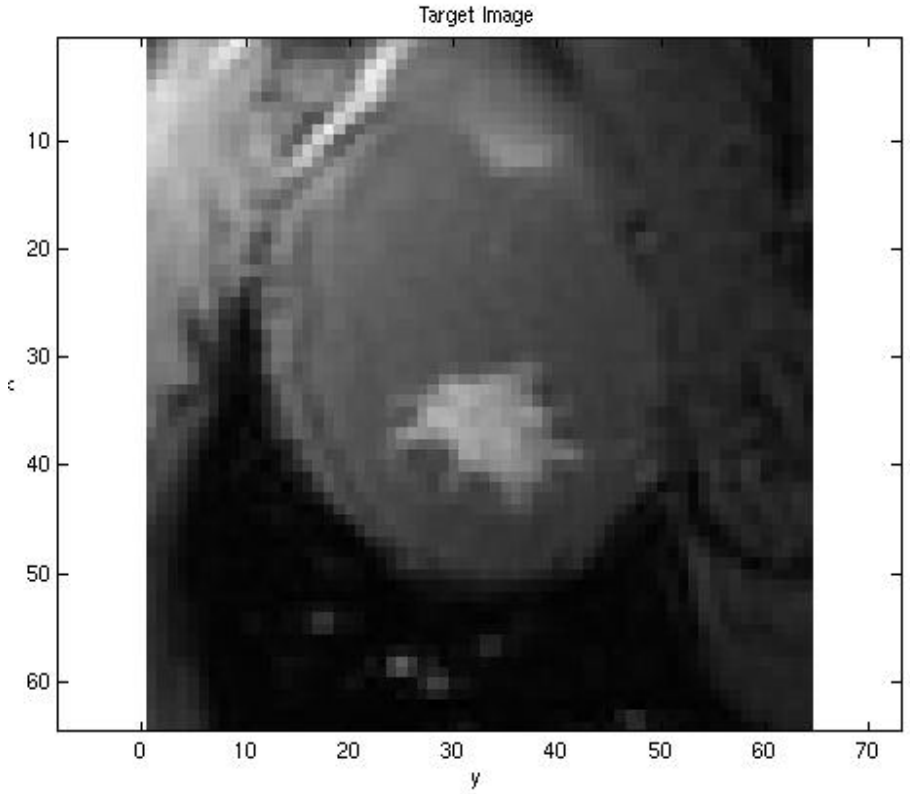

Warping Map

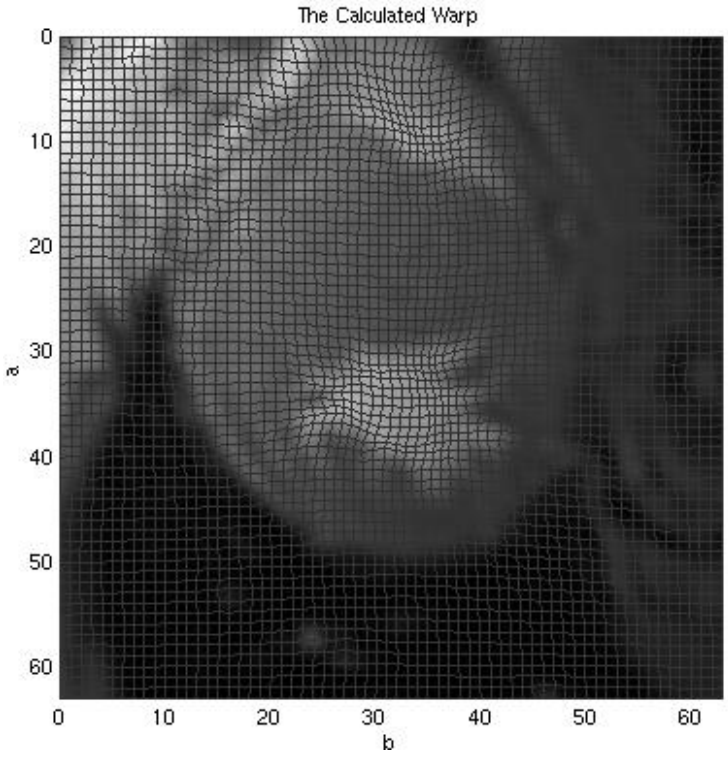

$$M = \inf_{u \in \mathrm{AP}} \int (F \circ u - G)^2 + \alpha^2 \int |Du|^2$$

$$F : \Omega_0 \to \mathbf{R},\ G : \Omega_1 \to \mathbf{R}$$

F and G are the image intensities and we infimize over all area-preserving maps:

$$u : \Omega_0 \to \Omega_1$$

And now for the details……..